

The shallow decay segment of GRB X-ray afterglow revisited

Submitted to APJ 2019 March 9; Accepted 2019 June 27

LITAO ZHAO,¹ BINBIN ZHANG,² HE GAO,³ LIN LAN,⁴ HOUJUN LÜ,⁴ AND BING ZHANG⁵

¹Department of Astronomy, Beijing Normal University, Beijing, China;

²School of Astronomy and Space Science, Nanjing University, Nanjing 210093, China;

³Department of Astronomy, Beijing Normal University, Beijing, China;

⁴Guangxi Key Laboratory for Relativistic Astrophysics, Department of Physics, Guangxi University, Nanning 530004, China;

⁵Department of Physics and Astronomy, University of Nevada, Las Vegas, NV 89154, USA

ABSTRACT

Based on the early-year observations from Neil Gehrels *Swift* Observatory, Liang et al. (2007) performed a systematic analysis for the shallow decay component of gamma-ray bursts (GRBs) X-ray afterglow, in order to explore its physical origin. Here we revisit the analysis with an updated sample (with Swift/XRT GRBs between February 2004 and July 2017). We find that with a larger sample, 1) the distributions of the characteristic properties of the shallow decay phase (e.g. t_b , S_X , $\Gamma_{X,1}$, and $\alpha_{X,1}$) still accords with normal or lognormal distribution; 2) $\Gamma_{X,1}$ and Γ_γ still show no correlation, but the tentative correlations of durations, energy fluences, and isotropic energies between the gamma-ray and X-ray phases still exist; 3) for most GRBs, there is no significant spectral evolution between the shallow decay segment and its follow-up segment, and the latter is usually consistent with the external-shock models; 4) assuming that the central engine has a power-law luminosity release history as $L(t) = L_0(\frac{t}{t_0})^{-q}$, we find that the value q is mainly distributed between -0.5 and 0.5, with an average value of 0.16 ± 0.12 ; 5) the tentative correlation between $E_{\text{iso},X}$ and t'_b disappears, so that the global 3-parameter correlation ($E_{\text{iso},X} - E'_p - t'_b$) becomes less significant; 6) the anti-correlation between L_X and t'_b and the three-parameter correlation ($E_{\text{iso},\gamma} - L_X - t_b$) indeed exist with a high confidence level. Overall, our results are generally consistent with Liang et al. (2007), confirming their suggestion that the shallow decay segment in most bursts is consistent with an external forward shock origin, probably due to a continuous energy injection from a long-lived central engine.

1. INTRODUCTION

Gamma-ray bursts (GRBs) are considered as the most extreme explosive events in the universe, which contains two phenomenological emission phases: prompt phase (with an initial prompt γ -ray emission) and afterglow phase (with a longer-lived broadband emission) (Zhang 2019). Although there are many uncertainties in the detailed physics of the prompt emission, mainly due to our poorly understanding the degree of magnetization of the GRB jet (Zhang 2014a; Kumar & Zhang 2015), a generic synchrotron external shock model has been constructed for interpreting the broadband afterglow data (Rees & Meszaros 1992, 1994; Meszaros & Rees 1993; Mészáros & Rees 1997; Gao et al. 2013; Wang et al. 2015).

In the pre-*Swift* era, the simple external shock signal was found to successfully explain a bunch of late-time afterglow data (Wijers et al. 1997; Waxman 1997; Wijers & Galama 1999; Huang et al. 1999, 2000; Panaiteescu & Kumar 2001, 2002; Yost et al. 2003). With the successful launch of the Neil Gehrels *Swift* Observatory, unprecedented new information about early-time afterglows was revealed (Tagliaferri et al. 2005; Burrows et al. 2005a; Zhang et al. 2006; Nousek et al. 2006; O'Brien et al. 2006; Evans et al. 2009), especially in the X-ray band, thanks mainly to the rapid slewing and precise localization capability of its on-board X-Ray Telescope (XRT) (Burrows et al. 2005b). After 6 months data accumulating, a five-segment canonical X-ray afterglow light curve was proposed (Zhang et al. 2006),

including a distinct rapidly decaying component, a shallow decay component, a normal decay component, a post jet break component and X-ray flares. With 2 years data collecting (with ~ 100 GRBs), a series of systematic analysis of the Swift XRT data was performed, in order to explore the physical origin for each segment of the canonical light curve (Zhang et al. 2007b; Liang et al. 2007; Willingale et al. 2007; Liang et al. 2008; Evans et al. 2009).

After fourteen years of operation, thousands of *Swift* GRBs were detected by XRT, it is of great interest to revisit the early analysis and see whether the previous results still consistent with the larger sample. In this work, we focus on the analysis of shallow decay component from Liang et al. (2007) (hereafter L07). L07 made a comprehensive analysis of the properties of the shallow decay segment with a sample of 53 long Swift GRBs detected before 2007 February. Their statistic results are summarized as follows: (1) the distributions of shallow decay segment parameters are normal and lognormal, with $\log_{10} t_b(s) = 4.09 \pm 0.61$, $\log_{10} S_X(\text{ergs cm}^{-2}) = -6.52 \pm 0.69$, $\Gamma_{X,1} = 2.09 \pm 0.21$ and $\alpha_1 = 0.35 \pm 0.35$; (2) The spectrum of the shallow decay phase is softer than that of the prompt gamma-ray phase, while the X-ray fluence and isotropic energy are almost linearly correlated with gamma-ray fluence and gamma-ray energy, respectively; (3) there is no significant spectral evolution between the shallow decay segment and its follow-up segment, and the follow-up segment in most bursts is consistent with the closure relations of external-shock models; (4) within the scenario of refreshed external shocks, the average energy injection index $q \sim 0$, suggesting a roughly constant injection luminosity from the central engine; (5) there is an empirical multivariate relation between parameters $E_{\text{iso},X} - E'_p - t'_b$ (henceforth the prime marks properties in the burst rest frame). Based on these results, L07 proposed that the shallow decay segment in most bursts is consistent with an external forward shock origin with continuous energy injection from a long-lived central engine. For a small fraction of bursts, whose post-break phase significantly deviate from the external-shock models, the shallow decay phase might be of internal origin and demand a long-lived emission component directly from the central engine.

In this work, we revisit the results of L07 with *Swift* observed GRBs between February 2004 and July 2017. In addition, it has been discovered that there exists a rough anti-correlation between the rest frame X-ray plateau end time (t'_b) and X-ray luminosity L_X (Dainotti et al. 2008, 2010, 2011a). The slope is roughly -1 (Dainotti et al. (2013a)). This suggests that the total plateau energy has relatively small scatter: a longer plateau tends to have a lower luminosity and vice versa. Dainotti et al. (2011b) analysed and suggested correlations between L_X with several prompt emission parameters, including the isotropic energy $E_{\text{iso},\gamma}$. Xu & Huang (2012) claimed that a three-parameters collection, expressed as $L_X \propto t_b^{0.87} E_{\text{iso},\gamma}^{0.88}$, becomes tighter. On the other hand, Dainotti et al. (2016, 2017) extend the $L_X - t'_b$ correlation by adding a third parameter (the peak luminosity in the prompt emission L_{peak}), and find that the new $L_X - t'_b - L_{\text{peak}}$ correlation becomes much tighter, which is 37% tighter than the Xu & Huang (2012) correlation. In this work, we also test these relations based on our new sample.

2. DATA REDUCTION AND SAMPLE SELECTION

The XRT light curves data were downloaded from the Swift/XRT team website¹ (Belokurov et al. 2009), and processed with HEASOFT v6.12. 1291 Swift GRBs were detected by Swift/XRT between February 2004 and July 2017, with 625 GRBs having well-sampled XRT light curves, which contains at least 6 data points, excluding upper limits. We then fit the XRT light curves (in logarithmic scale) with multi-segment broken power law function. Here the multivariate adaptive regression spline (MARS) technique (e.g. Friedman (1991)) is adopted, which can automatically determine both variable selection and functional form, resulting in an explanatory predictive model. It has been proven that MARS can automatically fit the XRT light curve with multi-segment broken power-law function (results consistent with fitting results provided by the XRT GRB online catalog), detect and optimize all breaks, and record all break times and power-law indices for each segment (see Zhang et al. (2014b) and Gao et al. (2017) for details). We find that the distribution of the index difference between adjacent segments for all GRBs could be fitted with a Gaussian function (with mean value as 0.6 and standard deviation as 0.3). To avoid the potential over-fitting problem from MARS technique, we treat the adjacent segments with index difference smaller than 0.3 as one component when calculating the segment time span.

We define segments with decay slope shallower than 0.8 and time span in log scale larger than 0.4 dex² as the shallow decay component candidates. 284 GRBs are excluded due to the lack of any shallow decay candidates. Among the rest 341 GRBs, 67 bursts are further excluded since there are too few data points or there seem seems to be weak flare

¹ http://www.swift.ac.uk/xrt_curves/

² We have tested that reasonably adjusting the criteria values of 0.8 and 0.4 might slightly change the size of the final sample but would not affect the main conclusions.

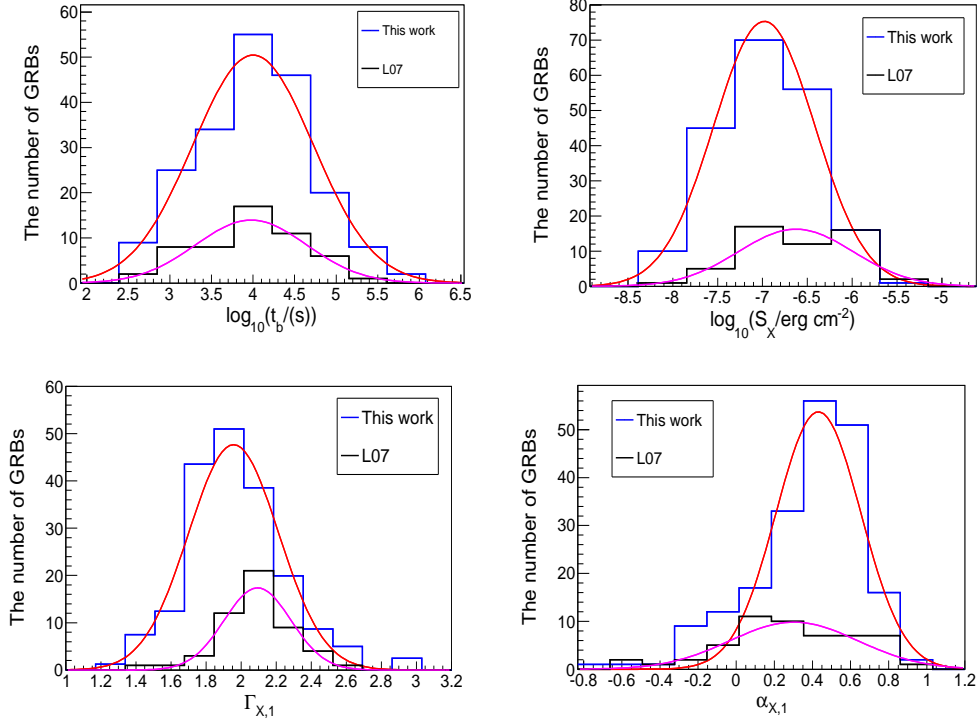


Figure 2. Distributions of the characteristic properties of the shallow decay phase for GRBs in our sample, comparing with L07’s results. The solid red and pink lines are the results of Gaussian fits.

signatures in the shallow decay segments. Moreover, we excluded 54 GRBs whose shallow decay candidate.segments lacks of a follow-up segment, namely the shallow decay segment is the only segment or the last segment in the light curve. 18 GRBs are excluded since they consist more than one nonadjacent shallow decay candidates, which would be discussed in a separate work. GRB 060218 is excluded since its early shallow decay behavior in the X-ray light curve should be mainly determined by the shock break-out emission instead of external shock emission (Campana et al. 2006).

For the remaining 201 GRBs, we record the beginning time (t_1) of the shallow decay segment and the end time (t_2) of its follow-up segment. We then fit the light curve in the time interval $[t_1, t_2]$ with a smoothed broken power law (BPL) function

$$f(t) = f_0 \left[\left(\frac{t}{t_b} \right)^{w\alpha_1} + \left(\frac{t}{t_b} \right)^{w\alpha_2} \right]^{-1/w} \quad (1)$$

with α_1 and α_2 representing the decay scopes of pre-break segment and post-break segment, and w determining the sharpness of the break. Here we adopt $w = 3$ as suggested in L07, in order to make better comparison with their results. All fitting light curves are shown in Fig.1, and the best fitting parameters are collected in Table.1 . The X-ray fluence (S_X) of the shallow decay segment is obtained by integrating the fitted light curve from t_1 to t_b . Note that here we further exclude three bursts in our sample since the difference between their α_1 and α_2 are smaller than 0.3.

There is no spectral evolution during the shallow decay and followed normal decay phases(Liang et al. 2007), so that we extract the time-integrated spectra in the time interval of $[t_1, t_b]$ and $[t_b, t_2]$. We fit the X-ray spectrum with the Xspec package, and an absorbed power-law model is invoked to fit the spectrum, i.e., abs \times zabs \times zdust \times power law, where zdust is the dust extinction of the GRB host galaxy, abs and zabs are the absorption models for the Milky Way and the GRB host galaxy, respectively. Then, we derived the photon indices $\Gamma_{X,1}$ and $\Gamma_{X,2}$ for shallow decay and followed normal decay phases.

3. L07 REVISITED

3.1. *Distributions of the characteristic properties of the shallow decay phase*

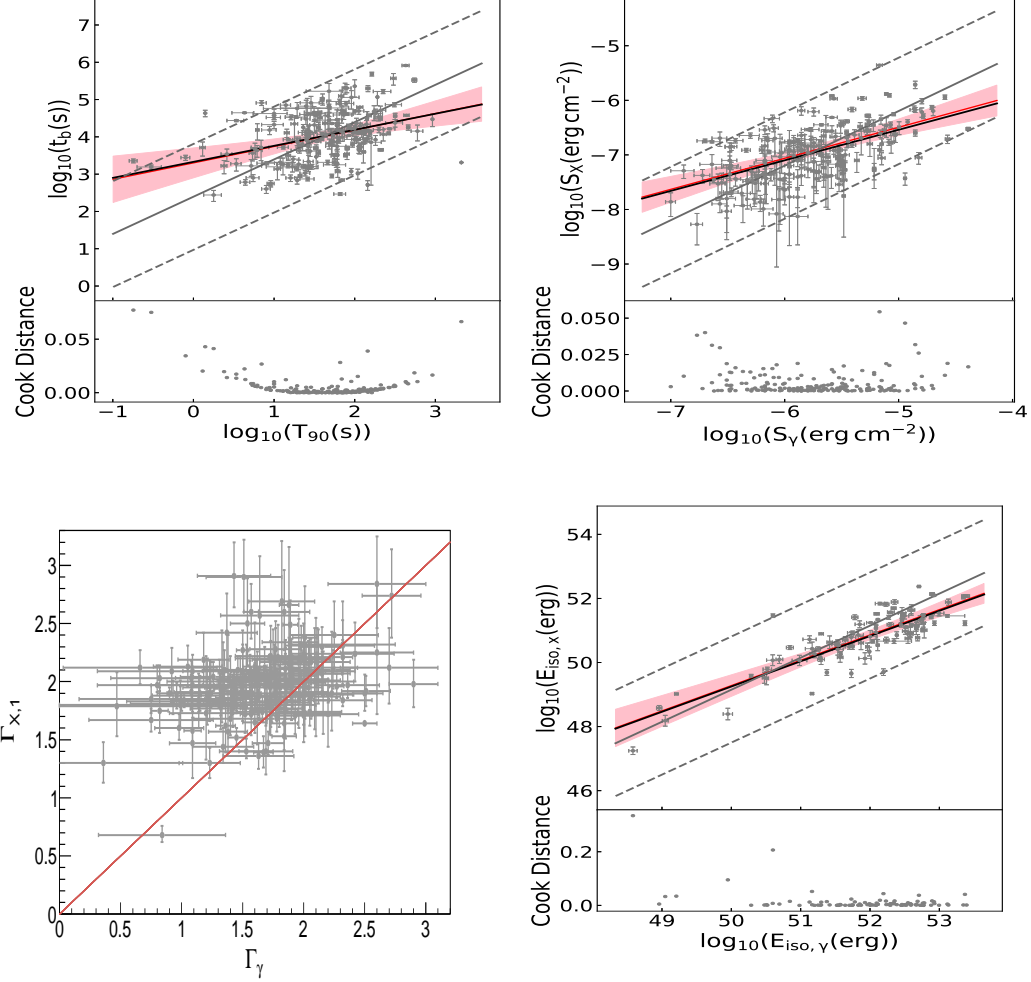


Figure 3. Parameters relationship between shallow decay phase and prompt emission phase, including t_b - T_{90} , S_X - S_γ , $\Gamma_{X,1}$ - Γ_γ and $E_{iso,X}$ - $E_{iso,\gamma}$. The black solid line represents the best fit with least square regression method. The red solid line present the best fit with the bivariate linear regression method and the pink shadowed region show the intrinsic scatter to the population $3\sigma_{int}$. The grey lines mark the best fitting results (solid) and its 2σ linear correlation region (dotted), which is defined with $y = x + A \pm 2\delta_A$, where y and x are the two quantities in question and A and σ_A are the mean and its 1σ standard error for the y - x correlation. The orange solid lines show $y = x$.

For our sample, we find that the distributions of the characteristic properties of the shallow decay phase (e.g. t_b , S_X , $\Gamma_{X,1}$, and $\alpha_{X,1}$) accords with normal or lognormal distribution³, with $\log_{10}(t_b) = 4 \pm 0.72$, $\log_{10}(S_X(\text{ergs cm}^{-2})) = -6.97 \pm 0.56$, $\Gamma_{X,1} = 1.96 \pm 0.26$ and $\alpha_{X,1} = 0.43 \pm 0.22$. For comparison, we plot our result together with L07's result in Fig.2. It is found that when larger sample being involved, the distributions for all the parameters become slightly broader, but the peaks of each distribution barely change, for instance, the mean value for distributions of $\log_{10}(t_b)$, $\log_{10}(S_X)$, $\Gamma_{X,1}$, and $\alpha_{X,1}$ differs by 3%, 7%, 6%, and 23% respectively, between L07 results and our results.

3.2. Relationship of the shallow decay phase to the prompt gamma-ray phase

In order to investigate the relationship of the shallow decay phase to the prompt gamma-ray phase, we first collect relevant parameters of prompt gamma-ray emission for our sample, including the duration (T_{90}), fluence (S_γ), photon indices (Γ_γ), and the peak energy of the νF_ν spectrum (E_p) through published articles and GCN Circulars (the results

³ In our analysis, we have checked several different distribution functions, including Weibull distribution, Beta distribution, Gamma distribution, normal distribution, lognormal distribution, Exponential distribution and so on. We compare these distribution functions by comparing their fitting square error (sum of squared discrepancies between histogram frequencies and fitted-distribution frequencies), and find that normal or lognormal functions are always the best or very close to the best to fit our interested distributions. In order to better compare our results with L07 findings, and considering that normal or lognormal functions have stronger physical meaning than other functions, here we only use normal and lognormal functions to fit relevant distributions.

are presented in Table 2). For BAT spectrum that can be fitted by a single power-law, we estimate E_p through the correlation between the BAT photon index Γ and E_p ((Zhang et al. 2007a; Sakamoto et al. 2009a; Virgili et al. 2012)), namely

$$\log_{10}(E_p) = (4.34 \pm 0.475) - (1.32 \pm 0.219)\log_{10}(\Gamma) \quad (2)$$

Within our sample, 97 GRBs have redshift measurements, whose isotropic-equivalent radiation energies ($E_{\text{iso},\gamma}$, $E_{\text{iso},X}$) in the prompt phase and in the shallow decay phase could be calculated as

$$E_{\text{iso},(\gamma,X)} = \frac{4\pi D_L^2 S_{(\gamma,X)}}{1+z} \quad (3)$$

where D_L is the luminosity distance. Here $H_0 = 71 \text{ km s}^{-1} \text{ Mpc}^{-1}$, $\Omega_M = 0.3$, $\Omega_A = 0.7$ are adopted for calculating D_L . We then calculate the bolometric energy $E_{\text{iso},(\gamma,X)}^b$ in the $1 \sim 10^4$ keV band with the k-correction method proposed by Bloom et al. (2001),

$$E_{\text{iso},(\gamma,X)}^b = k E_{\text{iso},(\gamma,X)}, \quad (4)$$

where

$$k = \frac{\int_{1/(1+z)}^{10^{4/(1+z)}} EN(E)dE}{\int_{15}^{150} EN(E)dE}. \quad (5)$$

assuming the gamma-ray spectrum for all GRBs following Band function with photon indices -1 and -2.3 before and after E_p .

Fig.3 shows parameter relationships of the shallow decay phase to the prompt gamma-ray phase, including t_b - T_{90} , S_X - S_γ , $\Gamma_{X,1} - \Gamma_\gamma$ and $E_{\text{iso},X}$ - $E_{\text{iso},\gamma}$ relationships. We find that with larger sample, $\Gamma_{X,1}$ and Γ_γ still show no correlation, with $\Gamma_{X,1}$ systematically larger than Γ_γ . The result is consistent with the relevant findings in Dainotti et al. (2015). The tentative correlations of duration, energy fluences, and isotropic energies between the gamma-ray and X-ray phases still exist, with the best fit as $\log_{10}(t_b) = (0.43 \pm 0.08)\log_{10}(T_{90}) + (3.33 \pm 0.15)$ (Spearman correlation coefficient $r = 0.39$, significance level $p < 10^{-4}$ for $N = 198$, fraction of the variance $R^2 = 14.1\%$, and significance of Anderson-Darling test $p_{AD} = 0.647$), $\log_{10}(S_X) = (0.56 \pm 0.06)\log_{10}(S_\gamma) + (-3.74 \pm 0.37)$ ($r = 0.55$, $p < 10^{-4}$ for $N = 198$, $R^2 = 35.3\%$ and $p_{AD} = 0.44$) and $\log_{10}(E_{\text{iso},X}) = (0.788 \pm 0.05)\log_{10}(E_{\text{iso},\gamma}) + (9.85 \pm 2.58)$ ($r = 0.77$, $p < 10^{-4}$ for $N = 198$, $R^2 = 72.4\%$ and $p_{AD} = 0.566$). With the exception of $E_{\text{iso},X}$ - $E_{\text{iso},\gamma}$, the correlations of t_b - T_{90} and $E_{\text{iso},X}$ - $E_{\text{iso},\gamma}$ become weaker with larger sample, and the correlation coefficients were reduced by approximately 18% (for duration) and 21% (for energy fluence). The fitting results and Cook distance for the fitting are shown in figure 3. Here we also apply the bivariate linear regression procedure to fit the data (Kelly 2007, for details). We find that the best fit results for different regression methods are consistent. The intrinsic scatter to the population σ_{int} is shown in Fig.3. In order to compare with L07, we also check the possible linear correlations for the quantities in the two phases by defining 2σ linear correlation regions⁴ (see Figure.3 for details), and we find that most of our GRBs fall in this region, suggesting that the radiation during the shallow decay phase might indeed be correlated with that in the prompt gamma-ray phase.

3.3. Test physical origin of the shallow decay segment

We first check whether there is any spectral evolution between shallow decay segment and its follow-up segment. The left panel of Fig.4 plots $\Gamma_{X,2}$ as a function of $\Gamma_{X,1}$. We find that all GRBs in our sample fall in the 2σ linear correlation regions. The middle of Fig.4 shows the comparison between the distributions of $\Gamma_{X,1}$ and $\Gamma_{X,2}$. For L07's sample, the Kolmogorov-Smirnov test suggests that these two distributions being consistent with the significance level of 0.96. With the larger sample, we find that the two distributions are still consistent, but the significance level of this consistency decreases to 0.40. As suggested by L07, here we define a new parameter as

$$\mu = \frac{\Gamma_{X,2} - \Gamma_{X,1}}{\sqrt{\delta\Gamma_{X,1}^2 + \delta\Gamma_{X,2}^2}}, \quad (6)$$

⁴ 2σ linear correlation regions is defined with $y = x + A \pm 2\delta_A$, where y and x are the two quantities in question and A and σ_A are the mean and its 1σ standard error for the y - x correlation

to verify this consistency within the observational uncertainty for individual bursts. The right panel of Fig.4 shows μ distribution. We find that 84% GRBs in our sample have $\mu \leq 1$, and only 2 GRBs (GRB 080903 and GRB 150201A) show significant spectral evolution ($\mu > 3$). Considering all these evidence, we confirm L07's conclusion that there is no significant spectral evolution between the shallow decay segment and its follow-up segment, indicating that the shallow decay phase is a refreshed forward shock(Rees & Mészáros 1998; Dai & Lu 1998; Zhang & Mészáros 2001; Zhang et al. 2006; Nousek et al. 2006).

In this scenario, the shallow decay's follow-up segment should be consistent with the predictions of the forward shock models, namely the observed spectral index $\beta_{X,2} = \Gamma_{X,2} - 1$ and temporal decay index α_2 should follow the so called “closure relations” (Gao et al. 2013, for a review). Although the closure correlations vary for different spectral regimes, different cooling schemes or different properties of the ambient medium, as illustrated in L07, three regimes are relevant here:

- regime 1: $\nu_x > \max(\nu_m, \nu_c)$ (for either ISM or wind medium), where $\alpha_2 = (3\beta_2 - 1)/2$;
- regime 2: $\nu_m < \nu_x < \nu_c$ (for ISM medium), where $\alpha_2 = 3\beta_2/2$;
- regime 3: $\nu_m < \nu_x < \nu_c$ (for wind medium), where $\alpha_2 = (3\beta_2 + 1)/2$.

We define a new parameter ϕ_i ($i = 1, 2, 3$) to test how well individual bursts being consistent with the closure relations under regime ($i = 1, 2, 3$):

$$\phi_i = \frac{|\alpha^{\text{obs}} - \alpha_i(\beta^{\text{obs}})|}{\sqrt{(\delta\alpha^{\text{obs}})^2 + [\delta\alpha_i(\beta^{\text{obs}})]^2}} \quad (7)$$

where α^{obs} and $\alpha_i(\beta^{\text{obs}})$ are the temporal decay slope from the observations and from the closure relations, and $\delta\alpha^{\text{obs}}$ and $\delta(\alpha_i(\beta^{\text{obs}}))$ represent their uncertainties. For an individual burst, if there existing $\phi_i < 3$, we conclude that this burst belongs to regime i model within $3 - \sigma$ significance. For those bursts that have more than one regimes satisfying $\phi_i < 3$, we choose the regime with smallest ϕ value.

Overall, we find that 66/198 bursts belong to regime 1, 82/198 bursts belong to regime 2, and 45/198 bursts belong to regime 3. For the other 5 bursts, we test their consistency with the curvature effect curve $\alpha = \beta + 2$ (Kumar & Panaitescu 2000; Panaitescu et al. 2006) with the ϕ parameter. We find that three bursts cannot be excluded within 3σ significance by curvature effect regime. These bursts could still be interpreted with external shock model once the jet break effect is invoked. We name regime 4 for these bursts. The other two bursts that could be excluded within 3σ significance by curvature effect regime are difficult to be interpreted under external shock framework. As suggested by many previous works, the early X-ray plateau for these cases should be of internal origin and is directly connected to a long-lasting central engine (Troja et al. 2007; Rowlinson et al. 2010, 2013, 2014; Dall'Osso et al. 2011; Lü & Zhang 2014; Lü et al. 2015; Gibson et al. 2017, 2018; Gompertz et al. 2013, 2014, 2015; Rea et al. 2015; Gompertz & Fruchter 2017; Stratta et al. 2018). We did not assign these bursts into either regime. Above all, we divided the GRBs of our sample into four groups, *case*¹, *case*², *case*³ and *case*⁴. Which case of each GRB in our sample belongs to and which regime is consistent with are listed in Table 2. The relationship of $\alpha_{X,2}$ and $\beta_{X,2}$ in difference cases are shown in Fig.5.

The normal decay phases for 196/198 bursts in our sample are consistent with the external-shock models, inferring that their shallow decay phase might also be of external origin and may be related to continuous energy injection from the central engine. Here we assume that the central engine has a power-law luminosity release history as $L(t) = L_0(\frac{t}{t_0})^{-q}$, so that the injected energy would be $E_{\text{inj}} = \frac{L_0 t_0^q}{1-q} t^{1-q}$ (Zhang & Mészáros (2001)). When E_{inj} is larger than the impulsively injected energy during the prompt emission phase, the dynamics of the external shock wave would be related to q as $\Gamma \propto t^{-\frac{q+2}{8}}$ ($\Gamma \propto t^{-\frac{q}{4}}$) and $R \propto t^{\frac{2-q}{4}}$ ($R \propto t^{\frac{2-q}{2}}$) for ISM (wind) case. Consequently, we have $\nu_m \propto t^{-1-q/2}(t^{-1-q/2})$, $\nu_c \propto t^{-1+q/2}(t^{1-q/2})$ and $F_{\nu, \text{max}} \propto t^{1-q}(t^{-q/2})$ for the ISM (wind) models for $p > 2$, and $\nu_m \propto t^{-\frac{(q+2)(p+2)}{8(p-1)}}(t^{\frac{4+pq}{4(1-q)}})$, $\nu_c \propto t^{-1+q/2}(t^{1-q/2})$ and $F_{\nu, \text{max}} \propto t^{1-q}(t^{-q/2})$ for the ISM (wind) models for $1 < p < 2$, where p is the electronic power law index, and $F_{\nu, \text{max}}$ is the observed peak flux. The relationship between decay slope α and energy injection index q for different spectral regimes could thus be derived (see results in Tables 13-16 of Gao et al. (2013)).

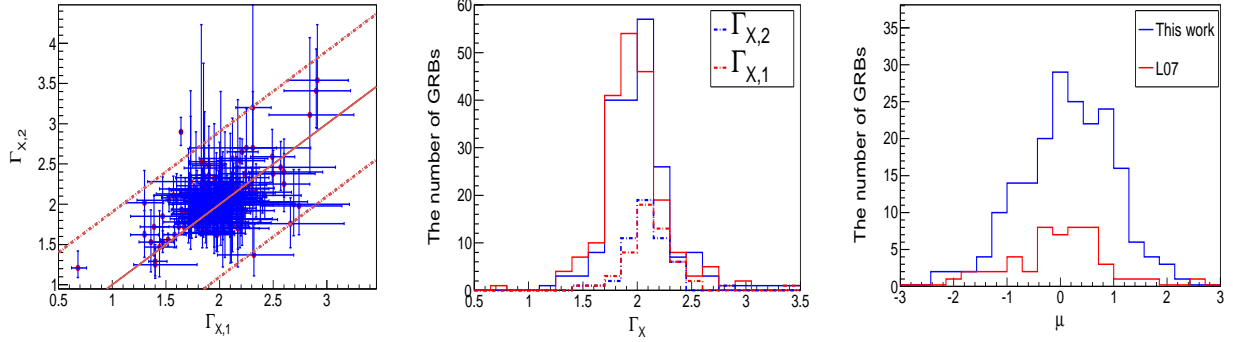


Figure 4. Left panel: Comparison between $\Gamma_{X,1}$ and $\Gamma_{X,2}$. The orange lines represent $\Gamma_{X,1} = \Gamma_{X,2}$ (solid) and its 2σ region (dotted). Middle panel: The distribution of $\Gamma_{X,1}$ and $\Gamma_{X,2}$, with solid lines showing our results and dotted lines showing L07's results. Right panel: The distribution of μ .

In this case, the decay indices difference between shallow decay segment and its follow-up segment in different regimes would be (Gao et al. 2013).

$$\begin{aligned}
 \Delta\alpha &= \frac{1}{16}(p+14)(1-q), \text{ regime 1, } 1 < p < 2 \\
 \Delta\alpha &= \frac{1}{16}(p+18)(1-q), \text{ regime 2, } 1 < p < 2 \\
 \Delta\alpha &= \frac{1}{8}(p+4)(1-q), \text{ regime 3, } 1 < p < 2 \\
 \Delta\alpha &= \frac{1}{4}(p+2)(1-q), \text{ regime 1, } p > 2 \\
 \Delta\alpha &= \frac{1}{4}(p+3)(1-q), \text{ regime 2, } p > 2 \\
 \Delta\alpha &= \frac{1}{4}(p+1)(1-q), \text{ regime 3, } p > 2
 \end{aligned} \tag{8}$$

where p could be derived from the observed spectral index, depending on the observed spectral regime. Given the regime models for each burst (here we only test bursts in regimes 1-3), its energy injection parameter q could be thus derived based on $\alpha_{X,1}$ and $\alpha_{X,2}$. The upper panels of Fig.6 shows the distributions of these GRBs in the two-dimensional q - $\Delta\alpha$ and q - p planes along with the contours of constant p and $\Delta\alpha$. The distribution of derived p and q values are plotted in the lower panels of Fig.6. We find that q values are mainly distributed between -0.5 and 0.5, with an average value of 0.16 ± 0.12 , which is well consistent with the model prediction (q -value around zero) where a spinning-down pulsar as the energy injection central engine (Dai & Lu 1998; Zhang & Mészáros 2001). With the derived q value, we can further test whether the $\alpha_{X,1}$ and $\beta_{X,1}$ satisfy the corresponding closure relations with energy injection (see Table 14 and 16 in Gao et al. (2013)) with ϕ parameter. It turns out the shallow decay phases for all 194 GRBs satisfy the closure relations with energy injection, and their corresponding spectral regime for 189/196 (96.4%) bursts are consistent with their follow-up phases, which is expected since there are no systematic spectral evolution between these two segments⁵. The results reinforce the conclusion that the shallow decay segment in most bursts is consistent with an external forward shock origin, probably due to a continuous energy injection from a long-lived central engine.

3.4. Empirical relations revisited

3.4.1. Empirical relation among E_{iso} , E'_p and t'_p

⁵ There are 7 GRBs (050401, 060413, 071118, 100508A, 100902A, 110411A and 161202A) whose shallow decay phase and normal decay phase belong to different spectral regimes. For GRBs 050401, 071118, 110411A, and 161202A, too few data points around t_b might cause bigger uncertainty for $\alpha_{X,2}$ and/or $\beta_{X,2}$. GRBs 060413, 100508A and 100902A marginally belongs to regime 3 but with a large decay slope for the normal decay phase.

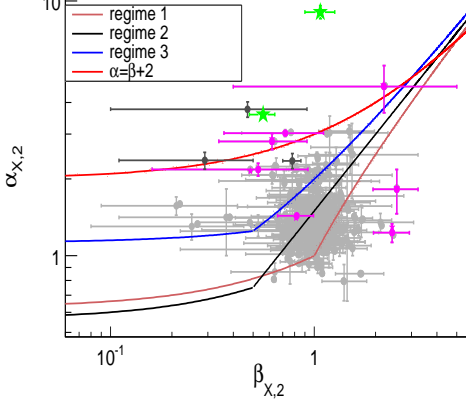


Figure 5. Temporal decay index $\alpha_{X,2}$ as a function of the spectral index $\beta_{X,2}$ for shallow decay's follow-up segment, compared with the closure correlations of various spectral regimes. The gray dots show GRBs belonging to regime 1-3(*case¹*). Pink dots show GRBs whose shallow decay segment and follow-up segment belongs to different spectrum regimes.(*case²*). Black dots show GRBs not belonging to regime 1-3 but cannot be excluded within 3σ significance by curvature effect regime(*case³*). Green dots show GRBs that could be excluded within 3σ significance by curvature effect(*case⁴*).

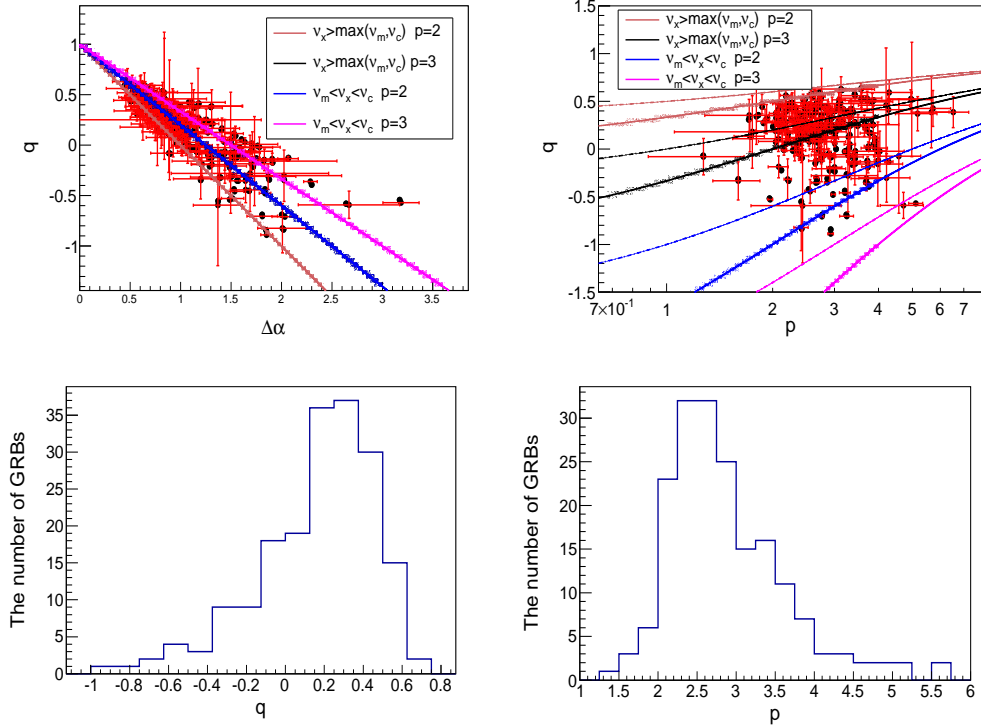


Figure 6. Upper panels: distributions of bursts in regimes 1-3 in the two-dimensional q - $\Delta\alpha$ and q - p planes, along with the model prediction for $v > \max(v_m, v_c)$ (thick solid lines) and $v_m < v < v_c$ (thin solid lines). Lower panels: distributions of p values and q values.

Based on their sample, L07 has investigated the relations among the energies $E_{\text{iso},X}$ and $E_{\text{iso},\gamma}$ and other parameters E'_p and t'_b , with a regression model as

$$\log_{10}(E_{\text{iso},(X,\gamma)}) = \kappa_0 + \kappa_1 \log_{10}(E'_p) + \kappa_2 \log_{10}(t'_b) \quad (9)$$

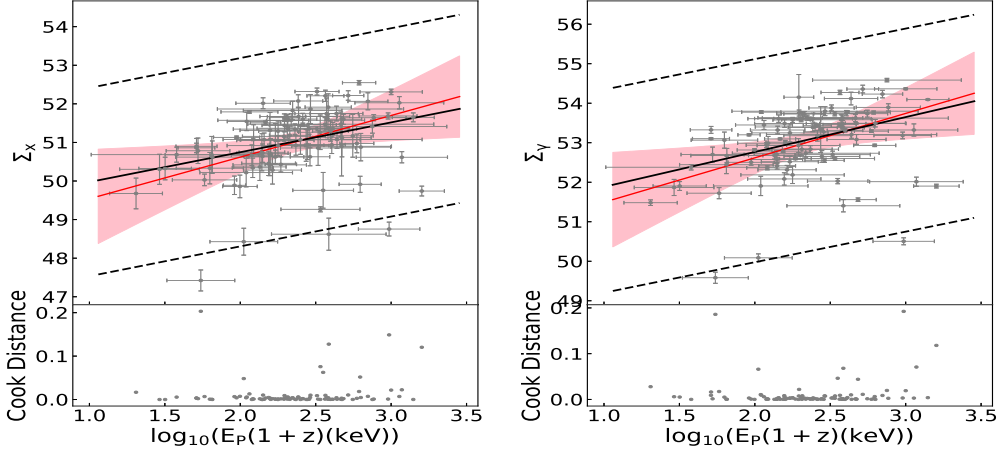


Figure 7. Left panel: the correlation between $\Sigma_X = \log_{10}(E_{\text{iso},X}) - \kappa_1 \log_{10}(t'_b)$ and E'_p . Right panel: the correlation between $\Sigma_\gamma = \log_{10}(E_{\text{iso},\gamma}^b) - \kappa_2 \log_{10}(t'_b)$ and E'_p . The black lines represent the best fitting results (solid) and its 3σ uncertainty region (dotted) with least square regression method. The red line presents the best fitting results with the bivariate linear regression method and the pink shadowed region show the intrinsic scatter to the population $3\sigma_{\text{int}}$.

where κ_0 , κ_1 and κ_2 are multiple regression coefficients. The probability from a t-test (p_t) was invoked to measure the significance of the dependence of each variable on the model and the probability from a F-test (p_F) was invoked to justify the global regression of the three parameter relation. For $E_{\text{iso},X} - E'_p - t'_b$ relation, L07 yields $\kappa_0 = 44.0 \pm 1.1$ ($p_t < 10^{-4}$) and $\kappa_1 = 1.82 \pm 0.33$ ($p_t < 10^{-4}$), $\kappa_2 = 0.61 \pm 0.18$ ($p_t < 3 \times 10^{-3}$), and the p_F is less than 10^{-4} . Their results suggest a strong correlation between $E_{\text{iso},X}$ and E'_p but a tentative correlation between $E_{\text{iso},X}$ and t'_b , and thus a tentative global 3-parameter correlation. We apply the regression model to our sample, we yield $\kappa_0 = 49.2 \pm 0.77$ ($p_t < 10^{-4}$), $\kappa_1 = 0.77 \pm 0.22$ ($p_t = 0.001$) and $\kappa_2 = -0.051 \pm 0.12$ ($p_t = 0.683$), with $p_F = 0.002$, $R^2 = 12.5\%$ and $p_{\text{AD}} = 0.555$. We find that with a larger sample, a strong correlation between $E_{\text{iso},X}$ and E'_p still exists but the tentative correlation between $E_{\text{iso},X}$ and t'_b is completely disappeared, so that the global 3-parameter correlation becomes less significant. Note that already in Dainotti et al. (2011b) it was clear that $E_{\text{iso},X} - t'_b$ was a weak correlation, while $L_{\text{peak}} - t'_b$ was a stronger correlation. Dainotti et al. (2016) thus proposed the $L_X - L_{\text{peak}} - t'_b$ correlation given the already established two-parameter $L_{\text{peak}} - t'_b$ (e.g. Dainotti et al. 2008) and $L_{\text{peak}} - L_X$ correlations (Dainotti et al. 2011b, 2015). With an extended sample (updated to July 2016) of long GRBs with X-ray plateau, Dainotti et al. (2017) yielded $\log_{10}L_X = (17.67 \pm 5.7) - (0.83 \pm 0.10)\log_{10}t'_b + (0.64 \pm 0.11)\log_{10}L_{\text{peak}}$, with the Pearson correlation coefficient $r = 0.90$ with a probability of the same sample occurring by chance, $P = 1.75 \times 10^{-17}$.

For $E_{\text{iso},\gamma} - E'_p - t'_b$ relation, L07 yields $\kappa_0 = 48.3 \pm 0.8$ ($p_t < 10^{-4}$) and $\kappa_1 = 1.7 \pm 0.25$ ($p_t < 10^{-4}$), $\kappa_2 = 0.07 \pm 0.13$ ($p_t = 0.486$), and the p_F is less than 10^{-4} . Their results suggest a strong correlation between $E_{\text{iso},\gamma}$ and E'_p but no correlation between $E_{\text{iso},\gamma}$ and t'_b . A tentative global 3-parameter correlation might exist. With a larger sample, we yield $\kappa_0 = 51 \pm 0.76$ ($p_t < 10^{-4}$), $\kappa_1 = 0.883 \pm 0.22$ ($p_t < 10^{-4}$), and $\kappa_2 = -0.19 \pm 0.12$ ($p_t = 0.11$), with $p_F < 10^{-4}$, $R^2 = 19.5\%$ and $p_{\text{AD}} = 0.403$. We confirm that a strong correlation between $E_{\text{iso},\gamma}$ and E'_p and a tentative global 3-parameter correlation exist and there is no correlation between $E_{\text{iso},\gamma}$ and t'_b . The data and regression modeling results are shown in Fig.7. It is worth noticing that Dainotti et al. (2011b) also investigated the $E_{\text{iso},\gamma}^b - t'_b$ relation with 62 long GRBs with known redshift, and the correlation coefficient and the random occurrence probability p for their sample are $r = -0.19$ and $p = 0.1$, also inferring that the correlation between $E_{\text{iso},\gamma}$ and t'_b was very weak.

3.4.2. Revisit correlations between t'_b (t_b), L_X and $E_{\text{iso},\gamma}$

Dainotti et al. (2008) discovered a formal anti-correlation between X-ray luminosity at the end of plateau L_X and rest frame plateau end time t'_b , described as $\log_{10}(L_X) = \kappa_0 + \kappa_1 \log_{10}(t'_b)$. Dainotti et al. (2010) fitted the correlation between L_X and t'_b and achieved the results $\kappa_0 = 51.06 \pm 1.02$, $\kappa_1 = -1.06^{+0.27}_{-0.28}$. It is of interest to justify this empirical relationship with our updated sample. With multivariate linear regression method, we find that the anti-correlation indeed exist between L_X and t'_b , with $\kappa_0 = 50.7 \pm 0.39$ ($p_t < 10^{-4}$) and $\kappa_1 = -1.15 \pm 0.1$ ($p_t < 10^{-4}$), where $p_F < 10^{-4}$, $R^2 = 54.9\%$ and $p_{\text{AD}} = 0.262$. In addition, the L_X for individual GRB in our sample are listed in Table 3. Basically

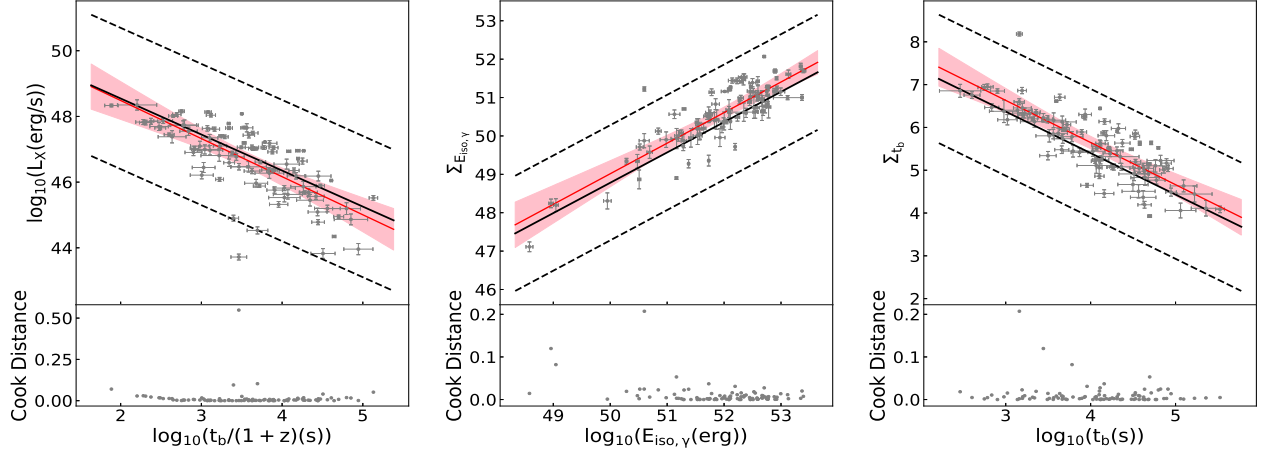


Figure 8. Left panel: the correlation between L_X and t'_b . Middle panel: the correlation between $\Sigma_{E_{\text{iso},\gamma}} = \log_{10}(L_X) - \kappa_1 \log_{10}(t_b)$ and $E_{\text{iso},\gamma}$. Right panel: the correlation between $\Sigma_{t_b} = \log_{10}(L_X) - \kappa_2 \log_{10}(E_{\text{iso},\gamma})$ and t_b . The black lines represent the best fitting results (solid) and its 3σ uncertainty region (dotted) with least square regression method. The red line presents the best fitting results with the bivariate linear regression method and the pink shadowed region show the intrinsic scatter to the population $3\sigma_{\text{int}}$.

speaking, our results in general agree well with Dainotti et al. (2013b), indicating that an intrinsic relationship between L_X and (t'_b) indeed exist. This correlation has been tested against selection bias robustly (Dainotti et al. 2013b). It is worth noticing that L_X is roughly inversely proportional to the timescale of the energy injection, inferring that the energy reservoir should be roughly a constant. This is consistent with the energy injection model, where the central engine is a newborn magnetars (Dai 2004).

Xu & Huang (2012) introduced a third parameter $E_{\text{iso},\gamma}$ to the above relation (and replacing t'_b by t_b) and claimed that the three-parameter correlation would be tighter. The relation could be expressed as $L_X = \kappa_0 + \kappa_1 \log_{10}(t_b) + \kappa_2 \log_{10}(E_{\text{iso},\gamma})$, with $\kappa_0 = 4.14$, $\kappa_1 = -0.87$ and $\kappa_2 = 0.88$. We have also justified this empirical relationship with our updated sample. With multiple regression analysis methods, we find that the three-parameter correlation indeed exist, with $\kappa_0 = 9.26 \pm 2.59$ ($p_t < 10^{-4}$), $\kappa_1 = -0.97 \pm 0.07$ ($p_t < 10^{-4}$) and $\kappa_2 = 0.79 \pm 0.05$ ($p_t < 10^{-4}$), where $p_F < 10^{-4}$, $R^2 = 73.3\%$ and $p_{AD} = 0.372$. The data and fitting results regarding this relationship are shown in Fig.8. It is interesting to note that besides the Xu & Huang (2012) correlation, more recently Dainotti et al. (2016, 2017) showed that the $L_X - L_{\text{peak}} - t'_b$ correlation is 37% tighter than the Xu & Huang (2012) correlation, making the $L_X - L_{\text{peak}} - t'_b$ correlation the tightest correlation in the literature so far involving the plateau emission.

4. CONCLUSIONS AND DISCUSSION

With Swift/XRT light curves of GRBs between February 2004 and July 2017, we revisit the analysis of shallow decay component from Liang et al. (2007). Our results and the comparison with L07's results are summarized as follows:

- We find that with a larger sample, the distributions of the characteristic properties of the shallow decay phase (e.g. t_b , S_X , $\Gamma_{X,1}$, and $\alpha_{X,1}$) still accords with normal or lognormal distribution with $\log_{10}(t_b) = 4 \pm 0.72$, $\log_{10}(S_X(\text{ergs cm}^{-2})) = -6.97 \pm 0.56$, $\Gamma_{X,1} = 1.96 \pm 0.26$ and $\alpha_{X,1} = 0.43 \pm 0.22$. Comparing with L07's results, the distributions for all the parameters become slightly broader but the peaks of each distribution barely change.
- We find that with a larger sample, $\Gamma_{X,1}$ and Γ_γ still show no correlation, with $\Gamma_{X,1}$ systemically larger than Γ_γ . The tentative correlations of durations, energy fluences, and isotropic energies between the gamma-ray and X-ray phases still exist, but all correlations become significantly weaker than L07's results.
- We find that for most GRBs, there is no significant spectral evolution between the shallow decay segment and its follow-up segment, and the follow-up segment for most bursts in our sample are consistent with the external-shock models. These two findings are consistent with L07's results, which infer that the shallow decay phase for most GRBs should be of external origin and may be related to continuous energy injection from the central engine.

- Assuming that the central engine has a power-law luminosity release history as $L(t) = L_0(\frac{t}{t_0})^{-q}$, we find that q values are mainly distributed between -0.5 and 0.5, with an average value of 0.16 ± 0.12 , which is consistent with L07's results and is well consistent with the model prediction (q-value around zero) where a spinning-down pulsar as the energy injection central engine (Dai & Lu 1998; Zhang & Mészáros 2001). With the derived q value, we find that the shallow decay phases for 196/198 GRBs satisfy the closure relations with energy injection, and their corresponding spectral regime for most bursts (96.4%) is consistent with their follow-up phases.
- We find that with a larger sample, L07 suggested correlation between $E_{\text{iso},X}$ and E'_p still exists but the tentative correlation between $E_{\text{iso},X}$ and t'_b is completely disappeared, so that the global 3-parameter correlation becomes less significant. On the other hand, we confirm that a strong correlation between $E_{\text{iso},\gamma}$ and E'_p and a tentative global 3-parameter correlation ($E_{\text{iso},\gamma} - E'_p - t'_b$) exist but there is no correlation between $E_{\text{iso},\gamma}$ and t'_b .
- We find that the anti-correlation indeed exist between L_X and (t'_b) (as suggested by Dainotti et al. (2008)), with $\kappa_0 = 50.7 \pm 0.39$ ($p_t < 10^{-4}$) and $\kappa_1 = -1.15 \pm 0.1$ ($p_t < 10^{-4}$), where the p_F is less than 10^{-4} . Xu & Huang (2012) introduced three-parameter correlation by involving $E_{\text{iso},\gamma}$ into the above relation (and replacing t'_b by t_b) and we find that with our updated sample, the three-parameter correlation indeed exist, with $\kappa_0 = 9.26 \pm 2.59$ ($p_t < 10^{-4}$), $\kappa_1 = -0.97 \pm 0.07$ ($p_t < 10^{-4}$) and $\kappa_2 = 0.79 \pm 0.05$ ($p_t < 10^{-4}$), where the p_F is $p_F < 10^{-4}$. More recently Dainotti et al. (2016, 2017) showed that the $L_X - L_{\text{peak}} - t'_b$ correlation is 37% tighter than the Xu & Huang (2012) correlation, making the $L_X - L_{\text{peak}} - t'_b$ correlation the tightest correlation in the literature involving plateau emission. In addition, we note that this correlation is the results of two correlation which have been tested for selection bias.

In conclusion, with an updated sample, our results are consistent with most of L07's results and confirm their suggestion that the shallow decay segment in most bursts is consistent with an external forward shock origin, probably due to a continuous energy injection from a long-lived central engine.

This work was supported by the National Natural Science Foundation of China (under Grant No. 11722324, 11603003, 11633001, 11690024, 11603006), and the Strategic Priority Research Program of the Chinese Academy of Sciences (Grant No. XDB23040100). L. H. J. acknowledges support by the GuangXi Science Foundation (grant Nos. 2017GXNSFFA198008 and 2016GXNSFCB380005), the One-Hundred-Talents Program of GuangXi colleges, and Bagui Young Scholars Program of GuangXi. BBZ acknowledges support from National Thousand Young Talents program of China and National Key Research and Development Program of China (2018YFA0404204) and The National Natural Science Foundation of China (Grant No. 11833003).

Software: XSPEC([Arnaud \(1996\)](#)), HEAsoft(v6.12;[Nasa High Energy Astrophysics Science Archive Research Center \(Heasarc\)](#)), root(v5.34;[Brun & Rademakers \(1997\)](#)), Linmix_err([Kelly \(2007\)](#))

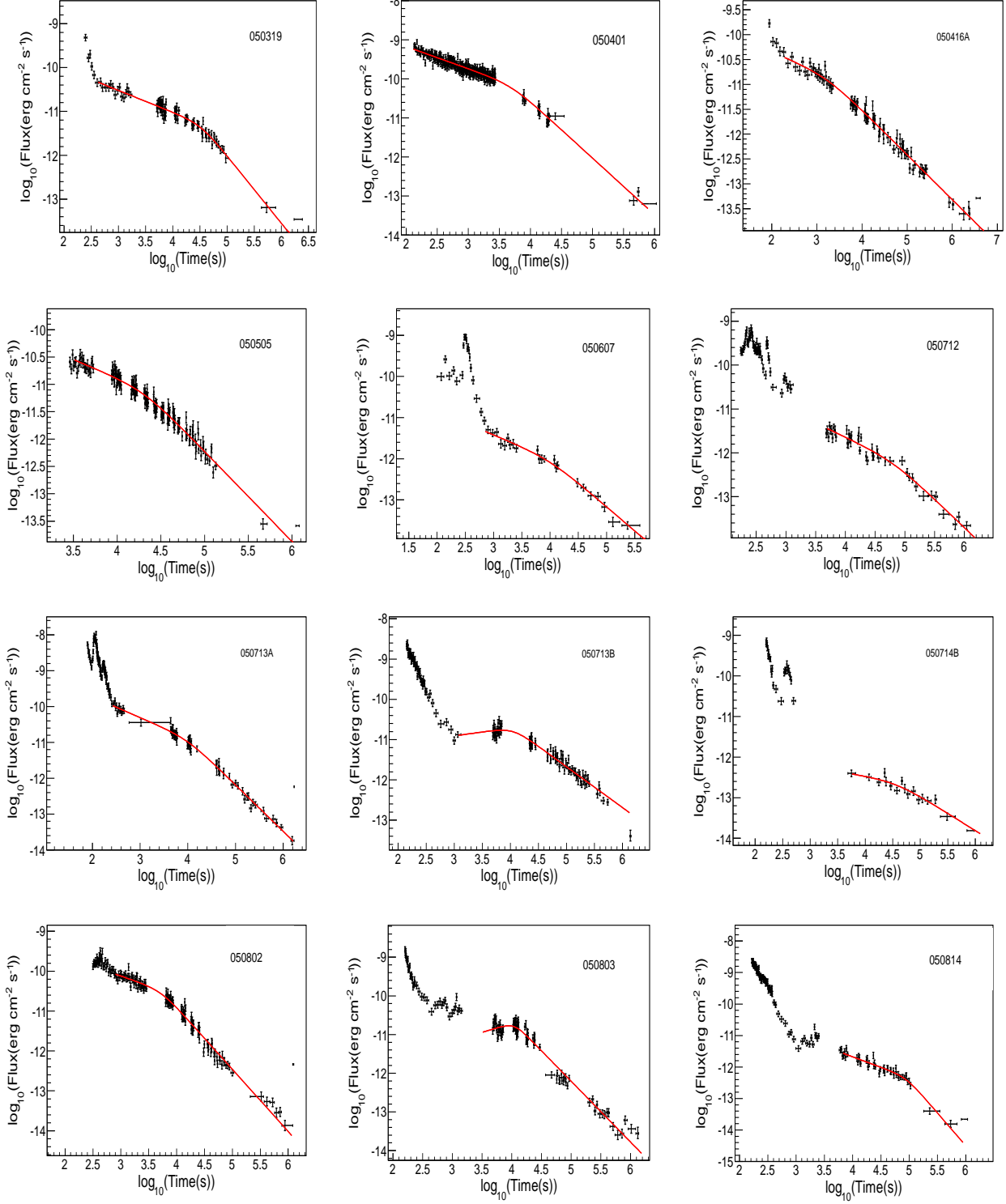


Figure 1. XRT light curves for the bursts in our sample. The solid red lines are the best fits with a smooth broken power law for the shallow decay phase and its follow-up decay phase.

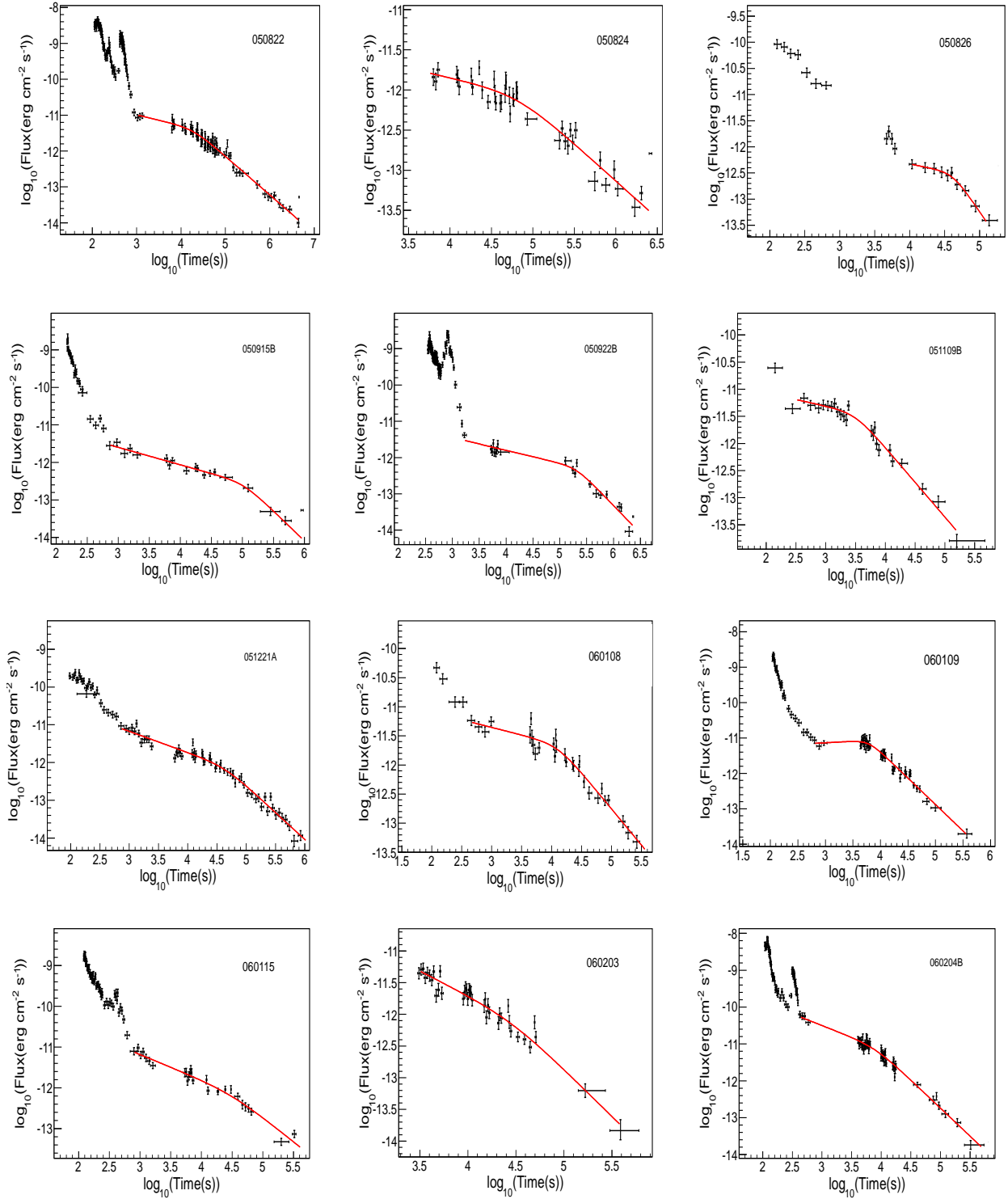
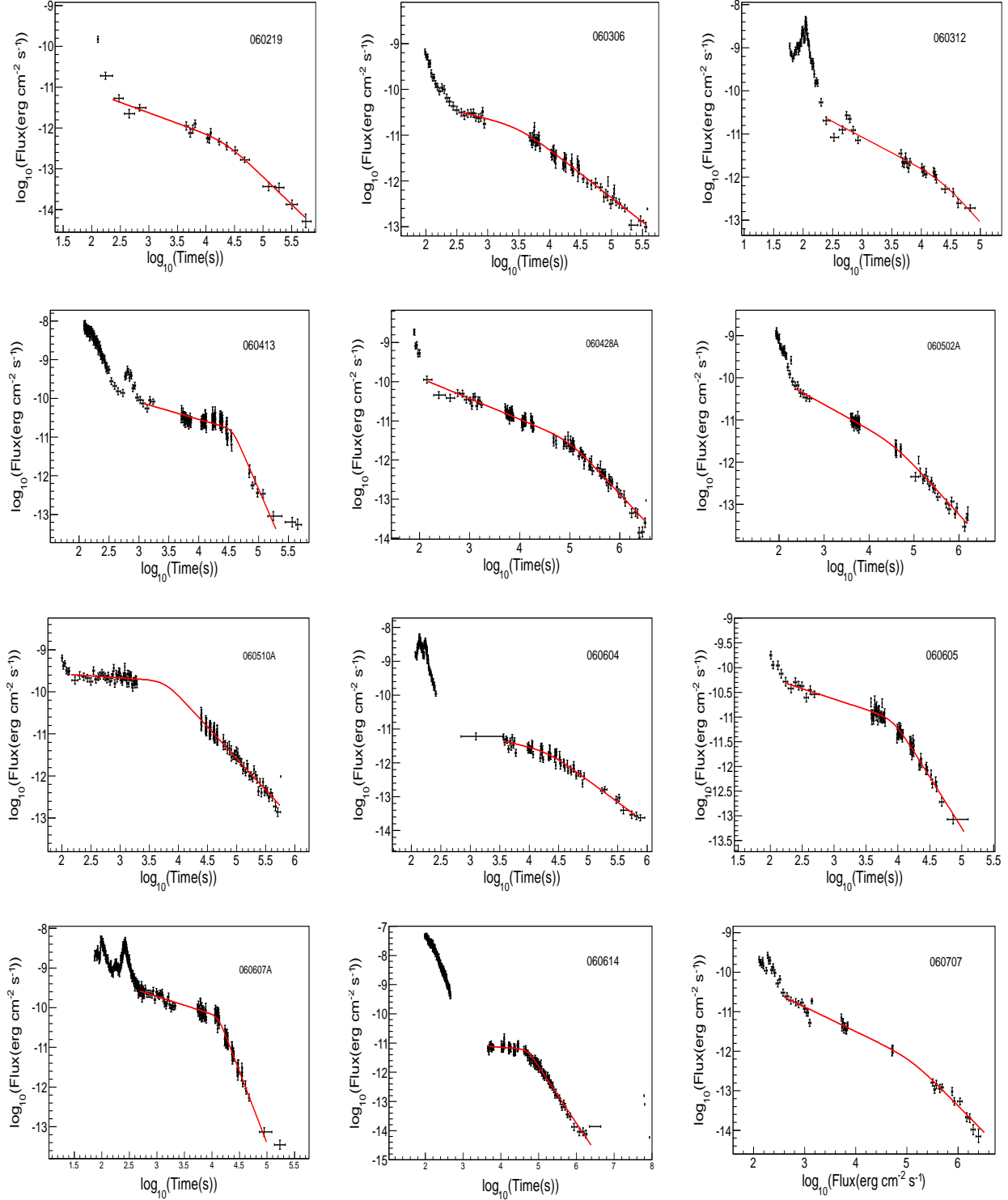
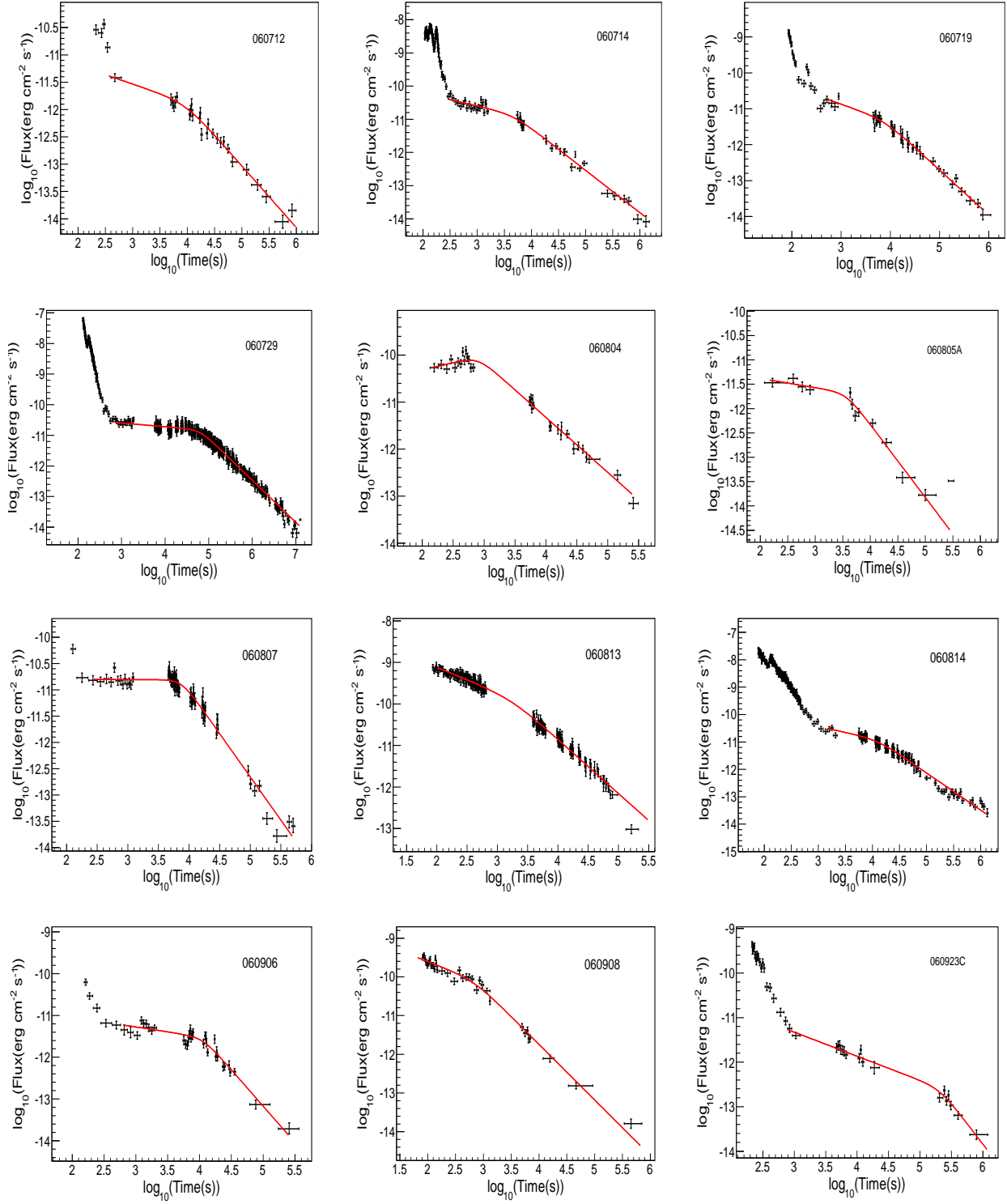
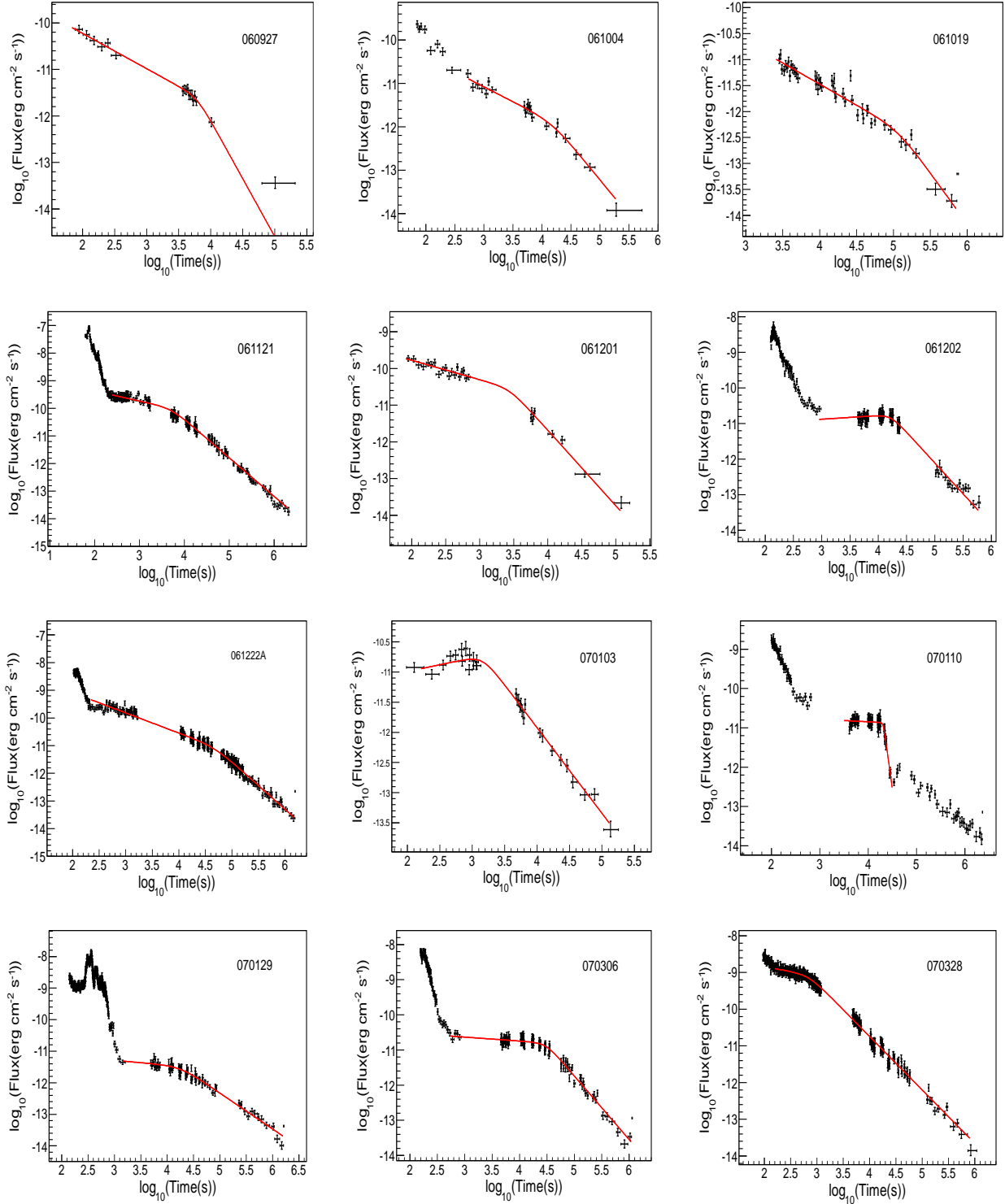
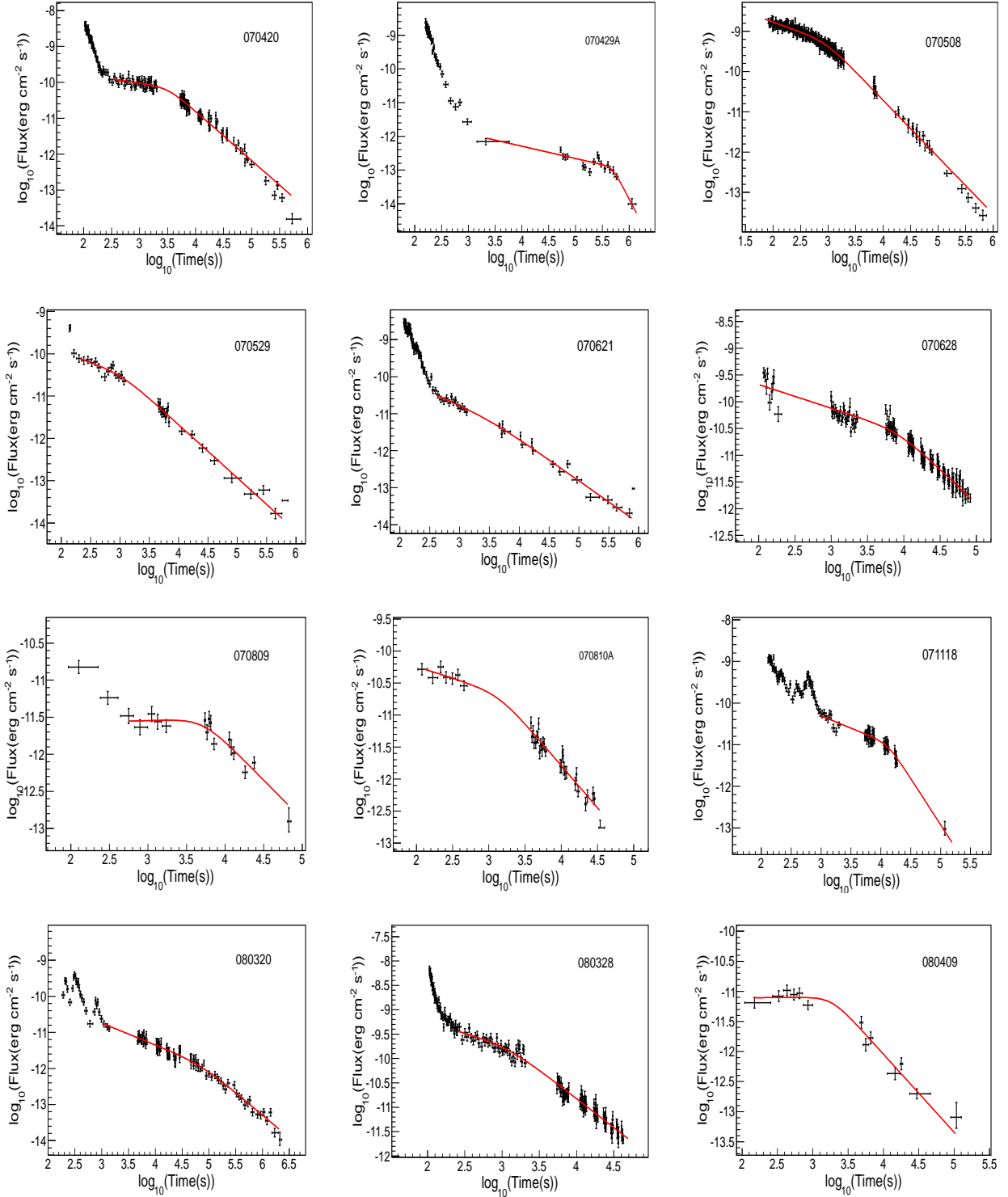


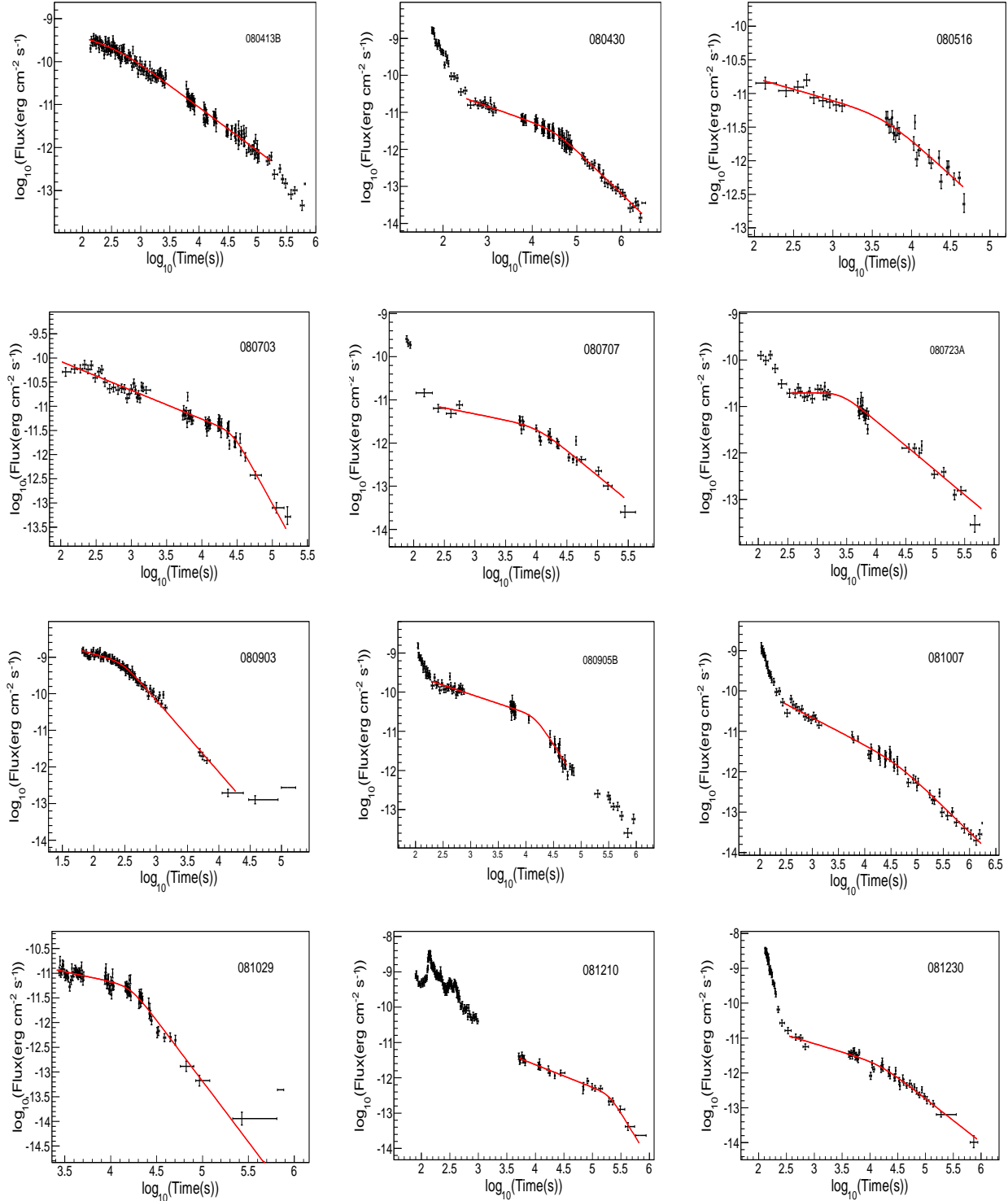
Figure 1. Continued.

**Figure 1.** Continued.

**Figure 1.** Continued.

**Figure 1.** Continued.

**Figure 1.** Continued.

**Figure 1.** Continued.

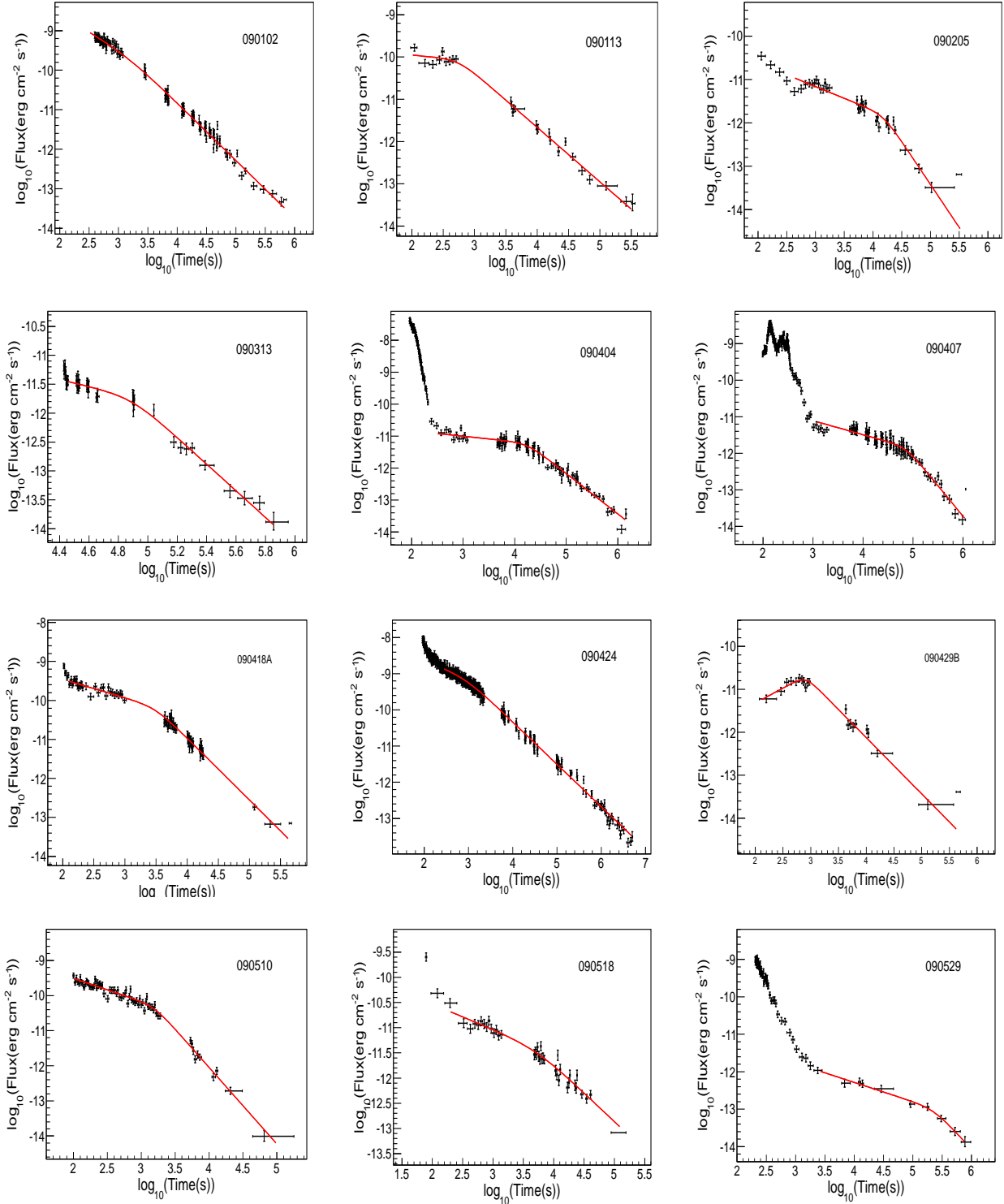
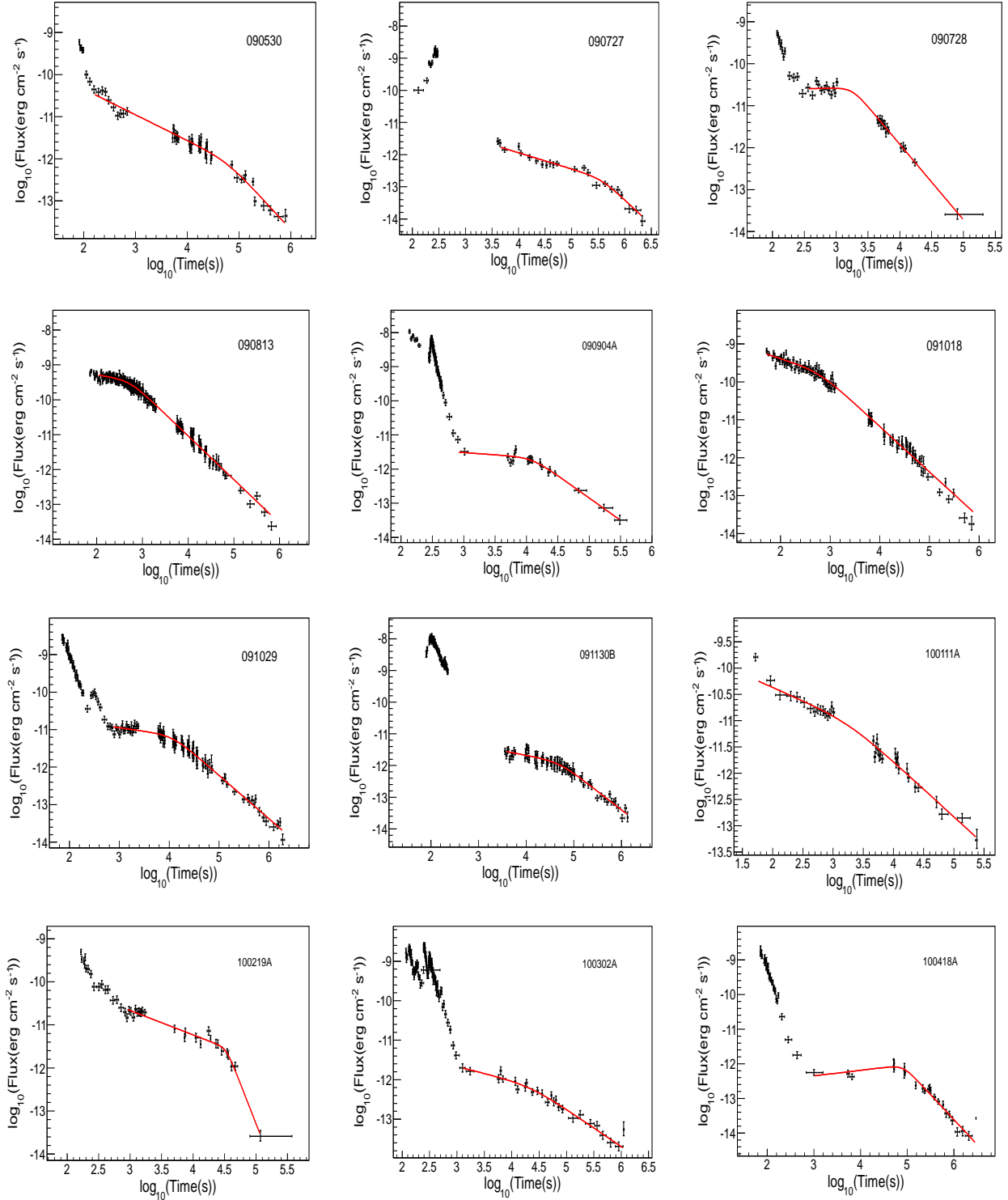


Figure 1. Continued.

**Figure 1.** Continued.

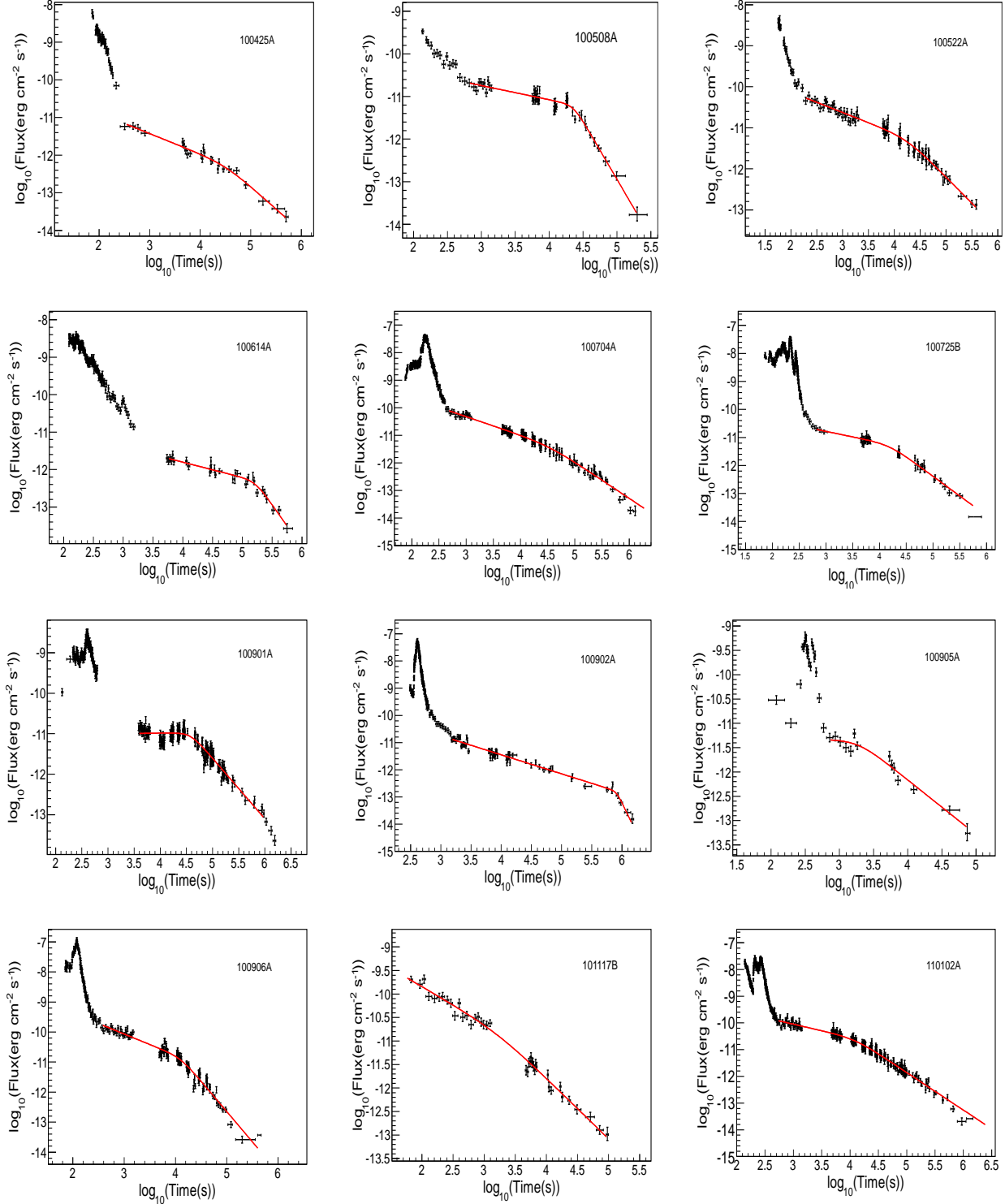
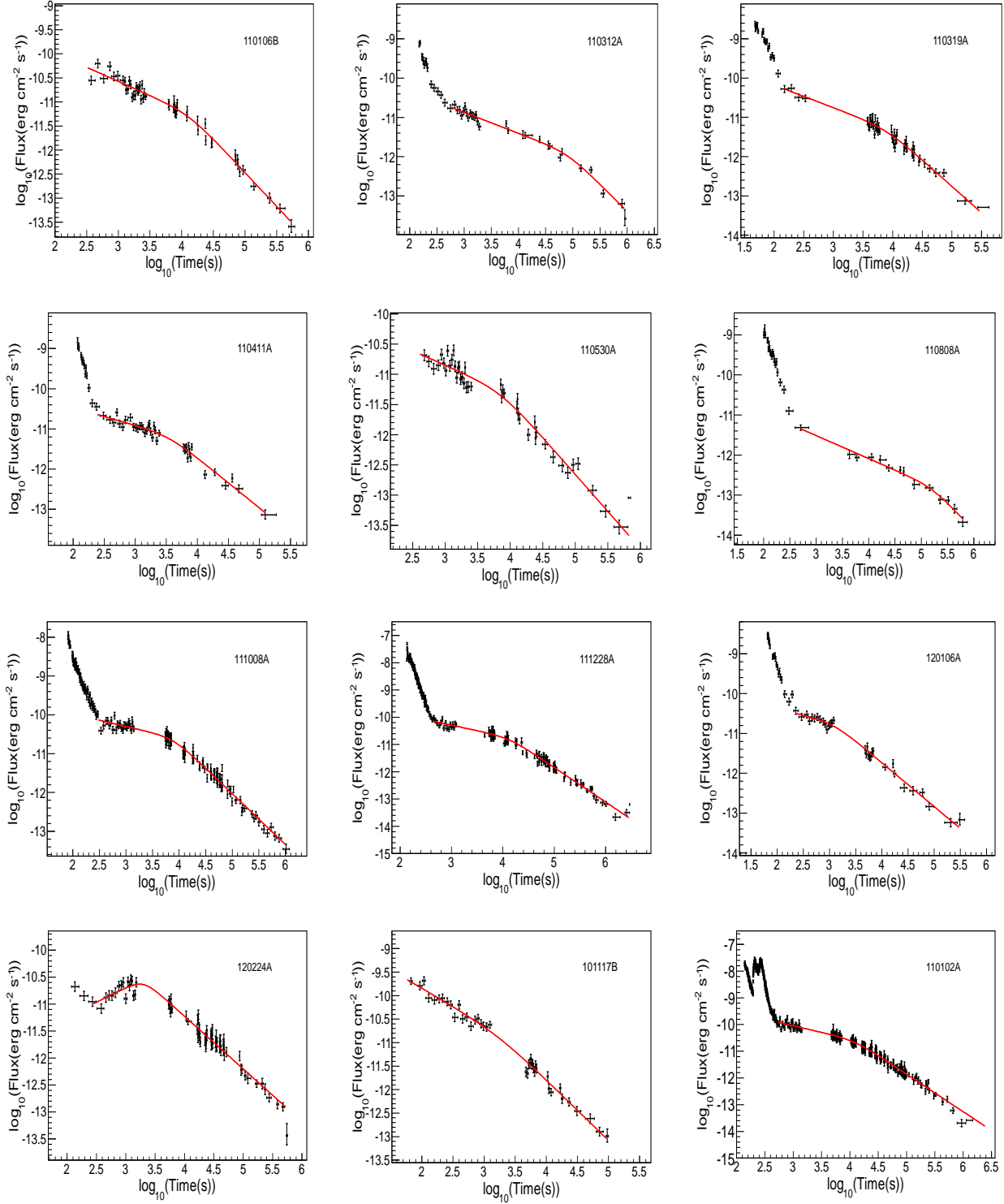
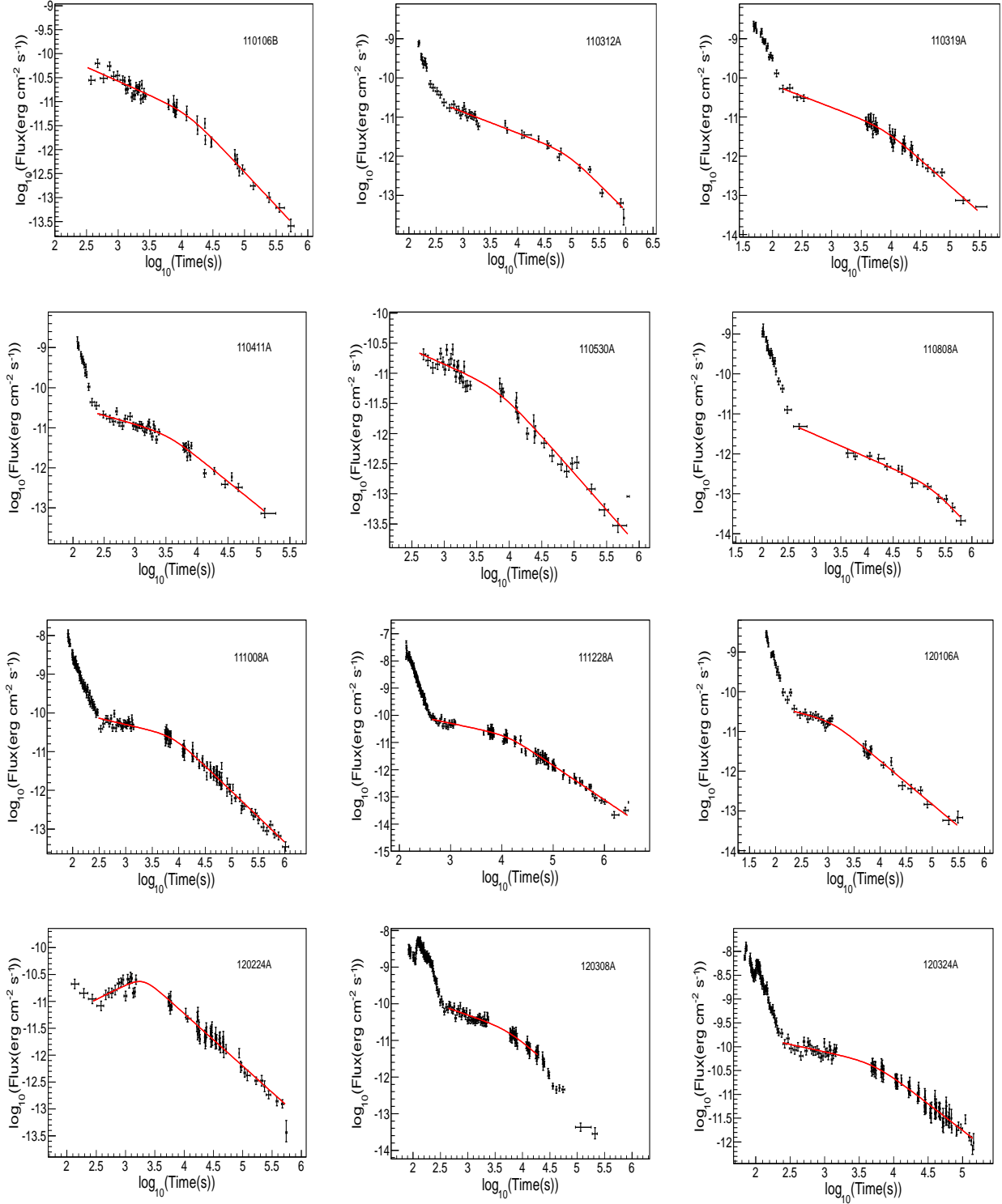


Figure 1. Continued.

**Figure 1.** Continued.

**Figure 1.** Continued.

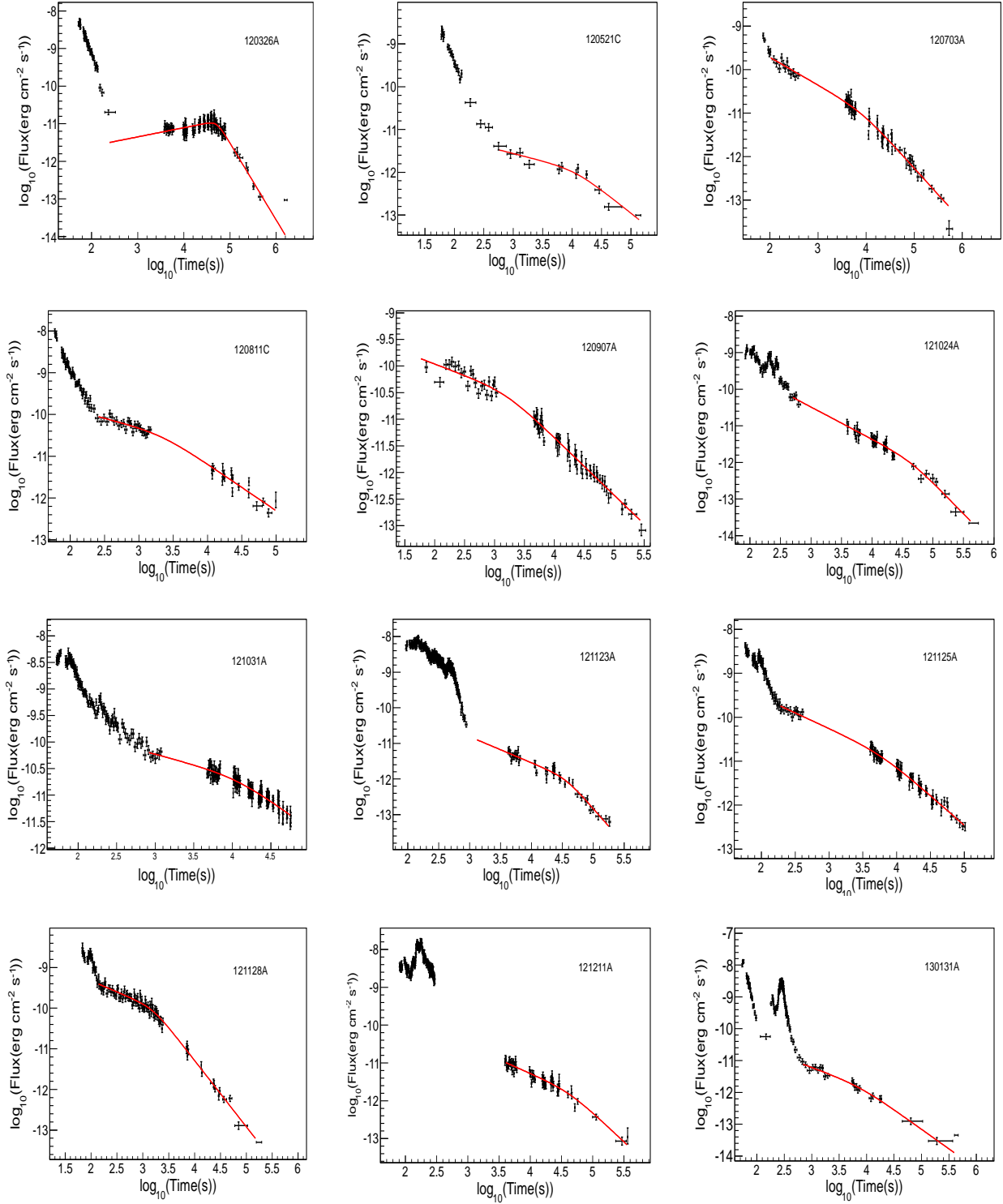
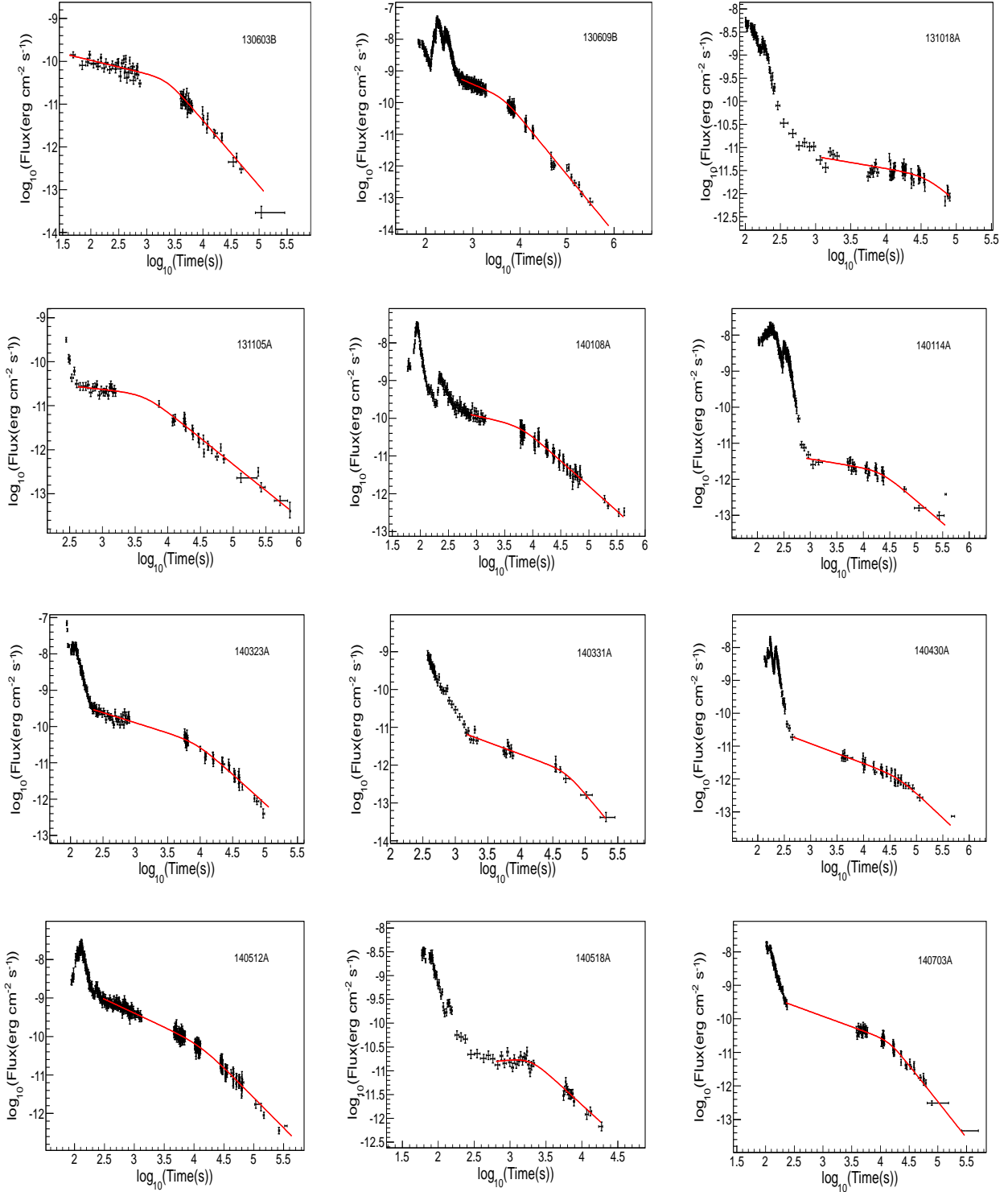


Figure 1. Continued.

**Figure 1.** Continued.

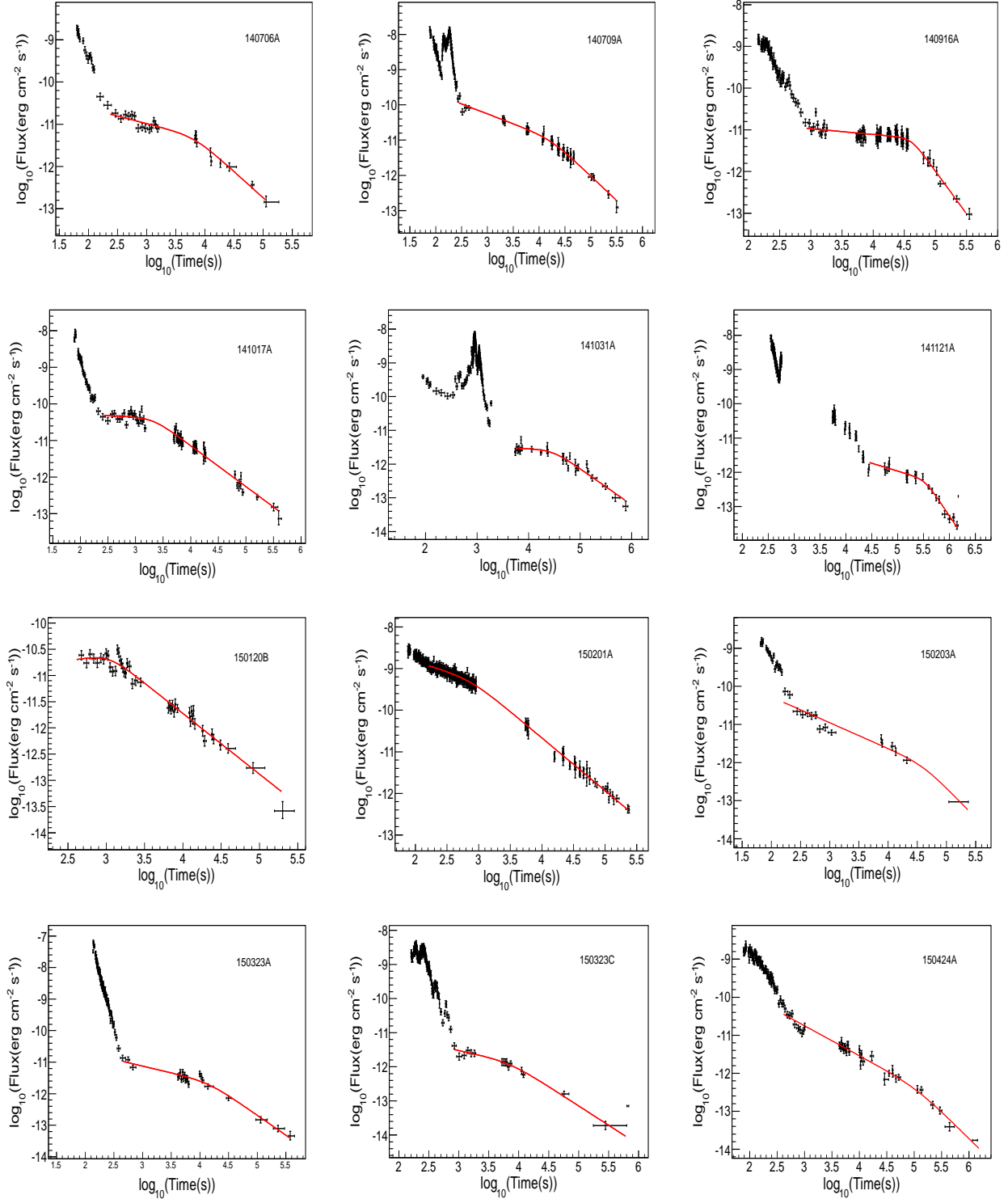


Figure 1. Continued.

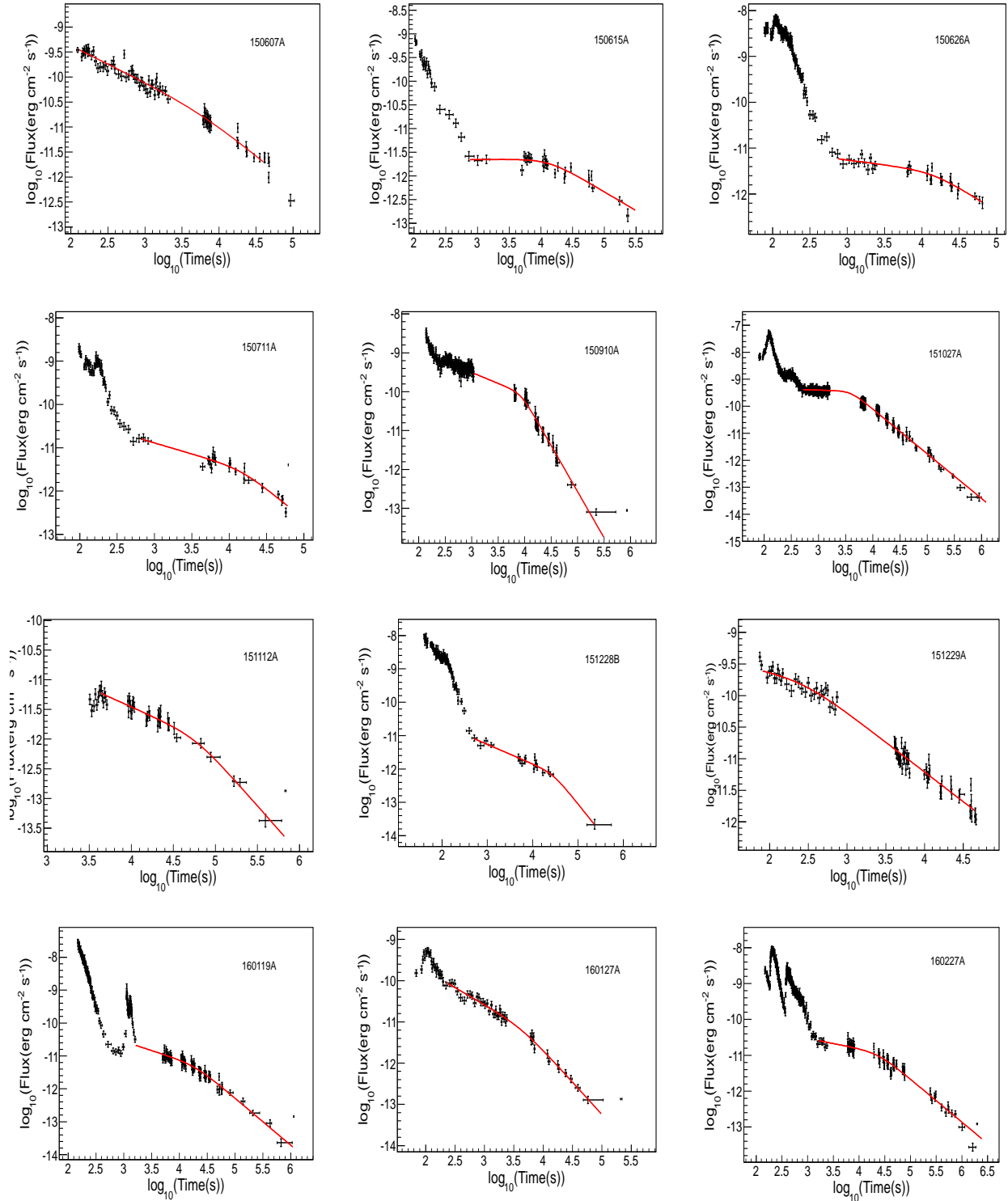
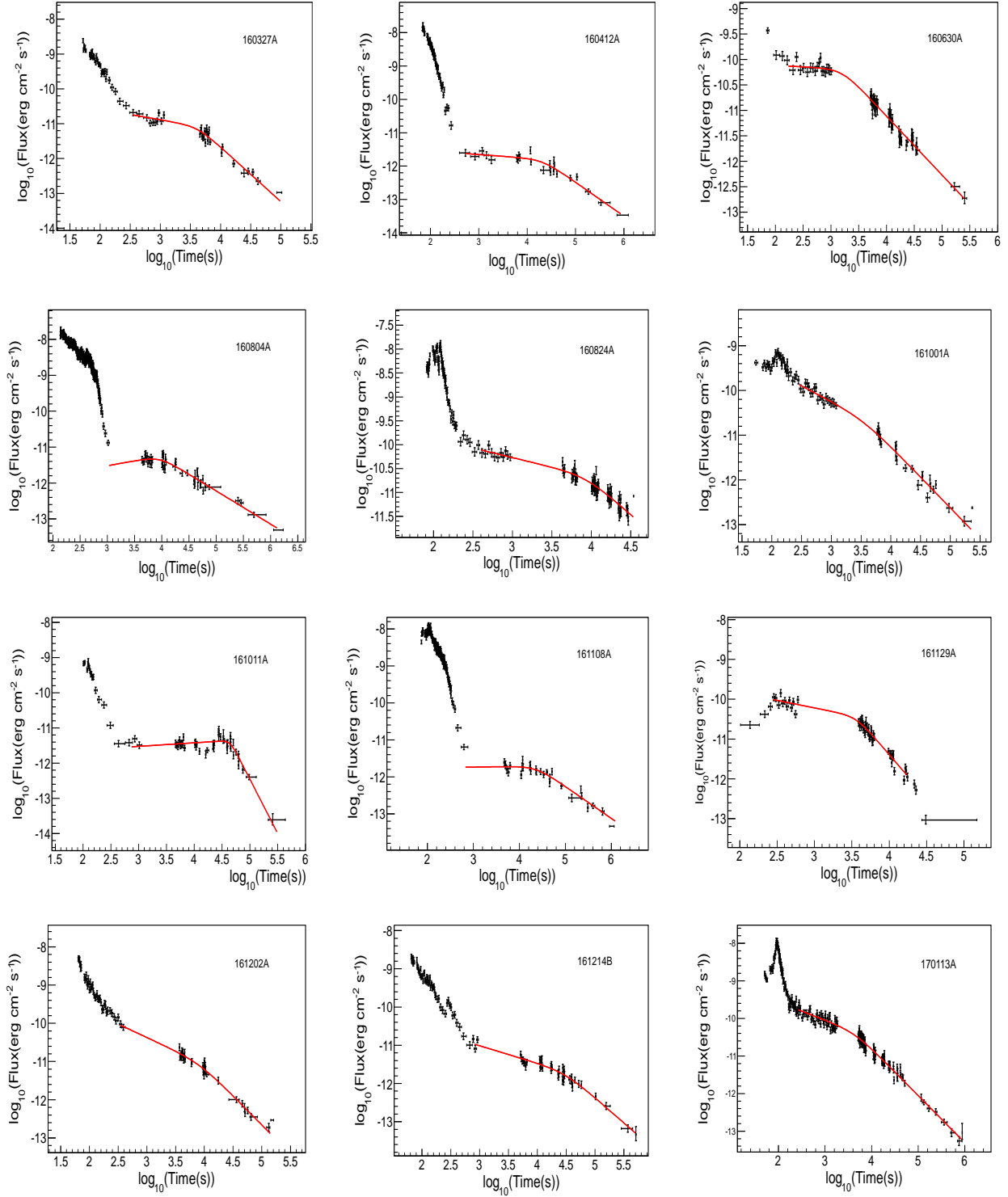


Figure 1. Continued.

**Figure 1.** Continued.

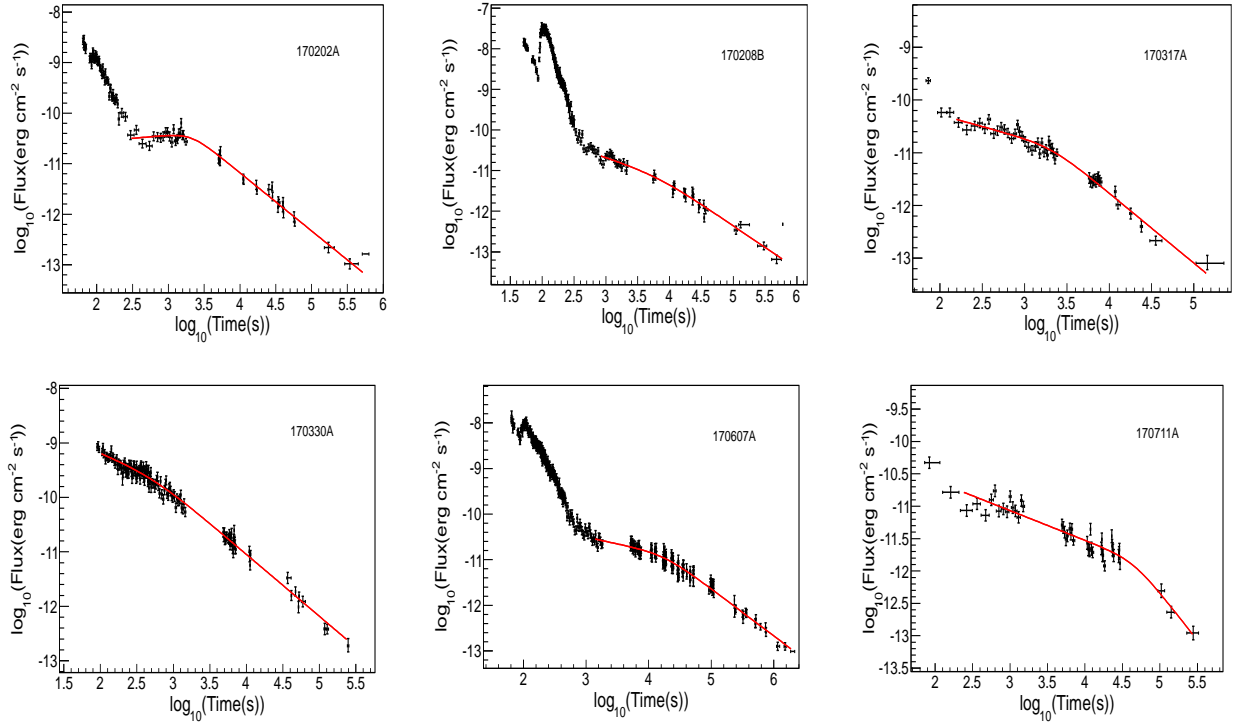


Figure 1. Continued.

Table 1. Part I. XRT observations and fitting results for our sample

GRBname	$\log_{10}(t_1)$ ^a	$\log_{10}(t_2)$ ^a	$\log_{10}(t_b)$ ^b	$\alpha_{X,1}$ ^b	$\alpha_{X,2}$ ^b	χ^2/dof ^b	S_X ^c	$\Gamma_{X,1}$ ^d	$\Gamma_{X,2}$ ^d
	s	s	s				$10^{-7} \text{ ergs cm}^{-2}$		
050319	2.61	6.32	4.52	0.5 ± 0.03	1.54 ± 0.11	96.98/91	3.1 ± 0.46	$1.89^{+0.08}_{-0.07}$	$2.12^{+0.18}_{-0.17}$
050401	2.1	5.91	3.67	0.55 ± 0.02	1.43 ± 0.04	429.9/317	6.51 ± 0.8	1.91 ± 0.04	$1.82^{+0.17}_{-0.16}$
050416A	2.26	6.77	3.22	0.39 ± 0.1	0.9 ± 0.02	111.4/91	0.31 ± 0.15	$1.98^{+0.21}_{-0.2}$	$2.08^{+0.15}_{-0.14}$
050505	3.5	6.2	4.31	0.68 ± 0.07	1.65 ± 0.06	233.1/188	2.32 ± 0.57	$1.97^{+0.09}_{-0.08}$	$2.01^{+0.09}_{-0.08}$
050607	2.84	6.21	3.99	0.57 ± 0.1	1.17 ± 0.08	19.9/20	0.15 ± 0.11	$1.71^{+0.21}_{-0.16}$	$2.17^{+0.52}_{-0.43}$
050712	3.68	6.19	4.82	0.65 ± 0.07	1.3 ± 0.1	75.22/41	0.74 ± 0.47	$2.04^{+0.19}_{-0.15}$	$1.85^{+0.35}_{-0.18}$
050713A	2.41	6.23	3.99	0.58 ± 0.03	1.29 ± 0.03	97.41/79	2.43 ± 0.64	$1.9^{+0.19}_{-0.18}$	$2.18^{+0.18}_{-0.17}$
050713B	3.06	6.14	4.04	-0.2 ± 0.1	1.02 ± 0.03	151/107	1.72 ± 0.22	$2.03^{+0.15}_{-0.14}$	1.83 ± 0.13
050714B	3.75	5.89	4.56	0.22 ± 0.29	0.85	17.6/11	0.1 ± 0.05	$2.25^{+0.6}_{-0.53}$	$2.7^{+0.49}_{-0.43}$
050802	2.89	6.08	3.72	0.48 ± 0.07	1.56 ± 0.02	208.4/143	2.18 ± 0.31	$1.65^{+0.1}_{-0.09}$	1.88 ± 0.08
050803	3.5	6.2	4.04	-0.46 ± 0.13	1.57 ± 0.02	307.2/104	1.51 ± 0.14	1.8 ± 0.14	2.07 ± 0.11
050814	3.82	5.96	4.95	0.67 ± 0.05	2.08 ± 0.16	44.62/40	0.76 ± 0.15	1.98 ± 0.16	$1.62^{+0.24}_{-0.14}$
050822	3.02	6.66	4.27	0.29 ± 0.07	1.08 ± 0.03	131.8/91	1 ± 0.23	$1.9^{+0.16}_{-0.15}$	$2.06^{+0.13}_{-0.12}$
050824	3.75	6.41	4.82	0.24 ± 0.1	0.93 ± 0.08	67.98/37	0.67 ± 0.34	$2.12^{+0.34}_{-0.31}$	$2.04^{+0.18}_{-0.17}$
050826	4.03	5.1	4.61	0.27 ± 0.33	1.96 ± 0.71	1.045/5	0.12 ± 0.06	$1.73^{+0.49}_{-0.4}$	$2.28^{+0.81}_{-0.66}$
050915B	2.86	5.97	5.03	0.46 ± 0.04	1.6 ± 0.28	10.68/14	0.53 ± 0.19	$2.16^{+0.34}_{-0.32}$	$1.99^{+0.6}_{-0.26}$
050922B	3.22	6.37	5.31	0.35 ± 0.05	1.53 ± 0.12	36.68/16	1.65 ± 10.43	$2.34^{+0.33}_{-0.31}$	$2.15^{+0.35}_{-0.31}$
051109B	2.51	5.2	3.5	0.24 ± 0.13	1.28 ± 0.07	21.88/19	0.13 ± 0.04	$2.2^{+0.34}_{-0.32}$	$1.81^{+0.35}_{-0.16}$
051221A	2.86	6.03	4.63	0.56 ± 0.04	1.43 ± 0.07	92.32/55	0.66 ± 0.15	1.91 ± 0.15	$1.89^{+0.24}_{-0.22}$
060108	2.66	5.57	4.11	0.26 ± 0.06	1.25 ± 0.08	46.49/25	0.36 ± 0.1	$1.99^{+0.34}_{-0.31}$	$2.12^{+0.3}_{-0.27}$
060109	2.8	5.57	3.79	-0.08 ± 0.07	1.49 ± 0.05	66.51/48	0.44 ± 0.05	$1.84^{+0.25}_{-0.24}$	$2.23^{+0.21}_{-0.20}$
060115	2.9	5.62	4.5	0.62 ± 0.05	1.2 ± 0.12	39.9/23	0.48 ± 0.28	$2.17^{+0.15}_{-0.13}$	$2.16^{+0.31}_{-0.20}$
060203	3.5	5.59	4.46	0.77 ± 0.15	1.49 ± 0.22	55.94/34	0.08 ± 0.7	$2.06^{+0.2}_{-0.19}$	$2.09^{+0.41}_{-0.28}$
060204B	2.63	5.8	3.9	0.63 ± 0.06	1.52 ± 0.05	79.3/59	1.23 ± 0.27	2.03 ± 0.11	$2.25^{+0.4}_{-0.35}$
060219	2.35	5.75	4.35	0.51 ± 0.05	1.35 ± 0.11	13.94/14	0.19 ± 0.08	$2.84^{+0.41}_{-0.38}$	$3.11^{+0.96}_{-0.72}$
060306	2.57	5.58	3.51	0.31 ± 0.14	1.06 ± 0.03	94.32/76	0.58 ± 0.33	$1.76^{+0.27}_{-0.25}$	2.1 ± 0.13
060312	2.39	5.46	4.37	0.72 ± 0.07	1.56 ± 0.46	54.06/21	0.5 ± 0.37	$1.95^{+0.15}_{-0.12}$	$1.68^{+0.28}_{-0.21}$
060413	3.07	5.3	4.41	0.17 ± 0.05	3.03 ± 0.1	393.1/145	7.16 ± 0.55	$1.39^{+0.14}_{-0.13}$	$1.72^{+0.39}_{-0.36}$
060428A	2.15	6.52	4.98	0.53 ± 0.02	1.37 ± 0.05	170/141	6.48 ± 1.15	$1.95^{+0.14}_{-0.13}$	$1.92^{+0.2}_{-0.19}$
060502A	2.35	6.2	4.57	0.59 ± 0.03	1.18 ± 0.05	64.41/62	2.22 ± 0.67	1.89 ± 0.13	$1.83^{+0.17}_{-0.16}$
060510A	2.14	5.76	3.77	0.09 ± 0.05	1.5 ± 0.02	196.2/158	11.4 ± 1	$1.74^{+0.14}_{-0.08}$	$1.84^{+0.07}_{-0.06}$
060604	3.56	6.2	4.32	0.39 ± 0.09	1.29 ± 0.06	98.72/66	0.51 ± 0.14	$2.07^{+0.17}_{-0.16}$	$2.08^{+0.16}_{-0.15}$
060605	2.24	5.25	3.92	0.42 ± 0.03	2.06 ± 0.08	85.71/74	1.22 ± 0.1	$1.95^{+0.12}_{-0.11}$	$2.10^{+0.15}_{-0.14}$
060607A	2.68	5	4.11	0.44 ± 0.02	3.58 ± 0.08	253.9/173	12.01 ± 0.71	$1.52^{+0.08}_{-0.07}$	1.56 ± 0.08
060614	3.66	6.4	4.69	0.09 ± 0.04	1.94 ± 0.04	181/150	3 ± 0.2	$1.74^{+0.1}_{-0.06}$	$1.84^{+0.13}_{-0.12}$
060707	2.58	6.53	5.09	0.62 ± 0.03	1.32 ± 0.12	59.43/33	1.91 ± 0.88	$2.12^{+0.15}_{-0.14}$	$1.73^{+0.38}_{-0.32}$
060712	2.55	6	3.97	0.34 ± 0.08	1.13 ± 0.05	23.93/22	0.17 ± 0.06	$2.57^{+0.51}_{-0.44}$	$2.46^{+0.32}_{-0.29}$
060714	2.47	6.11	3.67	0.38 ± 0.09	1.27 ± 0.04	81.86/47	0.88 ± 0.27	$1.88^{+0.15}_{-0.14}$	$2.01^{+0.19}_{-0.18}$
060719	2.71	5.88	3.87	0.48 ± 0.07	1.25 ± 0.04	60.03/50	0.55 ± 0.17	$2.24^{+0.26}_{-0.24}$	$2.38^{+0.22}_{-0.2}$
060729	2.83	7.1	4.8	0.12 ± 0.02	1.37 ± 0.01	1011/706	10.69 ± 0.38	$1; 96 \pm 0.05$	1.97 ± 0.05
060804	2.16	5.41	2.9	-0.31 ± 0.16	1.17 ± 0.06	38.76/28	0.5 ± 0.12	$1.82^{+0.29}_{-0.12}$	$1.92^{+0.27}_{-0.14}$
060805A	2.16	5.46	3.56	0.19 ± 0.17	1.5 ± 0.1	15.69/8	0.09 ± 0.03	$1.9^{+0.53}_{-0.32}$	$2.11^{+0.46}_{-0.38}$
060807	2.43	5.7	3.88	0.001 ± 0.04	1.64 ± 0.04	169.6/92	1.13 ± 0.08	1.9 ± 0.12	$2.36^{+0.19}_{-0.18}$
060813	2	5.5	3.24	0.6 ± 0.03	1.3 ± 0.02	333/234	4.08 ± 0.75	1.83 ± 0.08	1.78 ± 0.09
060814	3.15	6.12	4.1	0.44 ± 0.08	1.36 ± 0.03	272.1/161	1.96 ± 0.34	1.97 ± 0.12	2.08 ± 0.09
060906	2.8	5.41	4.05	0.24 ± 0.06	1.74 ± 0.09	66.64/32	0.39 ± 0.05	$2.1^{+0.23}_{-0.22}$	$1.76^{+0.22}_{-0.16}$
060908	1.8	5.94	2.84	0.56 ± 0.07	1.44 ± 0.04	62.81/33	0.86 ± 0.23	$2.02^{+0.42}_{-0.37}$	$2.09^{+0.21}_{-0.2}$
060923C	2.88	6.08	5.32	0.54 ± 0.06	1.85 ± 0.29	14.88/16	1.11 ± 0.38	$2.74^{+0.4}_{-0.36}$	$1.98^{+0.45}_{-0.36}$

Table 1. Part II. XRT observations and fitting results for our sample

GRBname	$\log_{10}(t_1)$ ^a	$\log_{10}(t_2)$ ^a	$\log_{10}(t_b)$ ^b	$\alpha_{X,1}$ ^b	$\alpha_{X,2}$ ^b	χ^2/dof ^b	S_X ^c	$\Gamma_{X,1}$ ^d	$\Gamma_{X,2}$ ^d
	s	s	s				$10^{-7} \text{ergs cm}^{-2}$		
060927	1.82	5	3.79	0.76 ± 0.05	2.49 ± 0.81	5.479/13	0.45 ± 0.16	$1.83^{+0.18}_{-0.11}$	$2.53^{+1.7}_{-0.59}$
061004	2.72	5.28	4.19	0.68 ± 0.07	1.64 ± 0.29	24.67/17	0.4 ± 0.24	$1.95^{+0.23}_{-0.19}$	$2.32^{+0.68}_{-0.32}$
061019	3.4	5.86	5.07	0.81 ± 0.05	1.96 ± 0.39	80.89/42	1.46 ± 0.73	$2.05^{+0.24}_{-0.23}$	$2.03^{+0.87}_{-0.69}$
061121	2.37	6.32	3.71	0.36 ± 0.03	1.4 ± 0.02	369.5/269	7.04 ± 0.84	$1.94^{+0.13}_{-0.12}$	1.79 ± 0.06
061201	1.9	5.08	3.44	0.54 ± 0.07	2.05 ± 0.11	33.23/23	1.39 ± 0.27	$1.3^{+0.18}_{-0.17}$	$2.02^{+0.4}_{-0.36}$
061202	2.94	5.78	4.22	-0.1 ± 0.05	1.73 ± 0.03	202.2/116	2.55 ± 0.15	$1.97^{+0.14}_{-0.13}$	$2.2^{+0.15}_{-0.14}$
061222A	2.33	6.19	4.68	0.73 ± 0.01	1.72 ± 0.03	516.3/327	12.37 ± 0.89	1.84 ± 0.06	2.05 ± 0.1
070103	2.2	5.13	3.16	-0.23 ± 0.14	1.42 ± 0.06	31.95/24	0.21 ± 0.04	$1.91^{+0.29}_{-0.28}$	$2.15^{+0.30}_{-0.28}$
070110	3.5	4.5	4.31	0.066 ± 0.05	9.05 ± 0.52	111.1/107	2.45 ± 0.13	2.04 ± 0.08	$2.07^{+0.19}_{-0.17}$
070129	3.15	6.21	4.25	0.15 ± 0.08	1.14 ± 0.03	102.4/80	0.62 ± 0.12	2.21 ± 0.16	$2.04^{+0.15}_{-0.14}$
070306	2.73	6.05	4.48	0.11 ± 0.03	1.81 ± 0.04	193.4/140	5.24 ± 0.34	1.8 ± 0.09	$2.02^{+0.17}_{-0.16}$
070328	2.18	5.92	2.84	0.25 ± 0.03	1.46 ± 0.01	683.4/531	5.57 ± 0.35	2.09 ± 0.04	1.9 ± 0.07
070420	2.51	5.72	3.51	0.23 ± 0.07	1.37 ± 0.02	230/139	2.53 ± 0.32	$2.03^{+0.15}_{-0.14}$	$1.78^{+0.24}_{-0.22}$
070429A	3.33	6.05	5.69	0.36 ± 0.08	3.03 ± 0.5	34.6/12	0.92 ± 0.14	$2.17^{+0.29}_{-0.27}$	$2.19^{+1.11}_{-0.75}$
070508	1.83	5.9	2.46	0.18 ± 0.32	0.95 ± 0.18	611/484	0.15 ± 0.55	1.8 ± 0.06	1.76 ± 0.04
070529	2.31	5.78	3.02	0.48 ± 0.16	1.25 ± 0.04	38.09/30	0.42 ± 0.17	$1.57^{+0.27}_{-0.18}$	$2.11^{+0.24}_{-0.22}$
070621	2.60	5.90	3.47	0.68 ± 0.19	1.14 ± 0.06	31.29/25	0.18 ± 0.83	$2.6^{+0.24}_{-0.23}$	$2.25^{+0.38}_{-0.34}$
070628	2	4.91	3.93	0.44 ± 0.02	1.29 ± 0.03	301.4/192	4.12 ± 0.26	1.9 ± 0.13	2.01 ± 0.11
070809	2.74	4.82	3.78	-0.06 ± 0.19	1.30 ± 0.15	16.71/11	0.16 ± 0.07	$1.4^{+0.39}_{-0.2}$	$1.25^{+0.2}_{-0.17}$
070810A	2.1	4.54	3.14	0.36 ± 0.25	1.32 ± 0.06	46.44/31	0.37 ± 0.24	$2.09^{+0.26}_{-0.24}$	$2.06^{+0.2}_{-0.19}$
071118	2.99	5.06	4.11	0.59 ± 0.06	2.18 ± 0.13	83.57/60	2.52 ± 0.4	1.36 ± 0.11	$1.53^{+0.4}_{-0.37}$
080320	3	6.32	4.85	0.60 ± 0.04	1.25 ± 0.06	131/96	2.03 ± 0.6	1.97 ± 0.11	$2.18^{+0.25}_{-0.23}$
080328	2.4	4.7	3.08	0.43 ± 0.09	1.19 ± 0.03	235.6/155	2.33 ± 0.64	1.72 ± 0.16	$1.94^{+0.39}_{-0.36}$
080409	2.16	5.03	3.27	-0.01 ± 0.14	1.3 ± 0.14	15.24/8	0.14 ± 0.04	$2.01^{+0.54}_{-0.48}$	$2^{+0.58}_{-0.51}$
080413B	2.1	5.24	2.6	0.38 ± 0.12	1 ± 0.01	328.2/225	0.73 ± 0.27	$2.04^{+0.13}_{-0.12}$	1.84 ± 0.07
080430	2.5	6.48	4.53	0.43 ± 0.02	1.16 ± 0.03	128.2/141	1.78 ± 0.28	1.97 ± 0.1	1.95 ± 0.13
080516	2.1	4.67	3.67	0.33 ± 0.09	1.07 ± 0.11	37.66/27	0.3 ± 0.1	$2.69^{+0.52}_{-0.47}$	$2^{+0.43}_{-0.39}$
080703	2	5.21	4.40	0.6 ± 0.03	2.36 ± 0.17	108.2/68	1.73 ± 0.32	$1.4^{+0.11}_{-0.06}$	$1.29^{+0.21}_{-0.18}$
080707	2.4	5.45	4.03	0.28 ± 0.07	1.17 ± 0.1	42.8/22	0.33 ± 0.14	$2.19^{+0.27}_{-0.26}$	$1.7^{+0.26}_{-0.24}$
080723A	2.53	5.67	3.4	-0.04 ± 0.13	1.06 ± 0.03	62.74/35	0.44 ± 0.1	$2.03^{+0.25}_{-0.23}$	$1.71^{+0.55}_{-0.49}$
080903	1.8	4.28	2.26	0.07 ± 0.26	1.57 ± 0.12	382.1/90	1.4 ± 0.53	$0.68^{+0.08}_{-0.06}$	$1.21^{+0.21}_{-0.12}$
080905B	2.27	4.75	4.16	0.47 ± 0.02	2.18 ± 0.25	103.5/69	6.19 ± 1.05	$1.68^{+0.12}_{-0.11}$	$1.91^{+0.19}_{-0.18}$
081007	2.43	6.24	4.62	0.67 ± 0.03	1.27 ± 0.06	81.85/58	1.83 ± 0.61	1.92 ± 0.13	$1.97^{+0.26}_{-0.24}$
081029	3.4	5.84	4.21	0.4 ± 0.05	2.46 ± 0.09	125.3/80	1.03 ± 0.01	$1.82^{+0.1}_{-0.09}$	$2.03^{+0.22}_{-0.2}$
081210	3.71	5.83	5.3	0.64 ± 0.04	2.67 ± 0.57	16.29/21	1.4 ± 0.3	$1.86^{+0.19}_{-0.14}$	$2.5^{+0.65}_{-0.54}$
081230	2.53	5.94	4.19	0.48 ± 0.07	1.25 ± 0.1	57.91/39	0.48 ± 0.2	$2.07^{+0.27}_{-0.25}$	$1.95^{+0.21}_{-0.19}$
090102	2.5	5.84	3.16	0.89 ± 0.05	1.45 ± 0.01	166.6/138	4.96 ± 0.67	$1.62^{+0.24}_{-0.23}$	1.72 ± 0.08
090113	2	5.52	2.75	0.13 ± 0.16	1.29 ± 0.04	37.88/22	0.45 ± 0.11	$2.13^{+0.38}_{-0.35}$	$2.2^{+0.31}_{-0.28}$
090205	2.63	5.53	4.18	0.54 ± 0.06	1.98 ± 0.23	61.18/30	0.42 ± 0.12	$2.07^{+0.19}_{-0.15}$	$2.02^{+0.34}_{-0.31}$
090313	4.45	5.86	4.89	0.6 ± 0.18	2.3 ± 0.12	28.47/34	1.27 ± 0.33	$2.02^{+0.2}_{-0.19}$	$2.27^{+0.32}_{-0.29}$
090404	2.49	6.16	4.23	0.20 ± 0.07	1.25 ± 0.06	200.1/109	1.24 ± 0.33	$2.21^{+0.15}_{-0.14}$	$2.65^{+0.16}_{-0.15}$
090407	3.07	6.05	4.86	0.38 ± 0.03	1.67 ± 0.09	177.4/107	1.65 ± 0.22	$2.22^{+0.13}_{-0.12}$	$2.11^{+0.29}_{-0.27}$
090418A	2.09	5.64	3.49	0.47 ± 0.05	1.58 ± 0.04	109.7/101	3.3 ± 0.6	$2^{+0.22}_{-0.21}$	1.98 ± 0.1
090424	2.43	6.70	2.97	0.57 ± 0.17	1.17 ± 0.02	517.5/510	7.94 ± 0.45	1.9 ± 0.05	1.99 ± 0.08
090429B	2.1	5.64	2.9	-0.7 ± 0.23	1.31 ± 0.08	22.16/16	0.1 ± 0.02	$1.79^{+0.29}_{-0.26}$	$2.02^{+0.4}_{-0.35}$
090510	2	4.81	3.19	0.65 ± 0.04	2.18 ± 0.08	103.2/69	1.42 ± 0.22	$1.6^{+0.12}_{-0.1}$	$2.05^{+0.33}_{-0.3}$
090518	2.29	5.06	3.72	0.51 ± 0.09	1.14 ± 0.12	48.83/34	0.33 ± 0.22	$2.5^{+0.39}_{-0.36}$	$2.38^{+0.29}_{-0.27}$
090529	3.41	5.89	5.36	0.51 ± 0.1	1.69 ± 0.43	3.054/5	0.43 ± 0.24	$1.71^{+0.56}_{-0.23}$	$1.78^{+0.32}_{-0.26}$

Table 1. Part III. XRT observations and fitting results for our sample

GRBname	$\log_{10}(t_1)$ ^a	$\log_{10}(t_2)$ ^a	$\log_{10}(t_b)$ ^b	$\alpha_{X,1}$ ^b	$\alpha_{X,2}$ ^b	χ^2/dof ^b	S_X ^c	$\Gamma_{X,1}$ ^d	$\Gamma_{X,2}$ ^d
	s	s	s				$10^{-7} \text{ergs cm}^{-2}$		
090530	2.2	5.90	4.77	0.61 ± 0.02	1.35 ± 0.1	84.28/49	1.27 ± 0.35	$1.97^{+0.14}_{-0.13}$	$1.87^{+0.3}_{-0.28}$
090727	3.65	6.33	5.57	0.5 ± 0.05	1.56 ± 0.25	26.34/17	1.22 ± 0.45	$1.9^{+0.27}_{-0.12}$	$2.1^{+0.63}_{-0.34}$
090728	2.56	4.90	3.25	-0.03 ± 0.22	1.8 ± 0.09	22.97/22	0.37 ± 0.08	$1.74^{+0.15}_{-0.12}$	$1.83^{+0.27}_{-0.25}$
090813	2.03	5.82	2.73	0.23 ± 0.06	1.25 ± 0.01	403.4/286	1.78 ± 0.21	2.01 ± 0.07	1.79 ± 0.09
090904A	2.91	5.49	4.1	0.13 ± 0.12	1.31 ± 0.09	13.19/15	0.29 ± 0.07	$2.38^{+0.44}_{-0.4}$	$2.04^{+0.35}_{-0.24}$
091018	1.7	5.9	2.78	0.43 ± 0.05	1.2 ± 0.02	232/137	1.53 ± 0.31	$1.87^{+0.18}_{-0.17}$	1.88 ± 0.09
091029	2.86	6.28	4.07	0.19 ± 0.04	1.15 ± 0.02	183.4/125	0.91 ± 0.13	2.1 ± 0.12	2.01 ± 0.11
091130B	3.58	6.13	4.70	0.29 ± 0.06	1.17 ± 0.05	147.7/96	0.78 ± 0.17	$2.3^{+0.17}_{-0.16}$	$2.27^{+0.19}_{-0.18}$
100111A	1.75	5.38	3.26	0.5 ± 0.09	1.05 ± 0.06	38.72/31	0.3 ± 0.17	$1.83^{+0.23}_{-0.21}$	$1.84^{+0.24}_{-0.23}$
100219A	2.95	5.07	4.53	0.56 ± 0.03	3.75 ± 0.3	28.34/22	1.82 ± 0.31	$1.44^{+0.16}_{-0.14}$	$1.47^{+0.45}_{-0.37}$
100302A	3.10	6.04	4.35	0.35 ± 0.12	0.95 ± 0.08	18.49/20	0.2 ± 0.1	$1.8^{+0.43}_{-0.25}$	$1.87^{+0.21}_{-0.19}$
100418A	3	6.47	4.91	-0.16 ± 0.06	1.44 ± 0.08	31.65/22	0.63 ± 0.1	$1.89^{+0.37}_{-0.34}$	$1.93^{+0.29}_{-0.26}$
100425A	2.53	5.7	4.51	0.54 ± 0.05	1.2 ± 0.13	20.87/19	0.35 ± 0.2	$2.24^{+0.27}_{-0.24}$	$1.92^{+0.33}_{-0.29}$
100508A	2.82	5.3	4.37	0.36 ± 0.05	2.83 ± 0.2	71.43/48	2.1 ± 0.36	1.3 ± 0.13	$1.62^{+0.3}_{-0.28}$
100522A	2.28	5.59	4.31	0.5 ± 0.03	1.28 ± 0.06	128.3/98	1.8 ± 0.37	2.11 ± 0.15	$2.21^{+0.19}_{-0.18}$
100614A	3.76	5.75	5.22	0.41 ± 0.05	2.28 ± 0.27	28.87/26	1.21 ± 0.18	$2.15^{+0.23}_{-0.22}$	$2.14^{+0.51}_{-0.38}$
100704A	2.67	6.29	4.53	0.67 ± 0.03	1.32 ± 0.05	202/155	3.52 ± 0.85	2.09 ± 0.12	$1.95^{+0.13}_{-0.12}$
100725B	2.81	5.76	4.19	0.39 ± 0.06	1.4 ± 0.07	53.09/50	1.23 ± 0.24	$2.49^{+0.21}_{-0.2}$	$2.59^{+0.34}_{-0.32}$
100901A	3.59	5.98	4.58	-0.02 ± 0.03	1.5 ± 0.03	543.9/264	3.56 ± 0.16	2.02 ± 0.07	$2.15^{+0.09}_{-0.08}$
100902A	3.18	6.17	5.93	0.71 ± 0.03	4.58 ± 0.96	84.64/53	3.67 ± 0.62	$2.31^{+0.17}_{-0.16}$	$3.2^{+2.8}_{-1.8}$
100905A	2.86	4.87	3.28	0.05 ± 0.4	1.12 ± 0.11	21/8	0.05 ± 0.03	$1.47^{+0.38}_{-0.3}$	$1.85^{+0.49}_{-0.4}$
100906A	2.57	5.62	4.1	0.7 ± 0.03	2.01 ± 0.05	344.3/127	4 ± 0.4	$1.9^{+0.1}_{-0.09}$	$1.95^{+0.15}_{-0.14}$
101117B	1.75	4.98	3.22	0.77 ± 0.06	1.29 ± 0.06	53.09/36	0.64 ± 0.39	$2.09^{+0.23}_{-0.22}$	$1.99^{+0.24}_{-0.23}$
110102A	2.72	6.4	4.09	0.49 ± 0.03	1.41 ± 0.02	397.7/294	5.12 ± 0.51	$2.06 \pm 0, 1$	1.98 ± 0.07
110106B	2.5	5.73	4.12	0.58 ± 0.05	1.41 ± 0.07	76.87/50	1.48 ± 0.41	$1.98 \pm 0, 16$	$1.66^{+0.26}_{-0.25}$
110312A	2.75	5.96	4.91	0.53 ± 0.04	1.38 ± 0.2	31.74/25	2 ± 1.06	$2.31^{+0.22}_{-0.21}$	$2.7^{+0.7}_{-0.59}$
110319A	2.16	5.48	3.89	0.58 ± 0.04	1.34 ± 0.08	72.05/52	0.82 ± 0.24	$2^{+0.19}_{-0.18}$	$2.45^{+0.22}_{-0.21}$
110411A	2.38	5.1	3.53	0.43 ± 0.12	1.23 ± 0.1	57.95/35	0.31 ± 0.22	$2.9^{+0.32}_{-0.3}$	$3.41^{+0.52}_{-0.46}$
110530A	2.6	5.84	3.85	0.47 ± 0.07	1.22 ± 0.05	93.57/39	0.6 ± 0.18	$1.87^{+0.2}_{-0.19}$	$2.09^{+0.26}_{-0.24}$
110808A	2.69	5.79	5.22	0.57 ± 0.05	1.41 ± 0.41	8.851/10	0.57 ± 0.38	$2.32^{+0.37}_{-0.34}$	$1.37^{+0.4}_{-0.26}$
111008A	2.47	6.01	3.9	0.32 ± 0.04	1.31 ± 0.03	207.2/135	2.69 ± 0.42	1.83 ± 0.1	1.84 ± 0.09
111228A	2.62	6.47	4.13	0.4 ± 0.03	1.27 ± 0.02	188.3/149	3.56 ± 0.44	$1.96^{+0.11}_{-0.1}$	2.01 ± 0.11
120106A	2.23	5.49	3.07	0.3 ± 0.15	1.1 ± 0.04	50.3/29	0.24 ± 0.1	$2.01^{+0.31}_{-0.29}$	$2.02^{+0.34}_{-0.32}$
120224A	2.43	5.74	3.29	-0.54 ± 0.11	0.98 ± 0.02	110.1/77	0.35 ± 0.04	$2.4^{+0.29}_{-0.28}$	$2.02^{+0.14}_{-0.13}$
120308A	2.64	4.28	3.75	0.52 ± 0.07	1.32 ± 0.13	107.6/86	1.68 ± 0.59	1.47 ± 0.1	$1.53^{+0.14}_{-0.13}$
120324A	2.38	5.16	3.73	0.31 ± 0.06	1.12 ± 0.04	224.4/149	3.2 ± 0.85	$2.08^{+0.26}_{-0.25}$	$2.08^{+0.13}_{-0.12}$
120326A	2.37	6.21	4.71	-0.24 ± 0.02	2.04 ± 0.06	364.1/191	4.87 ± 0.18	1.77 ± 0.06	$2^{+0.15}_{-0.14}$
120521C	2.75	5.15	4.06	0.35 ± 0.14	1.1 ± 0.2	5.505/7	0.17 ± 0.15	$1.78^{+0.31}_{-0.24}$	$2.18^{+0.72}_{-0.59}$
120703A	2	5.73	3.91	0.64 ± 0.04	1.22 ± 0.05	137/81	2.09 ± 0.75	$1.89^{+0.14}_{-0.13}$	$1.89^{+0.16}_{-0.15}$
120811C	2.4	5	3.34	0.43 ± 0.11	1.12 ± 0.08	61.36/45	0.96 ± 0.58	$1.68 \pm 0, 14$	$2.12^{+0.21}_{-0.2}$
120907A	1.75	5.45	3.2	0.43 ± 0.07	1.08 ± 0.03	140.4/86	0.79 ± 0.24	$1.77^{+0.17}_{-0.16}$	1.76 ± 0.11
121024A	2.69	5.63	4.64	0.88 ± 0.04	1.72 ± 0.27	66.73/48	1.76 ± 1.03	$1.85^{+0.12}_{-0.11}$	$2.36^{+1.39}_{-0.77}$
121031A	2.91	4.76	4.07	0.39 ± 0.06	1.05 ± 0.09	190.6/177	3.45 ± 1.35	$2.27^{+0.17}_{-0.16}$	2.24 ± 0.1
121123A	3.11	5.26	4.56	0.73 ± 0.07	1.99 ± 0.17	54.85/39	0.89 ± 0.22	1.88 ± 0.11	$1.71^{+0.27}_{-0.25}$
121125A	2.27	5.01	3.78	0.71 ± 0.05	1.35 ± 0.07	72.98/90	2.03 ± 1.03	$1.88^{+0.17}_{-0.16}$	2.03 ± 0.12
121128A	2.13	5.19	3.2	0.55 ± 0.04	1.63 ± 0.04	126.6/95	2.46 ± 0.39	$1.79^{+0.12}_{-0.08}$	1.89 ± 0.12
121211A	3.6	5.56	4.63	0.73 ± 0.06	1.55 ± 0.13	90.64/65	1.39 ± 0.53	$1.97^{+0.12}_{-0.11}$	$1.84^{+0.47}_{-0.42}$
130131A	2.83	5.61	3.88	0.63 ± 0.21	1.23 ± 0.16	11.51/17	0.16 ± 0.5	$2.12^{+0.33}_{-0.31}$	$2.57^{+0.5}_{-0.44}$

Table 1. Part IV. XRT observations and fitting results for our sample

GRBname	$\log_{10}(t_1)$ ^a	$\log_{10}(t_2)$ ^a	$\log_{10}(t_b)$ ^b	$\alpha_{X,1}$ ^b	$\alpha_{X,2}$ ^b	χ^2/dof ^b	S_X ^c	$\Gamma_{X,1}$ ^d	$\Gamma_{X,2}$ ^d
	s	s	s				$10^{-7} \text{ ergs cm}^{-2}$		
130603B	1.6	5.1	3.36	0.31 ± 0.05	1.53 ± 0.05	154.8/74	1.23 ± 0.17	$1.75^{+0.2}_{-0.19}$	2 ± 0.15
130609B	2.74	5.49	3.65	0.64 ± 0.04	1.82 ± 0.03	373.4/278	9.69 ± 1.07	1.81 ± 0.05	$1.96^{+0.1}_{-0.09}$
131018A	3.07	4.91	4.59	0.26 ± 0.05	1.35 ± 0.28	76.53/53	1.2 ± 0.31	$2.1^{+0.17}_{-0.16}$	$1.76^{+0.57}_{-0.49}$
131105A	2.61	5.87	3.66	0.16 ± 0.11	1.19 ± 0.04	63.77/49	0.88 ± 0.22	1.92 ± 0.17	$1.99^{+0.18}_{-0.17}$
140108A	2.88	5.63	3.8	0.33 ± 0.06	1.33 ± 0.03	240.5/150	4.5 ± 0.85	$1.76^{+0.32}_{-0.3}$	$2.08^{+0.17}_{-0.16}$
140114A	2.91	5.56	4.34	0.24 ± 0.06	1.25 ± 0.12	43.81/31	0.45 ± 0.13	$2.17^{+0.2}_{-0.19}$	$1.7^{+0.56}_{-0.48}$
140323A	2.34	5.07	3.95	0.56 ± 0.03	1.62 ± 0.08	162.3/105	6.07 ± 1.18	$2.1^{+0.17}_{-0.16}$	$2.2^{+0.68}_{-0.61}$
140331A	3.16	5.32	4.71	0.3 ± 0.06	2.07 ± 0.47	25.97/17	0.71 ± 0.24	$1.73^{+0.22}_{-0.2}$	$2.19^{+1.22}_{-0.75}$
140430A	2.66	5.66	4.68	0.6 ± 0.09	1.53 ± 0.4	45.08/37	1.17 ± 0.59	$2.19^{+0.2}_{-0.19}$	$2.07^{+0.26}_{-0.24}$
140512A	2.46	5.65	4.12	0.73 ± 0.02	1.57 ± 0.06	488.5/379	19.4 ± 3.03	1.8 ± 0.07	1.86 ± 0.1
140518A	2.8	4.27	3.28	-0.16 ± 0.31	1.38 ± 0.2	35.32/27	0.28 ± 0.11	$2.09^{+0.2}_{-0.19}$	$1.89^{+0.21}_{-0.2}$
140703A	2.34	5.48	4.16	0.62 ± 0.03	2.16 ± 0.09	122.8/76	6.82 ± 0.65	1.76 ± 0.11	1.94 ± 0.15
140706A	2.36	5.05	3.83	0.36 ± 0.07	1.25 ± 0.1	28.23/20	0.49 ± 0.16	$1.84^{+0.24}_{-0.23}$	$1.77^{+0.34}_{-0.31}$
140709A	2.43	5.5	4.22	0.56 ± 0.03	1.39 ± 0.07	72.03/74	3.63 ± 0.75	$1.84^{+0.19}_{-0.18}$	$2.03^{+0.2}_{-0.19}$
140916A	2.92	5.55	4.61	0.14 ± 0.02	2.05 ± 0.13	183.8/137	2.92 ± 0.23	2.09 ± 0.09	$2^{+0.32}_{-0.29}$
141017A	2.41	5.6	3.32	0.07 ± 0.13	1.12 ± 0.03	144.1/79	0.8 ± 0.17	$2.13^{+0.18}_{-0.17}$	2.01 ± 0.13
141031A	3.74	5.88	4.47	0.06 ± 0.18	1.07 ± 0.11	36.86/23	0.68 ± 0.3	$1.88^{+0.32}_{-0.25}$	$1.9^{+0.31}_{-0.28}$
141121A	4.45	6.17	5.52	0.46 ± 0.1	2.24 ± 0.18	25.1/20	2.86 ± 0.5	$1.87^{+0.26}_{-0.21}$	$1.65^{+0.26}_{-0.13}$
150120B	2.6	5.3	3.03	-0.23 ± 0.28	1.16 ± 0.04	61.48/40	0.15 ± 0.04	$1.72^{+0.3}_{-0.28}$	$2.19^{+0.2}_{-0.19}$
150201A	2.19	5.38	2.88	0.46 ± 0.04	1.27 ± 0.01	456.9/355	4.62 ± 0.73	1.84 ± 0.05	$2.28^{+0.14}_{-0.13}$
150203A	2.19	5.38	4.59	0.687 ± 0.07	1.56 ± 0.9	54.18/11	0.36 ± 2.03	$2.01^{+0.36}_{-0.24}$	$2.45^{+0.95}_{-0.81}$
150323A	2.65	5.58	4.16	0.43 ± 0.05	1.26 ± 0.09	30.87/18	0.52 ± 0.17	$2.11^{+0.25}_{-0.23}$	$1.77^{+0.57}_{-0.49}$
150323C	2.9	5.8	3.85	0.38 ± 0.22	1.13 ± 0.14	9.361/12	0.07 ± 0.17	$2^{+0.46}_{-0.41}$	$2.33^{+0.44}_{-0.39}$
150424A	2.6	5.8	5.06	0.79 ± 0.04	1.43 ± 0.17	62.65/39	$52 \pm 1.47 \pm 0.88$	$1.96^{+0.22}_{-0.21}$	$1.92^{+0.2}_{-0.18}$
150607A	2.1	4.61	3.76	0.73 ± 0.05	1.21 ± 0.14	114.9/76	2.7 ± 2.59	$1.81^{+0.15}_{-0.14}$	$1.79^{+0.18}_{-0.17}$
150615A	2.87	5.5	4.12	-0.01 ± 0.13	0.79 ± 0.13	27.83/23	0.3 ± 0.18	$2.6^{+0.36}_{-0.33}$	$2.4^{+0.41}_{-0.31}$
150626A	2.87	4.81	4.15	0.21 ± 0.09	1.03 ± 0.19	25.99/28	0.51 ± 0.26	$2.42^{+0.34}_{-0.31}$	$2.11^{+0.31}_{-0.29}$
150711A	2.82	4.79	4.18	0.5 ± 0.07	1.43 ± 0.19	38.73/20	0.79 ± 0.32	$2.21^{+0.28}_{-0.27}$	$1.82^{+0.36}_{-0.33}$
150910A	3.03	5.5	3.94	0.61 ± 0.14	2.36 ± 0.16	201.9/101	11.9 ± 4.84	$1.79^{+0.19}_{-0.18}$	1.78 ± 0.08
151027A	2.71	6.1	3.6	0.06 ± 0.03	1.65 ± 0.02	635.3/447	13.8 ± 0.61	2.03 ± 0.04	1.77 ± 0.12
151112A	3.63	5.83	4.76	0.64 ± 0.08	1.6 ± 0.25	34.09/38	1.09 ± 0.63	$2.28^{+0.24}_{-0.23}$	$2.14^{+0.25}_{-0.23}$
151228B	2.7	5.37	4.45	0.59 ± 0.06	1.7 ± 0.33	16.02/14	0.41 ± 0.31	$1.97^{+0.26}_{-0.23}$	$1.94^{+0.41}_{-0.34}$
151229A	1.9	4.66	2.44	0.27 ± 0.15	0.94 ± 0.03	108.3/75	0.42 ± 0.2	$1.53^{+0.33}_{-0.3}$	2.05 ± 0.14
160119A	3.2	6.05	4.29	0.55 ± 0.08	1.43 ± 0.06	138/106	1.58 ± 0.39	$1.97^{+0.16}_{-0.15}$	2.14 ± 0.13
160127A	2.35	5	3.64	0.83 ± 0.06	1.57 ± 0.1	38.51/41	0.79 ± 0.35	$1.8^{+0.21}_{-0.2}$	$1.82^{+0.21}_{-0.18}$
160227A	3.2	6.4	4.37	0.28 ± 0.09	1.2 ± 0.04	196/102	3.41 ± 0.92	1.67 ± 0.1	1.72 ± 0.1
160327A	2.53	5	3.62	0.3 ± 0.14	1.56 ± 0.09	56.85/28	0.42 ± 0.14	$1.64^{+0.26}_{-0.23}$	$2.13^{+0.23}_{-0.21}$
160412A	2.72	5.95	4.32	0.11 ± 0.08	1.01 ± 0.1	33.55/18	0.37 ± 0.15	$2.66^{+0.5}_{-0.45}$	$1.76^{+0.32}_{-0.3}$
160630A	2.22	5.41	3.2	0.06 ± 0.11	1.16 ± 0.03	92.93/73	0.97 ± 0.17	$1.81^{+0.23}_{-0.22}$	$1.76^{+0.14}_{-0.13}$
160804A	3.02	6.13	3.96	-0.28 ± 0.27	0.92 ± 0.05	75.62/43	0.37 ± 0.1	$1.97^{+0.25}_{-0.24}$	$1.94^{+0.17}_{-0.16}$
160824A	2.59	4.54	3.93	0.4 ± 0.05	1.45 ± 0.14	111.5/85	2.74 ± 0.68	$1.88^{+0.23}_{-0.21}$	2.04 ± 0.17
161001A	2.45	5.36	3.53	0.69 ± 0.09	1.38 ± 0.05	65.41/41	1.46 ± 0.7	$1.83^{+0.24}_{-0.23}$	$2.12^{+0.24}_{-0.23}$
161011A	2.86	5.5	4.64	-0.1 ± 0.04	3.08 ± 0.18	131.9/48	1.71 ± 0.87	1.9 ± 0.15	$2.48^{+0.49}_{-0.43}$
161108A	2.81	5.96	4.36	-0.02 ± 0.16	0.86 ± 0.07	33.44/24	0.43 ± 0.18	$1.95^{+0.29}_{-0.27}$	$1.64^{+0.27}_{-0.25}$
161129A	2.44	4.24	3.56	0.38 ± 0.11	2.18 ± 0.11	80.76/51	1.75 ± 0.37	$1.72^{+0.19}_{-0.18}$	$1.82^{+0.18}_{-0.17}$
161202A	2.53	5.16	4.17	0.75 ± 0.13	1.82 ± 0.36	34.26/31	2.29 ± 3.73	$1.72^{+0.19}_{-0.18}$	$1.82^{+0.18}_{-0.17}$
161214B	2.9	5.71	4.48	0.45 ± 0.06	1.32 ± 0.1	41.46/40	0.98 ± 0.31	$1.97^{+0.18}_{-0.17}$	$2.26^{+0.38}_{-0.34}$
170113A	2.41	5.94	3.64	0.48 ± 0.04	1.25 ± 0.02	211/148	2.87 ± 0.52	1.85 ± 0.12	1.79 ± 0.08

Table 1. Part V. XRT observations and fitting results for our sample

GRBname	$\log_{10}(t_1)$ ^a	$\log_{10}(t_2)$ ^a	$\log_{10}(t_b)$ ^b	$\alpha_{X,1}$ ^b	$\alpha_{X,2}$ ^b	χ^2/dof ^b	S_X ^c	$\Gamma_{X,1}$ ^d	$\Gamma_{X,2}$ ^d
	s	s	s				$10^{-7} \text{ergs cm}^{-2}$		
170202A	2.47	5.73	3.32	-0.12 ± 0.1	1.15 ± 0.04	50.64/39	0.66 ± 0.11	$2.12_{-0.17}^{+0.18}$	$1.92_{-0.17}^{+0.18}$
170208B	2.91	5.78	3.83	0.53 ± 0.14	1.07 ± 0.06	47/40	0.56 ± 0.75	$2.19_{-0.22}^{+0.23}$	$2.54_{-0.26}^{+0.28}$
170317A	2.18	5.16	3.32	0.44 ± 0.08	1.33 ± 0.08	56.84/45	0.39 ± 0.14	$1.97_{-0.06}^{+0.17}$	$2.15_{-0.23}^{+0.31}$
170330A	2	5.39	2.71	0.56 ± 0.08	1.33 ± 0.08	210.1/164	1.59 ± 0.14	$2.01_{-0.26}^{+0.39}$	$1.92_{-0.12}^{+0.13}$
170607A	3.13	6.29	4.25	0.29 ± 0.05	1.03 ± 0.03	204.7/166	2.86 ± 0.63	$2.08_{-0.09}^{+0.1}$	1.93 ± 0.1
170711A	2.37	5.45	4.66	0.46 ± 0.03	1.48 ± 0.3	85.36/42	1.17 ± 0.51	$2.07_{-0.35}^{+0.38}$	$2.11_{-0.21}^{+0.22}$

^a t_1 and t_2 represent the beginning time (t_1) of the shallow decay segment and the end time (t_2) of its follow-up segment.

^b Break time and decay slopes before and after the break, and the fit χ^2/dof

^c The X-ray fluence of shallow decay segment.

^d Photon index of shallow decay segment and its follow-up segment.

Table 2. Part I BAT observations and redshift for our sample

GRBname	$T_{90}(s)$	S_γ^a	$\Gamma_{\gamma,1}^b$	E_p^b	BAT Ref ^c	z	z Ref ^c	Group of GRBs ^d
		s	10^{-7} ergs cm $^{-2}$	keV				
050319	10±2	8±0.8	2.2±0.2	33.41±12.22	3119	3.24	3136	<i>case</i> ¹ (regime 2)
050401	33±2	140±14	1.5±0.06	133.14±29.35	3173	2.9	3176	<i>case</i> ²
050416A	2.4±0.2	69	2.9±0.2	12.32±4.45	3273	0.6528	3542	<i>case</i> ¹ (regime 1)
050505	60±2	41±4	1.5±0.1	133.14±38.15	3364	4.27	3368	<i>case</i> ¹ (regime 2)
050607	26.5	8.9±1.2	1.93±0.14	53.6±16.4	3525	<i>case</i> ¹ (regime 1)
050712	48±2	18	1.56±0.18	115.56±42.64	3576	<i>case</i> ¹ (regime 2)
050713A	70±10	91±6	1.58±0.07	110.37±25.84	3597	<i>case</i> ¹ (regime 1)
050713B	54.2	82±10	1.56±0.13	115.56±34.64	3600	<i>case</i> ¹ (regime 2)
050714B	46.7	6.5±1.4	2.6±0.3	18.28±8.08	3615	2.438	...	<i>case</i> ¹ (regime 1)
050802	13 ± 2	28±3	1.6±0.1	105.47±28.37	3737	1.7102	3749	<i>case</i> ¹ (regime 2)
050803	85 ± 10	39±3	1.5±0.1	133.14±35.98	3757	<i>case</i> ¹ (regime 2)
050814	65±20	21.7±3.6	1.8±0.17	68.94±24.5	3803	5.3	3809	<i>case</i> ¹ (regime 3)
050822	102±2	34±3	2.5±0.1	21.06±6.04	3856	1.434	H12	<i>case</i> ¹ (regime 1)
050824	25±5	2.8±0.5	2.7±0.4	15.95±12.45	3871	0.8278	3874	<i>case</i> ¹ (regime 1)
050826	35±8	4.3±0.7	1.2±0.3	297.96±61.25	3888	0.296	5982	<i>case</i> ¹ (regime 2)
050915B	40±1	34±1	1.89±0.06	57.81±13.27	3993	<i>case</i> ¹ (regime 2)
050922B	80±10	18±3	1.89±0.23	57.81±24.92	4019	<i>case</i> ¹ (regime 2)
051109B	15±1	2.7±0.4	1.96±0.25	50.69±24.63	4237	<i>case</i> ¹ (regime 2)
051221A	1.4	32±1	1.08±0.14	403 $^{+93}_{-72}$	4363 4394	0.5465	4384	<i>case</i> ¹ (regime 2)
060108	14.4±1	3.7±0.4	2.01±0.17	46.29±15.58	4445	2.03	4539	<i>case</i> ¹ (regime 1)
060109	116±3	6.4±1	1.96±0.25	50.69±24.47	4476	<i>case</i> ¹ (regime 1)
060115	142±5	19±1	1.76±0.12	74.77±20.42	4518	3.5328	4520	<i>case</i> ¹ (regime 1)
060203	60±10	8.5±1.2	1.62±0.23	100.84±45.17	4656	<i>case</i> ¹ (regime 2)
060204B	134±5	30±2	0.82±0.4	96.8±41	4671	<i>case</i> ¹ (regime 1)
060219	62 ± 2	4.2± 0.8	2.6±0.4	18.28±11.64	4811	<i>case</i> ¹ (regime 1)
060306	61 ± 2	22± 1	1.85±0.1	62.45±16.47	4851	1.55	P13	<i>case</i> ¹ (regime 1)
060312	43 ± 3	18± 1	1.35±0.34	62.8±21.5	4864	<i>case</i> ¹ (regime 3)
060413	150 ± 10	36± 1	1.67±0.08	90.36±22.8	4961	<i>case</i> ²
060428A	39.4 ± 2	14± 1	2.04±0.11	43.88±13.27	5022	<i>case</i> ¹ (regime 2)
060502A	33 ± 5	22± 1	1.43±0.08	158.21±39.79	5053	1.5026	5052	<i>case</i> ¹ (regime 2)
060510A	21	255± 7	1.661±0.072	186 $^{+36}_{-24}$	5113	<i>case</i> ¹ (regime 2)
060604	10 ± 3	1.3± 0.3	1.9±0.41	56.72±31.64	5214	2.1357	5218	<i>case</i> ¹ (regime 1)
060605	15 ± 2	4.6± 0.4	1.34±0.15	200.06±75.23	5231	3.773	5226	<i>case</i> ¹ (regime 3)
060607A	100 ± 5	26± 1	1.45±0.07	150.47±35.27	5242	3.0749	5237	<i>case</i> ⁴
060614	102	409± 18	1.57±0.12	302 $^{+214}_{-85}$	5264	0.1257	5276	<i>case</i> ¹ (regime 3)
060707	68 ± 5	17± 2	0.66±0.63	66 $^{+25}_{-10}$	5289	3.4240	5298	<i>case</i> ¹ (regime 2)
060712	26 ± 5	13± 2	1.64±0.32	96.47±25.27	5304	<i>case</i> ¹ (regime 1)
060714	115 ± 5	30± 2	1.99±0.1	47.99±12.52	5334	2.7108	5320	<i>case</i> ¹ (regime 2)
060719	55 ± 5	16± 1	2±0.11	47.13±12.88	5349	1.5320	K12	<i>case</i> ¹ (regime 1)
060729	116 ± 10	27± 2	1.86±0.14	61.24±17.75	5370	0.5428	F09	<i>case</i> ¹ (regime 2)
060804	16 ± 2	5.1± 0.9	1.78±0.28	71.78±56.05	5395	<i>case</i> ¹ (regime 2)
060805A	5.4 ± 0.5	0.74± 0.2	2.23±0.42	31.81±12.26	5403	2.44	...	<i>case</i> ¹ (regime 2)
060807	34 ± 4	7.3± 0.9	1.57±0.2	112.93±12.14	5421	<i>case</i> ¹ (regime 1)
060813	14.9 ± 0.5	55± 1	1±0.09	176 ± 83	5443	<i>case</i> ¹ (regime 2)
060814	134 ± 4	269± 12	1.43±0.16	257 $^{+122}_{-58}$	5460	1.9229	K12	<i>case</i> ¹ (regime 1)
060906	43.6 ± 1	22.1± 1.4	2.02±0.11	45.47 ± 12.14	5534 5538	3.6856	5535	<i>case</i> ¹ (regime 3)
060908	19.3 ± 0.3	29± 1	1.33±0.07	205.54 ± 48.55	5551	1.8836	F09	<i>case</i> ¹ (regime 2)
060923C	76 ± 2	16± 2	2.72±0.24	15.53 ± 5.36	5611	<i>case</i> ¹ (regime 3)

Table 2. Part II BAT observations and redshift for our sample

GRBname	T_{90} s	S_γ^a $10^{-7} \text{ ergs cm}^{-2}$	$\Gamma_{\gamma,1}^b$	E_p^b keV	BAT Ref ^c	z	z Ref ^c	Group of GRBs ^d
060927	22.6 ± 0.3	11 ± 1	0.93 ± 0.38	71.7 ± 17.6	5639	5.467	5651	<i>case</i> ¹ (regime 2)
061004	6.2 ± 0.3	5.7 ± 0.3	1.81 ± 0.10	67.57 ± 18.13	5964	<i>case</i> ¹ (regime 1)
061019	191 ± 3	17 ± 2	1.85 ± 0.26	62.45 ± 31.63	5732	<i>case</i> ¹ (regime 3)
061121	81 ± 5	137 ± 2	1.32 ± 0.05	606^{+90}_{-72}	5831 5837	1.3145	5826	<i>case</i> ¹ (regime 2)
061201	0.8 ± 0.1	3.3 ± 0.3	0.36 ± 0.65	873^{+458}_{-284}	5882 5890	0.111	5952	<i>case</i> ¹ (regime 3)
061202	91 ± 5	35 ± 1	1.63 ± 0.27	98.63 ± 23.83	5887	<i>case</i> ¹ (regime 2)
061222A	72 ± 3	83 ± 2	1.02 ± 0.11	324^{+54}_{-41}	5984	2.088	P09	<i>case</i> ¹ (regime 2)
070103	19 ± 1	3.4 ± 0.5	2 ± 0.2	47.13 ± 17.93	5991	2.6208	K12	<i>case</i> ¹ (regime 1)
070110	85 ± 5	16 ± 1	1.57 ± 0.12	112.93 ± 35.26	6007	2.3521	6010	<i>case</i> ⁴
070129	460 ± 20	31 ± 3	2.05 ± 0.16	43.11 ± 14.57	6058	2.3384	K12	<i>case</i> ¹ (regime 1)
070306	209.5 ± 10	53.80 ± 2.86	1.72 ± 0.1	84.74 ± 22.84	6173	1.49594	6202	<i>case</i> ¹ (regime 3)
070328	69 ± 5	90.6 ± 1.79	1.09 ± 0.08	421.59 ± 111.87	6225 6230	<i>case</i> ¹ (regime 2)
070420	77 ± 4	140 ± 4.48	1.08 ± 0.13	167^{+20}_{-16}	6342 6344	<i>case</i> ¹ (regime 2)
070429A	163 ± 5	9.1 ± 1.43	2.11 ± 0.27	38.85 ± 15.97	6362	<i>case</i> ¹ (regime 3)
070508	21 ± 1	196 ± 2.73	0.81 ± 0.07	188 ± 8	6390 6403	0.82	6398	<i>case</i> ¹ (regime 1)
070529	109.2 ± 3	25.70 ± 2.45	1.38 ± 0.16	179.9 ± 57.53	6468	2.4996	6470	<i>case</i> ¹ (regime 1)
070621	33.3	33 ± 1	1.57 ± 0.06	112.93 ± 24.8	6560 6571	<i>case</i> ¹ (regime 1)
070628	39.1 ± 2	35 ± 2	1.91 ± 0.09	55.65 ± 14.86	6589	<i>case</i> ¹ (regime 2)
070809	1.3 ± 0.1	1 ± 0.1	1.69 ± 0.22	86.56 ± 38.97	6732	0.2187	7889	<i>case</i> ¹ (regime 3)
070810A	11 ± 1	6.9 ± 0.6	2.04 ± 0.14	43.88 ± 13.64	6748	2.17	6741	<i>case</i> ¹ (regime 1)
071118	71 ± 20	5 ± 1	1.63 ± 0.29	98.63 ± 15.24	7109	<i>case</i> ²
080320	14 ± 2	2.7 ± 0.4	1.7 ± 0.22	84.74 ± 36.47	7505	<i>case</i> ¹ (regime 1)
080328	90.6 ± 1.5	94 ± 2	1.52 ± 0.04	126.92 ± 25.43	7533	<i>case</i> ¹ (regime 2)
080409	20.2 ± 8	6.1 ± 0.7	2.1 ± 0.2	39.52 ± 13.18	7582	<i>case</i> ¹ (regime 2)
080413B	8 ± 1	32 ± 1	1.26 ± 0.27	73.3 ± 15.8	7606	1.1014	7601	<i>case</i> ¹ (regime 1)
080430	16.2 ± 2.4	12 ± 1	1.73 ± 0.09	79.55 ± 20.16	7656	0.767	7654	<i>case</i> ¹ (regime 2)
080516	5.8 ± 0.3	2.6 ± 0.4	1.82 ± 0.27	66.24 ± 41.3	7736	3.2	7747	<i>case</i> ¹ (regime 1)
080703	3.4 ± 0.8	2 ± 0.3	1.53 ± 0.22	123.95 ± 63.34	7938	<i>case</i> ³ (regime 4)
080707	27.1 ± 1.1	5.2 ± 0.6	1.77 ± 0.19	73.25 ± 29.4	7953	1.2322	7949	<i>case</i> ¹ (regime 2)
080723A	17.3 ± 3	3.3 ± 0.4	1.77 ± 0.21	73.25 ± 28.43	8007	<i>case</i> ¹ (regime 2)
080903	66 ± 11	14 ± 1	0.84 ± 0.52	60 ± 15	8176	<i>case</i> ¹ (regime 3)
080905B	128 ± 16	18 ± 2	1.78 ± 0.15	71.78 ± 23.48	8188	2.3739	8191	<i>case</i> ¹ (regime 3)
081007	10 ± 4.5	7.1 ± 0.8	2.51 ± 0.2	20.76 ± 7.15	8338	0.5295	8335	<i>case</i> ¹ (regime 2)
081029	270 ± 45	21 ± 2	1.43 ± 0.18	158.21 ± 63.37	8447	3.8479	8438	<i>case</i> ¹ (regime 3)
081210	146 ± 8	18 ± 2	1.42 ± 0.14	162.27 ± 55.22	8649	<i>case</i> ¹ (regime 3)
081230	60.7 ± 13.8	8.2 ± 0.8	1.97 ± 0.16	49.77 ± 16.49	8759	<i>case</i> ¹ (regime 2)
090102	27 ± 2.2	0.68 ± 0.02	1.36 ± 0.08	189.64 ± 47.5	8769	1.547	8766	<i>case</i> ¹ (regime 3)
090113	9.1 ± 0.9	7.6 ± 0.4	1.6 ± 0.1	105.47 ± 28.92	8808	1.7493	K12	<i>case</i> ¹ (regime 1)
090205	8.8 ± 1.8	1.9 ± 0.3	2.15 ± 0.23	36.3 ± 12.57	8886	4.6497	8892	<i>case</i> ¹ (regime 3)
090313	78 ± 19	14 ± 2	1.91 ± 0.29	55.65 ± 28.37	8986	3.375	8994	<i>case</i> ¹ (regime 3)
090404	84 ± 14	30 ± 1	2.32 ± 0.08	27.58 ± 7.22	9089	3	P13	<i>case</i> ¹ (regime 1)
090407	310 ± 70	11 ± 2	1.73 ± 0.29	79.55 ± 36.98	9104	1.4485	K12	<i>case</i> ¹ (regime 2)
090418A	56 ± 5	46 ± 2	1.48 ± 0.07	139.75 ± 32.45	9157	1.608	9151	<i>case</i> ¹ (regime 2)
090424	52	201	0.9 ± 0.02	177 ± 3	9230	0.544	9243	<i>case</i> ¹ (regime 2)
090429B	5.5 ± 1	3.1 ± 0.3	0.47 ± 0.77	42.1 ± 5.6	9290	9.4	C11	<i>case</i> ¹ (regime 2)
090510	0.3 ± 0.1	3.4 ± 0.4	0.98 ± 0.2	618.98 ± 30.97	9337	0.903	9353	<i>case</i> ¹ (regime 3)
090518	6.9 ± 1.7	4.7 ± 0.4	1.54 ± 0.14	121.07 ± 40.95	9393	<i>case</i> ¹ (regime 1)
090529	100	6.8 ± 1.7	2 ± 0.3	47.13 ± 26.19	9434	2.625	9457	<i>case</i> ¹ (regime 3)

Table 2. Part III BAT observations and redshift for our sample

GRBname	T_{90} s	S_γ^a $10^{-7} \text{ ergs cm}^{-2}$	$\Gamma_{\gamma,1}^b$	E_p^b keV	BAT Ref ^c	z	z Ref ^c	Group of GRBs ^d
090530	48 ± 36	11 ± 1	1.61 ± 0.17	103.12 ± 34.85	9443	1.266	15571	<i>case</i> ¹ (regime 2)
090727	302 ± 23	14 ± 2	1.24 ± 0.24	264.7 ± 140.61	9724	<i>case</i> ¹ (regime 2)
090728	59 ± 18	10 ± 2	2.05 ± 0.26	43.11 ± 19.87	9736	<i>case</i> ¹ (regime 3)
090813	9	13 ± 1	1.43 ± 0.08	158.21 ± 39.97	9792	<i>case</i> ¹ (regime 2)
090904A	122 ± 10	30 ± 2	2.01 ± 0.1	46.29 ± 12.36	9888	<i>case</i> ¹ (regime 2)
091018	4.4 ± 0.6	14 ± 1	1.77 ± 0.24	19.3^{+18}_{-11}	10040	0.971	10038	<i>case</i> ¹ (regime 2)
091029	39.2 ± 5	24 ± 1	1.46 ± 0.27	61.4 ± 17.5	10103	2.752	10100	<i>case</i> ¹ (regime 1)
091130B	112.5 ± 17.1	13 ± 1	2.15 ± 0.15	36.3 ± 12.26	10221	<i>case</i> ¹ (regime 1)
100111A	12.9 ± 2.1	6.7 ± 0.5	1.69 ± 0.13	86.56 ± 25.02	10322	<i>case</i> ¹ (regime 2)
100219A	18.8 ± 5	3.7 ± 0.6	1.34 ± 0.25	200 ± 93.9	10434	4.6667	10445	<i>case</i> ³ (regime 4)
100302A	17.9 ± 1.7	3.1 ± 0.4	1.72 ± 0.19	81.23 ± 29.1	10462	4.813	10466	<i>case</i> ¹ (regime 1)
100418A	7 ± 1	3.4 ± 0.5	2.16 ± 0.25	35.7 ± 13.96	10615	0.6235	10620	<i>case</i> ¹ (regime 2)
100425A	37 ± 2.4	4.7 ± 0.9	2.42 ± 0.32	23.68 ± 12.53	10685	1.755	10684	<i>case</i> ¹ (regime 2)
100508A	52 ± 10	7 ± 1.1	1.23 ± 0.25	272.55 ± 146.57	10732	<i>case</i> ²
100522A	35.3 ± 1.8	21 ± 1	1.89 ± 0.08	57.81 ± 14.68	10788	<i>case</i> ¹ (regime 1)
100614A	225 ± 55	27 ± 2	1.88 ± 0.15	58.92 ± 18.98	10852	<i>case</i> ¹ (regime 3)
100704A	197.5 ± 23.3	60 ± 2	1.73 ± 0.06	79.55 ± 17.95	10932	<i>case</i> ¹ (regime 2)
100725B	200 ± 30	68 ± 2	1.89 ± 0.06	57.81 ± 13.41	10993	<i>case</i> ¹ (regime 1)
100901A	439 ± 33	21 ± 3	1.59 ± 0.21	107.88 ± 53.74	11169	1.408	11164	<i>case</i> ¹ (regime 2)
100902A	428.8 ± 43	32 ± 2	1.98 ± 0.13	48.87 ± 14.16	11202	<i>case</i> ²
100905A	3.4 ± 0.5	1.7 ± 0.2	1.09 ± 0.19	421.59 ± 40.24		<i>case</i> ¹ (regime 2)
100906A	114.4 ± 1.6	120	1.78 ± 0.03	71.78 ± 14.63	11233	1.727	11230	<i>case</i> ¹ (regime 3)
101117B	5.2 ± 1.8	11 ± 1	1.5 ± 0.09	133.14 ± 34.9	11414	<i>case</i> ¹ (regime 2)
110102A	264 ± 8	165 ± 3	1.6 ± 0.04	105.47 ± 21.62	11511	<i>case</i> ¹ (regime 2)
110106B	24.8 ± 4.8	20 ± 1	1.76 ± 0.11	74.77 ± 20.26	11533	0.618	11538	<i>case</i> ¹ (regime 3)
110312A	28.7 ± 7.6	8.2 ± 1.3	2.32 ± 0.26	27.58 ± 10.97	11783	<i>case</i> ¹ (regime 1)
110319A	19.3 ± 1.6	14 ± 1	1.31 ± 0.43	21.9 ± 7	11811	<i>case</i> ¹ (regime 1)
110411A	80.3 ± 5.2	33 ± 2	1.51 ± 0.31	41 ± 8.1	11921	<i>case</i> ²
110530A	19.6 ± 3.1	3.3 ± 0.5	2.06 ± 0.24	42.36 ± 16.22	12049	<i>case</i> ¹ (regime 1)
110808A	48 ± 23	3.3 ± 0.8	2.32 ± 0.43	27.58 ± 49.72	12262	1.348	12258	<i>case</i> ¹ (regime 3)
111008A	63.46 ± 2.19	53 ± 3	1.86 ± 0.09	61.24 ± 16.32	12424	4.9898	12431	<i>case</i> ¹ (regime 2)
111228A	101.2 ± 5.42	85 ± 2	2.27 ± 0.06	29.84 ± 7.59	12749	0.716	12761	<i>case</i> ¹ (regime 2)
120106A	61.6 ± 4.1	9.7 ± 1.1	1.53 ± 0.17	123.95 ± 45.81	12815	<i>case</i> ¹ (regime 1)
120224A	8.13 ± 1.99	2.4 ± 0.5	2.25 ± 0.36	30.8 ± 32	12983	<i>case</i> ¹ (regime 1)
120308A	60.6 ± 17.1	12 ± 1	1.71 ± 0.13	82.96 ± 23.8	13022	<i>case</i> ¹ (regime 3)
120324A	118 ± 10	101 ± 3	1.34 ± 0.04	200.06 ± 38.03	13096	<i>case</i> ¹ (regime 1)
120326A	69.6 ± 8.3	26 ± 3	1.41 ± 0.34	41.1 ± 6.9	13120	1.798	13118	<i>case</i> ¹ (regime 3)
120521C	26.7 ± 4.4	11 ± 1	1.73 ± 0.11	79.55 ± 22.68	13333	6	13348	<i>case</i> ¹ (regime 1)
120703A	25.2 ± 4.3	35 ± 1	1.51 ± 0.06	129.98 ± 27.54	13414	<i>case</i> ¹ (regime 2)
120811C	26.8 ± 3.7	30 ± 3	1.4 ± 0.3	42.9 ± 5.7	13634	2.671	13628	<i>case</i> ¹ (regime 1)
120907A	16.9 ± 8.9	6.7 ± 1.1	1.73 ± 0.25	79.55 ± 42.57	13720	0.97	13723	<i>case</i> ¹ (regime 2)
121024A	69 ± 32	11 ± 1	1.41 ± 0.22	166.46 ± 100.22	13899	0.97	13890	<i>case</i> ¹ (regime 1)
121031A	226 ± 19	78 ± 2	1.5 ± 0.05	133.14 ± 28.49	13949	<i>case</i> ¹ (regime 1)
121123A	317 ± 14	150 ± 10	0.96 ± 0.2	65 ± 5.1	13990	<i>case</i> ¹ (regime 3)
121125A	53.2 ± 4.6	47 ± 1	1.52 ± 0.06	126.92 ± 27.68	13996	<i>case</i> ¹ (regime 2)
121128A	23.3 ± 1.6	69 ± 4	1.32 ± 0.18	64.5 ± 6.8	14011	2.2	14009	<i>case</i> ¹ (regime 3)
121211A	182 ± 39	13 ± 2.67	2.36 ± 0.26	25.93 ± 10.67	14067	1.023	14059	<i>case</i> ¹ (regime 3)
130131A	51.6 ± 2.4	3.1 ± 0.6	2.12 ± 0.32	38.19 ± 25.72	14163	<i>case</i> ¹ (regime 1)

Table 2. Part IV BAT observations and redshift for our sample

GRBname	T_{90} s	S_{γ}^{a}	$\Gamma_{\gamma,1}^{\text{b}}$	E_p^{b} keV	BAT Ref ^c	z	z Ref ^c	Group of GRBs ^d
		$10^{-7}\text{ergs cm}^{-2}$						
130603B	0.18 ± 0.02	6.3 ± 0.3	0.82 ± 0.07	1177.96 ± 322.01	14741	0.356	14744	<i>case</i> ¹ (regime 2)
130609B	210.6 ± 15.1	160	1.32 ± 0.04	211.22 ± 40.09	14867	<i>case</i> ¹ (regime 3)
131018A	73.22 ± 18.97	11 ± 1	2.24 ± 0.14	31.3 ± 9.47	15354	<i>case</i> ¹ (regime 2)
131105A	112.3 ± 4.1	71 ± 5	1.45 ± 0.11	150.47 ± 44.64	15459	1.686	15450	<i>case</i> ¹ (regime 2)
140108A	94 ± 4	70 ± 2	1.62 ± 0.05	100.84 ± 22.11	15717	<i>case</i> ¹ (regime 1)
140114A	139.7 ± 16.4	32 ± 1	2.06 ± 0.09	42.36 ± 11.23	15738	<i>case</i> ¹ (regime 2)
140323A	104.9 ± 2.6	160	1.35 ± 0.17	127.1 ± 59.2	16029	<i>case</i> ¹ (regime 2)
140331A	209 ± 33	6.7 ± 1.3	2.01 ± 0.29	46.29 ± 26.12	16063	<i>case</i> ¹ (regime 3)
140430A	173.6 ± 3.7	11 ± 2	2 ± 0.22	47.13 ± 20.29	16200	1.6	16194	<i>case</i> ¹ (regime 2)
140512A	154.8 ± 4.88	140 ± 3	1.45 ± 0.04	150.47 ± 29.96	16258	0.725	16310	<i>case</i> ¹ (regime 3)
140518A	60.5 ± 2.4	10 ± 1	0.92 ± 0.61	43.9 ± 7.6	16306	4.707	16301	<i>case</i> ¹ (regime 2)
140703A	67.1 ± 67.9	39 ± 3	1.74 ± 0.13	77.91 ± 23.87	16509	3.14	16505	<i>case</i> ¹ (regime 3)
140706A	48.3 ± 4.3	20 ± 1	1.8 ± 0.1	68.94 ± 18.46	16539	<i>case</i> ¹ (regime 2)
140709A	98.6 ± 7.7	53 ± 2	1.23 ± 0.27	78 ± 20.4	16553	<i>case</i> ¹ (regime 2)
140916A	80.1 ± 15.6	17 ± 3	2.15 ± 0.27	36.3 ± 16.26	16827	<i>case</i> ¹ (regime 3)
141017A	55.7 ± 2.8	31 ± 1	1.05 ± 0.28	80.4 ± 17.2	16927	<i>case</i> ¹ (regime 1)
141031A	920 ± 10	29 ± 5	1.21 ± 0.13	289.16 ± 99.79	17010	<i>case</i> ¹ (regime 1)
141121A	549.9 ± 37.4	53 ± 4	1.73 ± 0.13	79.55 ± 22.45	17083	1.47	17081	<i>case</i> ¹ (regime 3)
150120B	24.30 ± 3.39	5.4 ± 0.8	2.20 ± 0.25	33.41 ± 13.05	17330	<i>case</i> ¹ (regime 1)
150201A	26.1 ± 5.2	7.8 ± 1.2	2.32 ± 0.24	27.58 ± 11.34	17374	<i>case</i> ¹ (regime 1)
150203A	25.8 ± 5	9.1 ± 0.6	1.9 ± 0.12	56.72 ± 15.74	17410	<i>case</i> ¹ (regime 1)
150323A	149.6 ± 8.9	61 ± 2	1.85 ± 0.07	62.45 ± 14.78	17628	0.593	17616	<i>case</i> ¹ (regime 2)
150323C	159.4 ± 54	13 ± 3	2.09 ± 0.32	40.2 ± 24	17637	<i>case</i> ¹ (regime 1)
150424A	91 ± 22	15 ± 1	1.23 ± 0.15	272.55 ± 104.2	17761	0.3	17758	<i>case</i> ¹ (regime 2)
150607A	26.3 ± 0.7	23 ± 2	0.99 ± 0.41	84.9 ± 40.1	17907	<i>case</i> ¹ (regime 2)
150615A	27.6 ± 5.1	5.5 ± 0.7	1.84 ± 0.21	63.68 ± 27.83	17930	<i>case</i> ¹ (regime 1)
150626A	599.5 ± 99.3	18 ± 2	1.37 ± 0.25	92.5 ± 45.9	17941	<i>case</i> ¹ (regime 1)
150711A	64.2 ± 14.2	43 ± 2	1.79 ± 0.08	70.34 ± 17.49	18020	<i>case</i> ¹ (regime 2)
150910A	112.2 ± 38.3	48 ± 4	1.42 ± 0.12	162.27 ± 45.97	18268	1.359	18273	<i>case</i> ³ (regime 4)
151027A	129.69 ± 5.55	78 ± 2	1.72 ± 0.05	81.23 ± 17.55	18496	0.81	18487	<i>case</i> ¹ (regime 3)
151112A	19.32 ± 31.24	9.4 ± 1.2	1.77 ± 0.21	73.25 ± 28.15	18593	4.1	18603	<i>case</i> ¹ (regime 2)
151228B	48 ± 16	24 ± 1	1.09 ± 0.34	78.1 ± 27	18752	<i>case</i> ¹ (regime 3)
151229A	1.78 ± 0.44	5.9 ± 0.4	1.84 ± 0.1	63.68 ± 18.03	18751	<i>case</i> ¹ (regime 1)
160119A	116 ± 14	71 ± 2	1.68 ± 0.05	83.44 ± 19.62	18899	<i>case</i> ¹ (regime 1)
160127A	6.16 ± 0.94	3.3 ± 0.5	0.99 ± 1.11	25.6	18944	<i>case</i> ¹ (regime 3)
160227A	316.5 ± 75.4	31 ± 2	0.75 ± 0.51	65.8 ± 16.4	19106	2.38	19109	<i>case</i> ¹ (regime 2)
160327A	28 ± 9	14 ± 1	1.84 ± 0.11	63.68 ± 17.11	19240	4.99	19245	<i>case</i> ¹ (regime 2)
160412A	31.6 ± 4	19 ± 1	1.88 ± 0.08	58.92 ± 14.57	19301	<i>case</i> ¹ (regime 2)
160630A	29.5 ± 5.51	12 ± 1	1.32 ± 0.14	211.22 ± 76.23	19639	<i>case</i> ¹ (regime 2)
160804A	144.2 ± 19.2	114 ± 3	1.4 ± 0.23	52.7 ± 5.4	19765	0.736	19773	<i>case</i> ¹ (regime 1)
160824A	99.3 ± 7.8	26 ± 2	1.64 ± 0.11	96.47 ± 22.41	19861	<i>case</i> ¹ (regime 2)
161001A	2.6 ± 0.4	6.7 ± 0.4	1.14 ± 0.09	358.57 ± 99.67	19974	<i>case</i> ¹ (regime 1)
161011A	4.3 ± 1.3	2.3 ± 0.4	1.15 ± 0.35	347.44 ± 43.24	20032	<i>case</i> ¹ (regime 3)
161108A	105.1 ± 11.9	11 ± 1	1.85 ± 0.17	62.45 ± 22.88	20151	1.159	20150	<i>case</i> ¹ (regime 1)
161129A	35.53 ± 2.09	36 ± 1	1.57 ± 0.06	112.93 ± 24.12	20220	0.645	20245	<i>case</i> ¹ (regime 3)
161202A	181	86 ± 3	1.43 ± 0.3	222^{+201}_{-63}	20238	<i>case</i> ²
161214B	24.8 ± 3.1	21 ± 1	1.76 ± 0.09	74.77 ± 19	20270	<i>case</i> ¹ (regime 1)
170113A	20.66 ± 4.4	6.7 ± 0.7	0.75 ± 0.59	73.3 ± 33.6	20456	1.968	20458	<i>case</i> ¹ (regime 2)

Table 2. Part V BAT observations and redshift for our sample

GRBname	T_{90}	S_γ^a	$\Gamma_{\gamma,1}^b$	E_p^b	BAT Ref ^c	z	z Ref ^c	Group of GRBs ^d
	s	$10^{-7}\text{ergs cm}^{-2}$		keV				
170202A	46.2 ± 11.5	33 ± 1	1.68 ± 0.07	88.44 ± 20.87	20596	3.645	20584	<i>case</i> ¹ (regime 2)
170208B	128.07 ± 5.75	61 ± 2	1.18 ± 0.21	97.8 ± 27.4	20654	<i>case</i> ¹ (regime 1)
170317A	11.94 ± 4.87	13 ± 1	0.8 ± 0.49	58.8 ± 10.5	20896	<i>case</i> ¹ (regime 1)
170330A	144.73 ± 3.51	56 ± 3	1.38 ± 0.09	179.9 ± 45.88	20968	<i>case</i> ¹ (regime 2)
170607A	23	75 ± 3	1.61 ± 0.07	103.12 ± 23.51	21218	<i>case</i> ¹ (regime 1)
170711A	31.3 ± 7.6	14 ± 1	1.75 ± 0.1	76.32 ± 20.03	21331	<i>case</i> ¹ (regime 2)

^a S_γ represents the fluence of gamma rays in the 15-150 keV band.

^b $\Gamma_{\gamma,1}$ represents the power law index of the time-averaged spectrum.

^c The references of BAT observations and redshift for our sample.

^d External shock model regimes for individual bursts (adjusted by closure relations with temporal and spectrum properties of shallow decay's follow-up phase).

NOTE—References: (F09)Fynbo et al. (2009); (P09)Perley et al. (2009); (C11)Cucchiara et al. (2011a); (H12) Hjorth et al. (2012) ; (K12)Kruhler et al. (2012); (P13)Perley et al. (2013); (3119)Krimm et al. (2005a); (3136)Fynbo et al. (2005a); (3173)Sakamoto et al. (2005a); (3176)Fynbo et al. (2005b); (3273)Sakamoto et al. (2005b);(3364)Hullinger et al. (2005a);(3368)Berger et al. (2005a); (3525)Retter et al. (2005);(3542)Cenko et al. (2005); (3576)Markwardt et al. (2005a); (3597)Palmer et al. (2005a);(3600)Parsons et al. (2005a); (3615)Tueller et al. (2005a); (3737)Palmer et al. (2005b); (3749)Fynbo et al. (2005c); (3757)Parsons et al. (2005b); (3803)Tueller et al. (2005b); (3809)Jensen et al. (2005); (3856)Hullinger et al. (2005b); (3871)Krimm et al. (2005b); (3874)Fynbo et al. (2005d); (3888)Markwardt et al. (2005b); (3993)Cummings et al. (2005); (4019)Hullinger et al. (2005c); (4237)Hullinger et al. (2005d); (4363)Parsons et al. (2005c); (4384)Berger & Soderberg (2005b); (4394)Golenetskii et al. (2005); (4445)Sakamoto et al. (2006a); (4476)Palmer et al. (2006a); (4518)Barbier et al. (2006a); (4520)Piranomonte et al. (2006); (4539)Melandri et al. (2006); (4656)Krimm et al. (2006a);(4671)Markwardt et al. (2006a); (4811)Sakamoto et al. (2006b); (4851)Hullinger et al. (2006a); (4864)Krimm et al. (2006b); (4961)Barbier et al. (2006b); (5022)Markwardt et al. (2006b); (5052)Cucchiara et al. (2006); (5053)Parsons et al. (2006a); (5113)Golenetskii et al. (2006a); (5214)Parsons et al. (2006b); (5218)Castro-Tirado et al. (2006); (5226)Still et al. (2006); (5231)Sato et al. (2006a); (5237)Ledoux et al. (2006); (5242)Tueller et al. (2006a); (5264)Golenetskii et al. (2006b); (5276)Fugazza et al. (2006);(5289)Stamatikos et al. (2006a); (5298)Jakobsson et al. (2006a); (5304)Hullinger et al. (2006b); (5320)Jakobsson et al. (2006b); (5334)Krimm et al. (2006c); (5349)Sakamoto et al. (2006e); (5370)Parsons et al. (2006c); (5395)Tueller et al. (2006b); (5403)Barbier et al. (2006c); (5421)Barthelmy et al. (2006); (5443)Cummings et al. (2006); (5460)Golenetskii et al. (2006c); (5534)Sakamoto et al. (2006d); (5535)Vreeswijk et al. (2006); (5538)Sato et al. (2006b); (5551)Palmer et al. (2006b);(5611)Sakamoto et al. (2006f); (5639)Stamatikos et al. (2006b); (5651)Fynbo et al. (2006); (5732)Sakamoto et al. (2006g); (5826)Bloom et al. (2006); (5831)Fenimore et al. (2006); (5837)Golenetskii et al. (2006d); (5882)Markwardt et al. (2006c); (5887)Sakamoto et al. (2006h); (5890)Golenetskii et al. (2006e); (5952)Berger (2006); (5964)Tueller et al. (2006c); (5982)Halpern & Mirabal (2006); (5984)Pal'Shin (2006); (5991)Barbier et al. (2007); (6007)Cummings et al. (2007); (6010)Jaunsen et al. (2007a); (6058)Krimm et al. (2007a); (6173)Barthelmy et al. (2007a); (6202)Jaunsen et al. (2007b); (6225) Stamatikos et al. (2007); (6230)Golenetskii et al. (2007a); (6342)Parsons et al. (2007a); (6344)Golenetskii et al. (2007b); (6362)Cannizzo et al. (2007); (6390)Barthelmy et al. (2007b); (6398)Jakobsson et al. (2007); (6403)Golenetskii et al. (2007c); (6468)Parsons et al. (2007b); (6470)Berger et al. (2007); (6560)Sbarufatti et al. (2007); (6571)Fenimore et al. (2007); (6589)Krimm et al. (2007b); (6732)Krimm et al. (2007c); (6741)Thoene et al. (2007); (6748)Markwardt et al. (2007a); (7109)Markwardt et al. (2007b); (7505)McLean et al. (2008); (7533)Krimm et al. (2008a); (7582)Palmer et al. (2008a); (7601)Vreeswijk et al. (2008a); (7606)Barthelmy et al. (2008a); (7654)Cucchiara & Fox (2008); (7656)Stamatikos et al. (2008a); (7736)Krimm et al. (2008b); (7747)Filgas et al. (2008); (7889)Perley et al. (2008); (7938)Sakamoto et al. (2008); (7949)Fynbo et al. (2008); (7953)Schady & Marshall (2008); (8007)Stamatikos et al. (2008b); (8176)Tueller et al. (2008); (8188)Barthelmy et al. (2008b); (8191)Vreeswijk et al. (2008b); (8335)Berger et al. (2008); (8338)Markwardt et al. (2008); (8438)D'Elia et al. (2008); (8447)Cummings et al. (2008); (8649)Barthelmy et al. (2008c); (8759)Palmer et al. (2008b); (8766)de Ugarte Postigo et al. (2009); (8769)Sakamoto et al. (2009b); (8808)Tueller et al. (2009a); (8886)Cummings et al. (2009a); (8986)Sakamoto et al. (2009c); (9089)Tueller et al. (2009b); (9104)Ukwatta et al. (2009a); (9151)Chornock et al. (2009a); (9157)Fenimore et al. (2009); (9230)Connaughton (2009); (9243)Chornock et al. (2009b); (9290)Stamatikos et al. (2009), (9337)Ukwatta et al. (2009b); (9353)Rau et al. (2009); (9393)Cummings et al. (2009b); (9434)Markwardt et al. (2009a); (9443)Palmer et al. (2009a); (9457)Malesani et al. (2009b); (9724)Markwardt et al. (2009c); (9736)Palmer et al. (2009b); (9792)von Kienlin (2009); (9888)Palmer et al. (2009c); (10038)Chen et al. (2009); (10040)Markwardt et al. (2009d); (10100)Chornock et al. (2009c); (10103)Barthelmy et al. (2009); (10322)Krimm et al. (2010); (10445)de Ugarte Postigo et al. (2010);

NOTE—References Continued:(10462)Cummings et al. (2010a); (10466)Chornock et al. (2010a); (10615)Ukwatta et al. (2010); (10620)Antonelli et al. (2010); (10684)Goldoni et al. (2010); (10685)Markwardt et al. (2010); (10732)Stamatikos et al. (2010a); (10788)Barthelmy et al. (2010a); (10852)Sakamoto et al. (2010a). (10932)Cummings et al. (2010b); (10993)Sakamoto et al. (2010b); (11164)Chornock et al. (2010b); (11169)Sakamoto et al. (2010c); (11202)Stamatikos et al. (2010b); (11218)Barthelmy et al. (2010b); (11230)Tanvir et al. (2010); (11233)Barthelmy et al. (2010c); (11414)Baumgartner et al. (2010); (11511)Sakamoto et al. (2011a); (11533)Ukwatta et al. (2011); (11538)Chornock et al. (2011); (11691)Stamatikos et al. (2011); (11783)Barthelmy et al. (2011a); (11811)Fruchter et al. (2011); (11921)Barthelmy et al. (2011b); (12049)Baumgartner et al. (2011a); (12258)de Ugarte Postigo et al. (2011); (12262)Sakamoto et al. (2011b); (12424)Baumgartner et al. (2011b); (12431)Wiersema et al. (2011); (12749)Cummings et al. (2011); (12761)Cucchiara & Levan (2011b); (12815)Barthelmy et al. (2012a); (12983)Barthelmy et al. (2012b); (13022)Sakamoto et al. (2012); (13096)Cummings et al. (2012a); (13118)Tello et al. (2012); (13120)Barthelmy et al. (2012c); (13333)Markwardt et al. (2012); (13348)Tanvir et al. (2012a); (13414)Stamatikos et al. (2012a); (13628)Thoene et al. (2012); (13634) Krimm et al. (2012); (13720) Stamatikos et al. (2012b); (13723)Sanchez-Ramirez et al. (2012); (13890)Tanvir et al. (2012b); (13899)Barthelmy et al. (2012d); (13949)Cummings et al. (2012b); (13990)Barthelmy et al. (2012e); (13996)Barthelmy et al. (2012f); (14011)Palmer et al. (2012); (14067)Barthelmy et al. (2012g); (14163)Palmer et al. (2013); (14741)Barthelmy et al. (2013); (14867)Krimm & Cummings (2013); (15354)Ukwatta et al. (2013); (15459)Baumgartner et al. (2013); (15571)Goldoni et al. (2013); (15717)Cummings (2014); (15738)Krimm et al. (2014a); (16029)Sakamoto et al. (2014a); (16063)Stamatikos et al. (2014a); (16194)Kruehler et al. (2014); (16200)Krimm et al. (2014b); (16258)Sakamoto et al. (2014b); (16301)Chornock et al. (2014); (16306)Ukwatta et al. (2014a); (16310)de Ugarte Postigo et al. (2014); (16505)Castro-Tirado et al. (2014); (16509)Krimm et al. (2014c); (16539)Markwardt et al. (2014a); (16553)Markwardt et al. (2014b); (16827)Stamatikos et al. (2014b); (16927)Markwardt et al. (2014c); (17010)Ukwatta et al. (2014b); (17081)Perley et al. (2014); (17083)Krimm et al. (2014d); (17330)Markwardt et al. (2015a); (17374)Palmer et al. (2015a); (17410)Ukwatta et al. (2015); (17616)Perley & Cenko (2015a); (17628)Markwardt et al. (2015b); (17637)Palmer et al. (2015b); (17758)Castro-Tirado et al. (2015); (17761)Barthelmy et al. (2015); (17907)Palmer et al. (2015c); (17930)Sakamoto et al. (2015); (17941)Stamatikos et al. (2015); (18020)Krimm et al. (2015a); (18268)Lien et al. (2015a); (18273)Zheng et al. (2015); (18487)Perley et al. (2015b); (18496)Palmer et al. (2015d); (18593)Krimm et al. (2015b); (18603)Bolmer et al. (2015); (18751)Lien et al. (2015b); (18752)Krimm et al. (2015c); (18899)Stamatikos et al. (2016); (18944)Barthelmy et al. (2016); (19106)Sakamoto et al. (2016a); (19109)Xu et al. (2016a); (19240)Markwardt et al. (2016a); (19245)de Ugarte Postigo et al. (2016a); (19301)Ukwatta et al. (2016a); (19639)Krimm et al. (2016a); (19765)Krimm et al. (2016b); (19773)Xu et al. (2016b); (19861)Sakamoto et al. (2016b); (19974)Markwardt et al. (2016b); (20032)Ukwatta et al. (2016b); (20150)de Ugarte Postigo et al. (2016b); (20151)Palmer et al. (2016); (20220)Mooley et al. (2016); (20238)Kozlova et al. (2016); (20245)Cano et al. (2016); (20270)Krimm et al. (2016c); (20456)Markwardt et al. (2017a); (20458)Xu et al. (2017); (20584)de Ugarte Postigo et al. (2017); (20596)Barthelmy et al. (2017a); (20654)Barthelmy et al. (2017a); (20896)Barthelmy et al. (2017b); (20968)Lien et al. (2017); (21218)Markwardt et al. (2017b).

REFERENCES

- Antonelli, L. A., Maund, J. R., Palazzi, E., et al. 2010, GRB Coordinates Network, Circular Service, No. 10620, #1 (2010), 10620, 1
- Arnaud, K. A. 1996, Astronomical Data Analysis Software and Systems V, 17.
- Barbier, L., Barthelmy, S., Cummings, J., et al. 2006a, GRB Coordinates Network, 4518, 1
- Barbier, L., Barthelmy, S., Cummings, J., et al. 2006b, GRB Coordinates Network, 4961, 1
- Barbier, L., Barthelmy, S., Cummings, J., et al. 2006c, GRB Coordinates Network, 5403, 1
- Barbier, L., Barthelmy, S. D., Cummings, J., et al. 2007, GRB Coordinates Network, 5991, 1
- Barthelmy, S. D., Barbier, L., Cummings, J., et al. 2006, GRB Coordinates Network, 5421, 1
- Barthelmy, S. D., Barbier, L., Cummings, J., et al. 2007a, GRB Coordinates Network, 6173, 1
- Barthelmy, S. D., Barbier, L., Cummings, J., et al. 2007b, GRB Coordinates Network, 6390, 1
- Barthelmy, S. D., Baumgartner, W., Cummings, J., et al. 2008a, GRB Coordinates Network, 7606, 1
- Barthelmy, S. D., Baumgartner, W., Cummings, J., et al. 2008b, GRB Coordinates Network, 8188, 1
- Barthelmy, S. D., Baumgartner, W. H., Cummings, J. R., et al. 2008c, GRB Coordinates Network, 8649, 1
- Barthelmy, S. D., Baumgartner, W. H., Cummings, J. R., et al. 2009, GRB Coordinates Network, Circular Service, No. 10103, #1 (2009), 10103, 1
- Barthelmy, S. D., Baumgartner, W. H., Cummings, J. R., et al. 2010a, GRB Coordinates Network, Circular Service, No. 10788, #1 (2010c), 10788, 1
- Barthelmy, S. D., Baumgartner, W. H., Cummings, J. R., et al. 2010b, GRB Coordinates Network, Circular Service, No. 11218, #1 (2010a), 11218, 1
- Barthelmy, S. D., Baumgartner, W. H., Cummings, J. R., et al. 2010c, GRB Coordinates Network, Circular Service, No. 11233, #1 (2010b), 11233, 1
- Barthelmy, S. D., Baumgartner, W. H., Cummings, J. R., et al. 2011a, GRB Coordinates Network, Circular Service, No. 11783, #1 (2011b), 11783, 1
- Barthelmy, S. D., Baumgartner, W. H., Cummings, J. R., et al. 2011b, GRB Coordinates Network, Circular Service, No. 11921, #1 (2011a), 11921, 1
- Barthelmy, S. D., Sakamoto, T., Baumgartner, W. H., et al. 2012a, GRB Coordinates Network, Circular Service, No. 12815, #1 (2012a), 12815, 1
- Barthelmy, S. D., Baumgartner, W. H., Cummings, J. R., et al. 2012b, GRB Coordinates Network, Circular Service, No. 12983, #1 (2012b), 12983, 1
- Barthelmy, S. D., Sakamoto, T., Markwardt, C. B., et al. 2012c, GRB Coordinates Network, Circular Service, No. 13120, #1 (2012c), 13120, 1
- Barthelmy, S. D., Sakamoto, T., Baumgartner, W. H., et al. 2012d, GRB Coordinates Network, Circular Service, No. 13899, #1 (2012d), 13899, 1
- Barthelmy, S. D., Baumgartner, W. H., Cummings, J. R., et al. 2012e, GRB Coordinates Network, Circular Service, No. 13990, #1 (2012e), 13990, 1
- Barthelmy, S. D., Barlow, B. N., Baumgartner, W. H., et al. 2012f, GRB Coordinates Network, Circular Service, No. 13996, #1 (2012f), 13996, 1
- Barthelmy, S. D., Baumgartner, W. H., Cummings, J. R., et al. 2012g, GRB Coordinates Network, Circular Service, No. 14067, #1 (2012g), 14067, 1
- Barthelmy, S. D., Baumgartner, W. H., Cummings, J. R., et al. 2013, GRB Coordinates Network, Circular Service, No. 14741, #1 (2013), 14741, 1
- Barthelmy, S. D., Baumgartner, W. H., Beardmore, A. P., et al. 2015, GRB Coordinates Network, Circular Service, No. 17761, #1 (2015), 17761, 1
- Barthelmy, S. D., Amaral-Rogers, A., Cummings, J. R., et al. 2016, GRB Coordinates Network, Circular Service, No. 18944, #1 (2016), 18944, 1
- Barthelmy, S. D., Cummings, J. R., Gehrels, N., et al. 2017a, GRB Coordinates Network, Circular Service, No. 20596, #1 (2017a), 20596, 1
- Barthelmy, S. D., Cummings, J. R., Gehrels, N., et al. 2017b, GRB Coordinates Network, Circular Service, No. 20896, #1 (2017b), 20896, 1
- Baumgartner, W. H., Barthelmy, S. D., Cummings, J. R., et al. 2010, GRB Coordinates Network, Circular Service, No. 11414, #1 (2010), 11414, 1
- Baumgartner, W. H., Barthelmy, S. D., Cummings, J. R., et al. 2011a, GRB Coordinates Network, Circular Service, No. 12049, #1 (2011a), 12049, 1
- Baumgartner, W. H., Barthelmy, S. D., Cummings, J. R., et al. 2011b, GRB Coordinates Network, Circular Service, No. 12424, #1 (2011b), 12424, 1
- Baumgartner, W. H., Barthelmy, S. D., Cummings, J. R., et al. 2013, GRB Coordinates Network, Circular Service, No. 15459, #1 (2013), 15459, 1
- Belokurov, V., Walker, M. G., Evans, N. W., et al. 2009, MNRAS, 397, 1748
- Berger, E., Cenko, S. B., Steidel, C., Reddy, N., & Fox, D. B. 2005a, GRB Coordinates Network, 3368, 1
- Berger, E., & Soderberg, A. M. 2005b, GRB Coordinates Network, 4384, 1
- Berger, E. 2006, GRB Coordinates Network, 5952, 1

Table 3. Part I Rest-frame properties for bursts with known redshifts

GRBname	$\log_{10}(T'_{90})$	$\log_{10}(E'_p)$	$\log_{10}(E_{iso,\gamma})$	$\log_{10}(E_{iso,\gamma}^b)$	$\log_{10}(E_{iso,X})$	$\log_{10}(t'_b)$	$\log_{10}((L_X))$
	s	keV	ergs	ergs	ergs	s	ergs/s
050319	0.37 ± 0.08	2.15 ± 0.18	52.23 ± 0.04	52.58 ± 0.08	51.82 ± 0.06	3.89 ± 0.06	47.05 ± 0.05
050401	0.93 ± 0.03	2.72 ± 0.1	53.39 ± 0.04	53.77 ± 0.04	52.06 ± 0.05	3.08 ± 0.04	48.13 ± 0.03
050416A	0.16 ± 0.03	1.31 ± 0.17	50.47 ± 0.03	50.91 ± 0.06	49.52 ± 0.17	3 ± 0.14	46.21 ± 0.11
050505	1.06 ± 0.01	2.85 ± 0.13	53.13 ± 0.04	53.55 ± 0.05	51.88 ± 0.1	3.59 ± 0.07	47.43 ± 0.08
050714B	1.13	1.8 ± 0.22	51.93 ± 0.09	52.3 ± 0.09	50.13 ± 0.18	4.03 ± 0.19	45.53 ± 0.13
050802	0.68 ± 0.06	2.46 ± 0.13	52.29 ± 0.04	52.65 ± 0.06	51.18 ± 0.18	3.29 ± 0.04	47.38 ± 0.06
050814	1.01 ± 0.12	2.64 ± 0.17	52.99 ± 0.07	53.33 ± 0.11	51.54 ± 0.08	4.15 ± 0.06	46.35 ± 0.08
050822	1.62 ± 0.01	1.71 ± 0.14	52.24 ± 0.04	52.59 ± 0.04	50.7 ± 0.09	3.89 ± 0.08	46.34 ± 0.07
050824	1.14 ± 0.08	1.46 ± 0.27	50.6 ± 0.09	51 ± 0.11	50.07 ± 0.17	4.56 ± 0.16	45.2 ± 0.1
050826	1.43 ± 0.09	2.59 ± 0.38	49.95 ± 0.07	50.55 ± 0.5	48.39 ± 0.18	4.51 ± 0.15	43.83 ± 0.15
051109B	1.14 ± 0.03	1.74 ± 0.23	48.58 ± 0.06	48.92 ± 0.09	47.25 ± 0.12	3.46 ± 0.1	43.72 ± 0.09
051221A	-0.04	2.79 ± 0.14	51.38 ± 0.01	52.09 ± 0.07	49.69 ± 0.09	4.45 ± 0.08	44.78 ± 0.08
060108	0.68 ± 0.03	2.15 ± 0.17	51.55 ± 0.05	51.89 ± 0.05	50.53 ± 0.1	3.63 ± 0.1	46.34 ± 0.08
060115	1.5 ± 0.02	2.53 ± 0.14	52.67 ± 0.02	53 ± 0.11	51.07 ± 0.19	3.84 ± 0.18	46.27 ± 0.16
060306	1.38 ± 0.01	2.2 ± 0.13	52.11 ± 0.02	52.46 ± 0.08	50.54 ± 0.17	3.11 ± 0.16	46.97 ± 0.14
060502A	1.12 ± 0.06	2.6 ± 0.12	52.09 ± 0.02	52.53 ± 0.05	51.08 ± 0.11	4.17 ± 0.11	46.2 ± 0.1
060604	0.5 ± 0.11	2.25 ± 0.34	51.13 ± 0.09	51.46 ± 0.18	50.72 ± 0.11	3.83 ± 0.08	46.37 ± 0.08
060605	0.5 ± 0.05	2.98 ± 0.19	52.1 ± 0.04	52.57 ± 0.1	51.52 ± 0.03	3.25 ± 0.03	47.41 ± 0.03
060607A	1.39 ± 0.02	2.79 ± 0.11	52.71 ± 0.02	53.16 ± 0.05	52.37 ± 0.03	3.5 ± 0.01	48.08 ± 0.02
060614	1.95	2.53 ± 0.26	51.16 ± 0.02	51.71 ± 0.13	49.03 ± 0.03	4.64 ± 0.02	44.34 ± 0.03
060707	1.19 ± 0.03	2.47 ± 0.62	52.6 ± 0.05	52.95 ± 0.09	51.64 ± 0.16	4.45 ± 0.16	46.18 ± 0.15
060714	1.49 ± 0.02	2.25 ± 0.13	52.68 ± 0.03	52.99 ± 0.01	51.13 ± 0.11	3.1 ± 0.1	47.35 ± 0.11
060719	1.34 ± 0.04	2.08 ± 0.13	51.97 ± 0.03	52.28 ± 0.01	50.49 ± 0.12	3.47 ± 0.1	46.47 ± 0.1
060729	1.88 ± 0.04	1.98 ± 0.15	51.3 ± 0.03	51.63 ± 0.07	50.9 ± 0.02	4.61 ± 0.01	46.04 ± 0.01
060805A	0.2 ± 0.04	2.04 ± 0.31	50.98 ± 0.11	51.33 ± 0.22	50.06 ± 0.16	3.03 ± 0.14	46.45 ± 0.15
060814	1.66 ± 0.01	2.88 ± 0.49	53.37 ± 0.02	53.89 ± 0.1	51.23 ± 0.07	3.64 ± 0.05	47.02 ± 0.06
060906	0.97 ± 0.01	2.33 ± 0.14	52.76 ± 0.03	53.09 ± 0.01	51.01 ± 0.05	3.38 ± 0.05	46.89 ± 0.05
060908	0.83 ± 0.01	2.77 ± 0.11	52.39 ± 0.01	52.84 ± 0.05	50.85 ± 0.11	2.38 ± 0.08	47.85 ± 0.09
060927	0.54 ± 0.01	2.67 ± 0.62	52.72 ± 0.04	53.06 ± 0.03	51.32 ± 0.14	2.98 ± 0.12	47.1 ± 0.15
061121	1.54 ± 0.03	3.15 ± 0.14	52.77 ± 0.01	53.58 ± 0.04	51.48 ± 0.05	3.34 ± 0.04	47.65 ± 0.05
061201	-0.14 ± 0.05	2.99 ± 0.2	48.96 ± 0.04	49.86 ± 0.12	48.58 ± 0.08	3.4 ± 0.06	44.9 ± 0.09
061222A	1.37 ± 0.02	3 ± 0.21	52.92 ± 0.01	53.57 ± 0.05	52.1 ± 0.03	4.19 ± 0.03	46.96 ± 0.03
070103	0.72 ± 0.02	2.23 ± 0.19	51.70 ± 0.06	52.03 ± 0.06	50.49 ± 0.08	2.6 ± 0.06	47.44 ± 0.05
070110	1.4 ± 0.02	2.58 ± 0.15	52.3 ± 0.03	52.66 ± 0.07	51.48 ± 0.02	3.79 ± 0.01	47.22 ± 0.02
070129	2.14 ± 0.02	2.16 ± 0.16	52.58 ± 0.04	52.90 ± 0.15	50.88 ± 0.08	3.73 ± 0.06	46.61 ± 0.05
070306	0.48 ± 0.09	2.33 ± 0.13	50.92 ± 0.25	51.26 ± 0.09	51.46 ± 0.03	4.08 ± 0.02	46.94 ± 0.02
070508	1.06 ± 0.02	2.67 ± 0.33	52.52 ± 0.01	53.07 ± 0.11	50.79 ± 0.33	2.2 ± 0.24	48.35 ± 0.16
070529	1.49 ± 0.01	2.8 ± 0.2	52.55 ± 0.04	53 ± 0.11	50.75 ± 0.15	2.48 ± 0.11	47.69 ± 0.12
070809	0.03 ± 0.03	2.02 ± 0.22	49.05 ± 0.04	49.39 ± 0.25	48.24 ± 0.15	3.69 ± 0.13	44.53 ± 0.11
070810A	0.54 ± 0.04	2.14 ± 0.15	51.87 ± 0.04	52.21 ± 0.04	50.61 ± 0.21	2.64 ± 0.17	47.38 ± 0.19
080413B	0.58 ± 0.05	2.19 ± 0.18	52 ± 0.01	52.34 ± 0.02	50.34 ± 0.14	2.28 ± 0.1	47.83 ± 0.08
080430	0.96 ± 0.06	2.15 ± 0.12	51.25 ± 0.04	51.6 ± 0.07	50.42 ± 0.07	4.28 ± 0.06	45.68 ± 0.05
080516	0.14 ± 0.02	2.44 ± 0.25	51.73 ± 0.06	52.07 ± 0.14	50.79 ± 0.17	3.12 ± 0.16	47 ± 0.14
080707	1.08 ± 0.02	2.21 ± 0.2	51.3 ± 0.05	52.61 ± 0.12	50.1 ± 0.16	3.68 ± 0.14	45.97 ± 0.12
080905B	1.58 ± 0.05	2.38 ± 0.16	52.35 ± 0.05	52.7 ± 0.12	51.88 ± 0.07	3.64 ± 0.07	47.5 ± 0.05
081007	0.82 ± 0.16	1.5 ± 0.17	50.7 ± 0.05	51.06 ± 0.07	50.1 ± 0.3	4.44 ± 0.12	45.09 ± 0.12
081029	1.75 ± 0.07	2.88 ± 0.21	52.77 ± 0.04	53.22 ± 0.15	51.46 ± 0.03	3.53 ± 0.02	47.2 ± 0.03
090102	1.03 ± 0.03	2.68 ± 0.12	50.6 ± 0.02	51.06 ± 0.05	51.46 ± 0.06	2.75 ± 0.03	48.16 ± 0.04

- Berger, E., Fox, D. B., & Cucchiara, A. 2007, GRB Coordinates Network, 6470, 1
- Berger, E., Fox, D. B., Cucchiara, A., & Cenko, S. B. 2008, GRB Coordinates Network, 8335, 1
- Bloom, J. S., Frail, D. A., & Sari, R. 2001, AJ, 121, 2879
- Bloom, J. S., Perley, D. A., & Chen, H. W. 2006, GRB Coordinates Network, 5826, 1
- Bolmer, J., Knust, F., & Greiner, J. 2015, GRB Coordinates Network, Circular Service, No. 18603, #1 (2015), 18603, 1
- Brun, R., & Rademakers, F. 1997, Nuclear Instruments and Methods in Physics Research A, 389, 81
- Burrows, D. N., Romano, P., Falcone, A., et al. 2005a, Science, 309, 1833
- Burrows, D. N., Hill, J. E., Nousek, J. A., et al. 2005b, SSRv, 120, 165
- Campana, S., Mangano, V., Blustin, A. J., et al. 2006, Nature, 442, 1008
- Cannizzo, J., Barbier, L., Barthelmy, S. D., et al. 2007, GRB Coordinates Network, 6362, 1
- Cannizzo, J. K., Troja, E., & Gehrels, N. 2011, ApJ, 734, 35
- Cano, Z., Malesani, D., de Ugarte Postigo, A., et al. 2016, GRB Coordinates Network, Circular Service, No. 20245, #1 (2016), 20245, 1
- Castro-Tirado, A. J., Amado, P., Negueruela, I., et al. 2006, GRB Coordinates Network, 5218, 1
- Castro-Tirado, A. J., Cunniffe, R., Sanchez-Ramirez, R., et al. 2014, GRB Coordinates Network, Circular Service, No. 16505, #1 (2014), 16505, 1
- Castro-Tirado, A. J., Sanchez-Ramirez, R., Lombardi, G., & Rivero, M. A. 2015, GRB Coordinates Network, Circular Service, No. 17758, #1 (2015), 17758, 1
- Cenko, S. B., Kulkarni, S. R., Gal-Yam, A., & Berger, E. 2005, GRB Coordinates Network, 3542, 1
- Chen, H.-W., Helsby, J., Shectman, S., Thompson, I., & Crane, J. 2009, GRB Coordinates Network, Circular Service, No. 1038, #1 (2009), 10038, 1
- Chornock, R., Cenko, S. B., Griffith, C. V., et al. 2009a, GRB Coordinates Network, 9151, 1
- Chornock, R., Perley, D. A., Cenko, S. B., & Bloom, J. S. 2009b, GRB Coordinates Network, 9243, 1
- Chornock, R., Perley, D. A., & Cobb, B. E. 2009c, GRB Coordinates Network, Circular Service, No. 10100, #1 (2009c), 10100, 1
- Chornock, R., Cucchiara, A., Fox, D., & Berger, E. 2010a, GRB Coordinates Network, Circular Service, No. 10466, #1 (2010a), 10466, 1
- Chornock, R., Berger, E., Fox, D., et al. 2010b, GRB Coordinates Network, Circular Service, No. 11164, #1 (2010b), 11164, 1
- Chornock, R., Berger, E., & Fox, D. B. 2011, GRB Coordinates Network, Circular Service, No. 11538, #1 (2011), 11538, 1
- Chornock, R., Fox, D. B., Cucchiara, A., Perley, D. A., & Levan, A. 2014, GRB Coordinates Network, Circular Service, No. 16301, #1 (2014), 16301, 1
- Connaughton, V. 2009, GRB Coordinates Network, 9230, 1
- Cucchiara, A., Price, P. A., Fox, D. B., Cenko, S. B., & Schmidt, B. P. 2006, GRB Coordinates Network, 5052, 1
- Cucchiara, A., & Fox, D. B. 2008, GRB Coordinates Network, 7654, 1
- Cucchiara, A., Levan, A. J., Fox, D. B., et al. 2011a, ApJ, 736, 7
- Cucchiara, A., & Levan, A. J. 2011b, GRB Coordinates Network, Circular Service, No. 12761, #1 (2011b), 12761, 1
- Cummings, J., Ajello, M., Barbier, L., et al. 2005, GRB Coordinates Network, 3993, 1
- Cummings, J., Barbier, L., Barthelmy, S. D., et al. 2006, GRB Coordinates Network, 5443, 1
- Cummings, J., Barbier, L., Barthelmy, S. D., et al. 2007, GRB Coordinates Network, 6007, 1
- Cummings, J. R., Barthelmy, S. D., Baumgartner, W. H., et al. 2008, GRB Coordinates Network, 8447, 1
- Cummings, J. R., Barthelmy, S. D., Baumgartner, W. H., et al. 2009a, GRB Coordinates Network, 8886, 1
- Cummings, J. R., Barthelmy, S. D., Baumgartner, W. H., et al. 2009b, GRB Coordinates Network, 9393, 1
- Cummings, J. R., Barthelmy, S. D., Baumgartner, W. H., et al. 2010b, GRB Coordinates Network, Circular Service, No. 10462, #1 (2010a), 10462, 1
- Cummings, J. R., Barthelmy, S. D., Baumgartner, W. H., et al. 2010a, GRB Coordinates Network, Circular Service, No. 10932, #1 (2010b), 10932, 1
- Cummings, J. R., Barthelmy, S. D., Baumgartner, W. H., et al. 2011, GRB Coordinates Network, Circular Service, No. 12749, #1 (2011), 12749, 1
- Cummings, J. R., Barthelmy, S. D., Baumgartner, W. H., et al. 2012a, GRB Coordinates Network, Circular Service, No. 13096, #1 (2012b), 13096, 1
- Cummings, J. R., Barthelmy, S. D., Baumgartner, W. H., et al. 2012b, GRB Coordinates Network, Circular Service, No. 13949, #1 (2012a), 13949, 1
- Cummings, J. R. 2014, GRB Coordinates Network, Circular Service, No. 15717, #1 (2014), 15717, 1
- D'Agostini, G. 2005, arXiv:physics/0511182
- D'Elia, V., Covino, S., & D'Avanzo, P. 2008, GRB Coordinates Network, 8438, 1
- Dai, Z. G., & Lu, T. 1998, Physical Review Letters, 81, 4301

Table 3. Part II Rest-frame properties for bursts with known redshifts

GRBname	$\log_{10}(T'_{90})$	$\log_{10}(E'_p)$	$\log_{10}(E_{iso,\gamma})$	$\log_{10}(E_{iso,\gamma}^b)$	$\log_{10}(E_{iso,X})$	$\log_{10}(t'_b)$	$\log_{10}((L_X))$
	s	keV	ergs	ergs	ergs	s	ergs/s
090113	0.52 ± 0.04	2.46 ± 0.13	51.75 ± 0.02	52.12 ± 0.05	50.51 ± 0.1	2.31 ± 0.08	47.81 ± 0.07
090205	0.19 ± 0.08	2.31 ± 0.2	51.85 ± 0.06	52.18 ± 0.1	51.19 ± 0.11	3.43 ± 0.1	46.77 ± 0.11
090313	1.25 ± 0.09	2.39 ± 0.26	52.5 ± 0.06	52.80 ± 0.1	51.46 ± 0.1	4.25 ± 0.06	46.64 ± 0.09
090404	1.32 ± 0.07	2.04 ± 0.13	52.75 ± 0.01	53.08 ± 0.05	51.36 ± 0.1	3.63 ± 0.08	47.06 ± 0.07
090407	2.1 ± 0.09	2.29 ± 0.27	51.75 ± 0.07	52.12 ± 0.27	50.93 ± 0.05	4.47 ± 0.05	45.89 ± 0.04
090418A	1.33 ± 0.04	2.56 ± 0.11	52.46 ± 0.02	52.87 ± 0.04	51.31 ± 0.08	3.07 ± 0.06	47.64 ± 0.08
090424	1.53	2.44 ± 0.01	52.35 ± 0.25	52.8 ± 0.01	50.78 ± 0.18	2.79 ± 0.17	47.73 ± 0.16
090429B	-0.28 ± 0.07	2.64 ± 0.56	52.51 ± 0.04	52.83 ± 0.01	50.98 ± 0.1	1.88 ± 0.08	48.34 ± 0.04
090510	-0.8 ± 0.12	3.07 ± 0.3	50.84 ± 0.05	51.46 ± 0.13	50.47 ± 0.07	2.91 ± 0.05	47.03 ± 0.06
090529	1.44	2.23 ± 0.25	52 ± 0.1	52.34 ± 0.11	50.81 ± 0.19	2.91 ± 0.05	47.03 ± 0.18
090530	1.33 ± 0.24	2.37 ± 0.19	51.64 ± 0.04	52 ± 0.26	50.7 ± 0.11	4.42 ± 0.1	45.47 ± 0.09
091018	0.35 ± 0.06	1.58 ± 0.57	51.52 ± 0.03	51.91 ± 0.38	50.56 ± 0.08	2.49 ± 0.07	47.65 ± 0.06
091029	1.02 ± 0.05	2.36 ± 0.41	52.59 ± 0.02	52.93 ± 0.05	51.17 ± 0.06	3.5 ± 0.05	47.06 ± 0.04
100219A	0.52 ± 0.1	3.05 ± 0.29	52.14 ± 0.07	52.61 ± 0.31	51.83 ± 0.07	3.77 ± 0.03	47.05 ± 0.06
100302A	0.49 ± 0.04	2.67 ± 0.2	52.09 ± 0.05	52.4 ± 0.15	50.94 ± 0.22	3.58 ± 0.22	46.47 ± 0.16
100418A	0.63 ± 0.06	1.76 ± 0.21	50.52 ± 0.6	50.83 ± 0.13	49.79 ± 0.22	4.7 ± 0.06	44.95 ± 0.05
100425A	1.13 ± 0.03	1.81 ± 0.24	51.54 ± 0.08	51.91 ± 0.21	50.41 ± 0.18	4.07 ± 0.18	45.63 ± 0.14
100901A	2.26 ± 0.03	2.41 ± 0.22	52 ± 0.06	52.35 ± 0.32	51.24 ± 0.02	4.2 ± 0.02	46.72 ± 0.01
100906A	1.62 ± 0.01	2.29 ± 0.1	53.12 ± 0.25	53.46 ± 0.04	51.46 ± 0.04	3.66 ± 0.03	47.02 ± 0.05
110106B	1.19 ± 0.08	2.08 ± 0.14	51.28 ± 0.02	51.62 ± 0.1	50.14 ± 0.11	3.91 ± 0.1	45.76 ± 0.1
110808A	1.31 ± 0.17	1.81 ± 0.3	51.17 ± 0.09	51.52 ± 0.24	50.43 ± 0.21	4.85 ± 0.21	44.86 ± 0.16
111008A	1.03 ± 0.01	2.56 ± 0.12	53.35 ± 0.02	53.68 ± 0.01	52.05 ± 0.06	3.12 ± 0.06	48.04 ± 0.05
111228A	1.77 ± 0.02	1.71 ± 0.12	52.04 ± 0.01	52.4 ± 0.07	50.66 ± 0.05	3.89 ± 0.05	46.37 ± 0.04
120326A	1.4 ± 0.05	2.06 ± 0.19	52.3 ± 0.05	52.64 ± 0.01	51.57 ± 0.05	4.27 ± 0.01	46.96 ± 0.01
120521C	0.58 ± 0.07	2.75 ± 0.13	52.78 ± 0.04	53.12 ± 0.12	51 ± 0.24	3.22 ± 0.23	46.81 ± 0.17
120811C	0.86 ± 0.06	2.2 ± 0.2	52.67 ± 0.04	52.96 ± 0.01	51.17 ± 0.2	2.77 ± 0.17	47.74 ± 0.13
120907A	0.93 ± 0.18	2.2 ± 0.2	51.2 ± 0.07	51.53 ± 0.2	50.27 ± 0.2	4.35 ± 0.17	45.45 ± 0.1
121024A	1.54 ± 0.17	2.52 ± 0.25	51.42 ± 0.04	51.87 ± 0.25	50.63 ± 0.2	4.35 ± 0.17	45.45 ± 0.18
121128A	0.86 ± 0.03	2.31 ± 0.14	52.88 ± 0.03	53.22 ± 0.01	51.43 ± 0.07	2.7 ± 0.05	48.06 ± 0.06
121211A	1.95 ± 0.08	1.72 ± 0.21	51.53 ± 0.08	51.88 ± 0.19	50.56 ± 0.14	4.32 ± 0.11	45.69 ± 0.11
130603B	-0.88 ± 0.05	3.2 ± 0.15	50.29 ± 0.02	51.29 ± 0.11	49.58 ± 0.06	3.23 ± 0.05	46.08 ± 0.06
131105A	1.62 ± 0.02	2.61 ± 0.14	52.69 ± 0.03	53.14 ± 0.07	50.77 ± 0.1	3.23 ± 0.08	47.1 ± 0.08
140430A	1.82 ± 0.01	2.09 ± 0.2	51.83 ± 0.08	52.16 ± 0.07	50.86 ± 0.17	4.26 ± 0.16	45.86 ± 0.16
140512A	1.95 ± 0.01	2.41 ± 0.09	52.27 ± 0.01	52.71 ± 0.04	51.4 ± 0.06	3.88 ± 0.06	46.92 ± 0.06
140518A	1.03 ± 0.02	2.4 ± 0.4	52.58 ± 0.04	52.92 ± 0.01	50.94 ± 0.16	2.53 ± 0.12	47.86 ± 0.08
140703A	1.21 ± 0.3	2.51 ± 0.15	52.9 ± 0.03	53.21 ± 0.1	52.13 ± 0.04	3.54 ± 0.03	47.66 ± 0.04
141121A	2.35 ± 0.03	2.3 ± 0.15	52.45 ± 0.03	52.78 ± 0.12	51.18 ± 0.07	5.13 ± 0.05	45.52 ± 0.07
150323A	1.97 ± 0.03	2 ± 0.11	51.73 ± 0.01	52.06 ± 0.01	49.66 ± 0.13	3.96 ± 0.11	45.32 ± 0.09
150424A	1.85 ± 0.09	2.55 ± 0.2	50.51 ± 0.03	51.09 ± 0.12	49.51 ± 0.2	4.94 ± 0.18	43.96 ± 0.17
150910A	1.68 ± 0.13	2.58 ± 0.15	52.34 ± 0.04	52.81 ± 0.08	51.73 ± 0.15	3.56 ± 0.07	47.65 ± 0.12
151027A	1.86 ± 0.02	2.17 ± 0.1	52.11 ± 0.04	52.46 ± 0.03	51.34 ± 0.02	3.34 ± 0.02	47.78 ± 0.02
151112A	0.58 ± 0.42	2.57 ± 0.21	52.46 ± 0.05	52.81 ± 0.17	51.54 ± 0.18	4.06 ± 0.16	46.55 ± 0.15
160227A	1.97 ± 0.09	2.35 ± 0.33	52.59 ± 0.03	52.90 ± 0.04	51.63 ± 0.1	3.85 ± 0.09	47.18 ± 0.08
160327A	0.67 ± 0.12	2.58 ± 0.14	52.78 ± 0.03	53.09 ± 0.01	51.23 ± 0.13	2.84 ± 0.11	47.55 ± 0.13
160804A	1.92 ± 0.05	1.96 ± 0.07	52.19 ± 0.01	52.49 ± 0.01	49.7 ± 0.1	3.72 ± 0.07	45.88 ± 0.04
161108A	1.69 ± 0.05	2.13 ± 0.17	51.57 ± 0.04	51.91 ± 0.09	50.16 ± 0.15	4.03 ± 0.14	45.82 ± 0.08
161129A	1.33 ± 0.02	2.27 ± 0.1	51.57 ± 0.01	51.96 ± 0.03	50.26 ± 0.09	3.34 ± 0.07	46.59 ± 0.11
170113A	0.84 ± 0.08	2.34 ± 0.49	51.78 ± 0.04	52.13 ± 0.13	51.41 ± 0.07	3.16 ± 0.06	47.61 ± 0.06
170202A	1 ± 0.1	2.61 ± 0.11	52.93 ± 0.01	53.28 ± 0.04	51.22 ± 0.07	2.65 ± 0.06	48.01 ± 0.04

- Dai, Z. G. 2004, ApJ, 606, 1000
- Dainotti, M. G., Cardone, V. F., & Capozziello, S. 2008, MNRAS, 391, L79
- Dainotti, M. G., Willingale, R., Capozziello, S., Fabrizio Cardone, V., & Ostrowski, M. 2010, ApJL, 722, L215
- Dainotti, M. G., Fabrizio Cardone, V., Capozziello, S., Ostrowski, M., & Willingale, R. 2011a, ApJ, 730, 135
- Dainotti, M. G., Ostrowski, M., & Willingale, R. 2011b, MNRAS, 418, 2202
- Dainotti, M. G., Petrosian, V., Singal, J., & Ostrowski, M. 2013a, ApJ, 774, 157
- Dainotti, M. G., Cardone, V. F., Piedipalumbo, E., et al. 2013b, MNRAS, 436, 82
- Dainotti, M., Petrosian, V., Willingale, R., et al. 2015, MNRAS, 451, 3898
- Dainotti, M. G., Postnikov, S., Hernandez, X., & Ostrowski, M. 2016, ApJL, 825, L20
- Dainotti, M. G., Hernandez, X., Postnikov, S., et al. 2017, ApJ, 848, 88
- Dall'Osso, S., Stratta, G., Guetta, D., et al. 2011, A&A, 526, A121
- de Ugarte Postigo, A., Jakobsson, P., Malesani, D., et al. 2009, GRB Coordinates Network, 8766, 1
- de Ugarte Postigo, A., Thoene, C. C., Vergani, S. D., Milvang-Jensen, B., & Fynbo, J. 2010, GRB Coordinates Network, Circular Service, No. 10445, #1 (2010), 10445, 1
- de Ugarte Postigo, A., Fynbo, J. P. U., Jakobsson, P., et al. 2011, GRB Coordinates Network, Circular Service, No. 12258, #1 (2011), 12258, 1
- de Ugarte Postigo, A., Gorosabel, J., Xu, D., et al. 2014, GRB Coordinates Network, Circular Service, No. 16310, #1 (2014), 16310, 1
- de Ugarte Postigo, A., Tanvir, N. R., Cano, Z., et al. 2016a, GRB Coordinates Network, Circular Service, No. 19245, #1 (2016a), 19245, 1
- de Ugarte Postigo, A., Malesani, D., Perley, D. A., et al. 2016b, GRB Coordinates Network, Circular Service, No. 20150, #1 (2016b), 20150, 1
- de Ugarte Postigo, A., Izzo, L., Thoene, C., et al. 2017, GRB Coordinates Network, Circular Service, No. 20584, #1 (2017), 20584, 1
- Evans, P. A., Beardmore, A. P., Page, K. L., et al. 2009, MNRAS, 397, 1177
- Fenimore, E., Barbier, L., Barthelmy, S. D., et al. 2006, GRB Coordinates Network, 5831, 1
- Fenimore, E., Barbier, L., Barthelmy, S. D., et al. 2007, GRB Coordinates Network, 6571, 1
- Fenimore, E. E., Barthelmy, S. D., Baumgartner, W. H., et al. 2009, GRB Coordinates Network, 9157, 1
- Filgas, R., Tautenburg, T., Kupcu-Yoldas, A., et al. 2008, GRB Coordinates Network, 7747, 1
- Friedman, J. L. 1991, Annals of the New York Academy of Sciences, 647, 620
- Fruchter, A., Misra, K., Graham, J., et al. 2011, GRB Coordinates Network, Circular Service, No. 11881, #1 (2011), 11881, 1
- Fugazza, D., Malesani, D., Romano, P., et al. 2006, GRB Coordinates Network, 5276, 1
- Fynbo, J. P. U., Hjorth, J., Jensen, B. L., et al. 2005a, GRB Coordinates Network, 3136, 1
- Fynbo, J. P. U., Jensen, B. L., Hjorth, J., et al. 2005b, GRB Coordinates Network, 3176, 1
- Fynbo, J. P. U., Sollerman, J., Jensen, B. L., et al. 2005c, GRB Coordinates Network, 3749, 1
- Fynbo, J. P. U., Jensen, B. L., Sollerman, J., et al. 2005d, GRB Coordinates Network, z3874, 1
- Fynbo, J. P. U., Jakobsson, P., Jensen, B. L., et al. 2006, GRB Coordinates Network, 5651, 1
- Fynbo, J. P. U., Malesani, D., & Milvang-Jensen, B. 2008, GRB Coordinates Network, 7949, 1
- Fynbo, J. P. U., Jakobsson, P., Prochaska, J. X., et al. 2009, ApJS, 185, 526
- Gao, H., Lei, W.-H., Zou, Y.-C., Wu, X.-F., & Zhang, B. 2013, NewAR, 57, 141
- Gao, H., Ren, A.-B., Lei, W.-H., et al. 2017, ApJ, 845, 51
- Gibson, S. L., Wynn, G. A., Gompertz, B. P., & O'Brien, P. T. 2017, MNRAS, 470, 4925
- Gibson, S. L., Wynn, G. A., Gompertz, B. P., & O'Brien, P. T. 2018, MNRAS, 478, 4323
- Gompertz, B. P., O'Brien, P. T., Wynn, G. A., & Rowlinson, A. 2013, MNRAS, 431, 1745
- Gompertz, B. P., O'Brien, P. T., & Wynn, G. A. 2014, MNRAS, 438, 240
- Gompertz, B. P., van der Horst, A. J., O'Brien, P. T., Wynn, G. A., & Wiersema, K. 2015, MNRAS, 448, 629
- Gompertz, B., & Fruchter, A. 2017, ApJ, 839, 49
- Goldoni, P., Flores, H., Malesani, D., et al. 2010, GRB Coordinates Network, Circular Service, No. 10684, #1 (2010), 10684, 1
- Goldoni, P., de Ugarte Postigo, A., & Fynbo, J. P. U. 2013, GRB Coordinates Network, Circular Service, No. 15571, #1 (2013), 15571, 1
- Golenetskii, S., Aptekar, R., Mazets, E., et al. 2005, GRB Coordinates Network, 4394, 1
- Golenetskii, S., Aptekar, R., Mazets, E., et al. 2006a, GRB Coordinates Network, 5113, 1
- Golenetskii, S., Aptekar, R., Mazets, E., et al. 2006b, GRB Coordinates Network, 5264, 1

- Golenetskii, S., Aptekar, R., Mazets, E., et al. 2006c, GRB Coordinates Network, 5460, 1
- Golenetskii, S., Aptekar, R., Mazets, E., et al. 2006d, GRB Coordinates Network, 5837, 1
- Golenetskii, S., Aptekar, R., Mazets, E., et al. 2006e, GRB Coordinates Network, 5890, 1
- Golenetskii, S., Aptekar, R., Mazets, E., et al. 2007a, GRB Coordinates Network, 6230, 1
- Golenetskii, S., Aptekar, R., Mazets, E., et al. 2007b, GRB Coordinates Network, 6344, 1
- Golenetskii, S., Aptekar, R., Mazets, E., et al. 2007c, GRB Coordinates Network, 6403, 1
- Granot, J., & Kumar, P. 2006, MNRAS, 366, L13
- Halpern, J. P., & Mirabal, N. 2006, GRB Coordinates Network, 5982, 1
- Hjorth, J., Malesani, D., Jakobsson, P., et al. 2012, ApJ, 756, 187
- Huang, Y. F., Dai, Z. G., & Lu, T. 1999, MNRAS, 309, 513
- Huang, Y. F., Gou, L. J., Dai, Z. G., & Lu, T. 2000, ApJ, 543, 90
- Hullinger, D., Barbier, L., Barthelmy, S., et al. 2005a, GRB Coordinates Network, 3364, 1
- Hullinger, D., Angelini, L., Barbier, L., et al. 2005b, GRB Coordinates Network, 3856, 1
- Hullinger, D., Barbier, L., Barthelmy, S., et al. 2005c, GRB Coordinates Network, 4019, 1
- Hullinger, D., Barbier, L., Barthelmy, S., et al. 2005d, GRB Coordinates Network, 4237, 1
- Hullinger, D., Angelini, L., Barbier, L., et al. 2006a, GRB Coordinates Network, 4851, 1
- Hullinger, D., Barbier, L., Barthelmy, S. D., et al. 2006b, GRB Coordinates Network, 5304, 1
- Jakobsson, P., Tanvir, N., Jensen, B. L., et al. 2006a, GRB Coordinates Network, 5298, 1
- Jakobsson, P., Vreeswijk, P., Fynbo, J. P. U., et al. 2006b, GRB Coordinates Network, 5320, 1
- Jakobsson, P., Fynbo, J. P. U., Andersen, M. I., et al. 2007, GRB Coordinates Network, 6398, 1
- Jaunsen, A. O., Malesani, D., Fynbo, J. P. U., Sollerman, J., & Vreeswijk, P. M. 2007a, GRB Coordinates Network, 6010, 1
- Jaunsen, A. O., Thoene, C. C., Fynbo, J. P. U., Hjorth, J., & Vreeswijk, P. 2007b, GRB Coordinates Network, 6202, 1
- Jensen, B. L., Fynbo, J. P. U., Hjorth, J., et al. 2005, GRB Coordinates Network, 3809, 1
- K.-M. Osei-Bryson and O. Ngwenyama (eds.), Advances in Research Methods 93 for Information Systems Research, Integrated Series in Information Systems 34, Springer Science+Business Media New York 2014
- Kelly, B. C. 2007, ApJ, 665, 1489
- Kozlova, A., Golenetskii, S., Aptekar, R., et al. 2016, GRB Coordinates Network, Circular Service, No. 20238, #1 (2016), 20238, 1
- Krühler, T., Malesani, D., Milvang-Jensen, B., et al. 2012, ApJ, 758, 46
- Krimm, H., Sakamoto, T., Barthelmy, S., et al. 2005a, GRB Coordinates Network, 3119, 1
- Krimm, H., Barbier, L., Barthelmy, S., et al. 2005b, GRB Coordinates Network, 3871, 1
- Krimm, H., Barbier, L., Barthelmy, S., et al. 2006a, GRB Coordinates Network, 4656, 1
- Krimm, H., Barbier, L., Barthelmy, S., et al. 2006b, GRB Coordinates Network, 4864, 1
- Krimm, H., Barbier, L., Barthelmy, S. D., et al. 2006c, GRB Coordinates Network, 5334, 1
- Krimm, H., Barbier, L., Barthelmy, S. D., et al. 2007a, GRB Coordinates Network, 6058, 1
- Krimm, H., Barbier, L., Barthelmy, S. D., et al. 2007b, GRB Coordinates Network, 6589, 1
- Krimm, H., Barbier, L., Barthelmy, S. D., et al. 2007c, GRB Coordinates Network, 6732, 1
- Krimm, H., Barthelmy, S. D., Cummings, J., et al. 2008a, GRB Coordinates Network, 7533, 1
- Krimm, H., Barthelmy, S. D., Baumgartner, W., et al. 2008b, GRB Coordinates Network, 7736, 1
- Krimm, H. A., Barthelmy, S. D., Baumgartner, W. H., et al. 2010, GRB Coordinates Network, Circular Service, No. 10322, #1 (2010), 10322, 1
- Krimm, H. A., Barlow, B. N., Barthelmy, S. D., et al. 2012, GRB Coordinates Network, Circular Service, No. 13634, #1 (2012), 13634, 1
- Krimm, H. A., & Cummings, J. R. 2013, GRB Coordinates Network, Circular Service, No. 14867, #1 (2013), 14867, 1
- Krimm, H. A., Barthelmy, S. D., Baumgartner, W. H., et al. 2014a, GRB Coordinates Network, Circular Service, No. 15738, #1 (2014a), 15738, 1
- Krimm, H. A., Barthelmy, S. D., Baumgartner, W. H., et al. 2014b, GRB Coordinates Network, Circular Service, No. 16200, #1 (2014b), 16200, 1
- Krimm, H. A., Barthelmy, S. D., Baumgartner, W. H., et al. 2014c, GRB Coordinates Network, Circular Service, No. 16509, #1 (2014c), 16509, 1
- Krimm, H. A., Barthelmy, S. D., Baumgartner, W. H., et al. 2014d, GRB Coordinates Network, Circular Service, No. 17083, #1 (2014d), 17083, 1
- Krimm, H. A., Barthelmy, S. D., Cummings, J. R., et al. 2015a, GRB Coordinates Network, Circular Service, No. 18020, #1 (2015a), 18020, 1

- Krimm, H. A., Barthelmy, S. D., Cummings, J. R., et al. 2015b, GRB Coordinates Network, Circular Service, No. 18593, #1 (2015b), 18593, 1
- Krimm, H. A., Barthelmy, S. D., Cummings, J. R., et al. 2015c, GRB Coordinates Network, Circular Service, No. 18752, #1 (2015c), 18752, 1
- Krimm, H. A., Barthelmy, S. D., Cummings, J. R., et al. 2016a, GRB Coordinates Network, Circular Service, No. 19639, #1 (2016a), 19639, 1
- Krimm, H. A., Barthelmy, S. D., Cummings, J. R., et al. 2016b, GRB Coordinates Network, Circular Service, No. 19765, #1 (2016b), 19765, 1
- Krimm, H. A., Barthelmy, S. D., Cummings, J. R., et al. 2016c, GRB Coordinates Network, Circular Service, No. 20270, #1 (2016c), 20270, 1
- Kruehler, T., Malesani, D., de Ugarte Postigo, A., Melandri, A., & Fynbo, J. P. U. 2014, GRB Coordinates Network, Circular Service, No. 16194, #1 (2014), 16194, 1
- Kumar, P., & Panaiteescu, A. 2000, ApJL, 541, L9
- Kumar, P., & Zhang, B. 2015, PhR, 561, 1
- Ledoux, C., Vreeswijk, P., Smette, A., Jaunsen, A., & Kaufer, A. 2006, GRB Coordinates Network, 5237, 1
- Liang, E.-W., Zhang, B.-B., & Zhang, B. 2007, ApJ, 670, 565
- Liang, E.-W., Racusin, J. L., Zhang, B., Zhang, B.-B., & Burrows, D. N. 2008, ApJ, 675, 528
- Lien, A. Y., Barthelmy, S. D., Cummings, J. R., et al. 2015a, GRB Coordinates Network, Circular Service, No. 18268, #1 (2015a), 18268, 1
- Lien, A. Y., Barthelmy, S. D., Cummings, J. R., et al. 2015b, GRB Coordinates Network, Circular Service, No. 18751, #1 (2015b), 18751, 1
- Lien, A. Y., Barthelmy, S. D., Cummings, J. R., et al. 2017, GRB Coordinates Network, Circular Service, No. 20968, #1 (2017), 20968, 1
- Lü, H.-J., & Zhang, B. 2014, ApJ, 785, 74
- Lü, H.-J., Zhang, B., Lei, W.-H., Li, Y., & Lasky, P. D. 2015, ApJ, 805, 89
- Markwardt, C., Ajello, M., Barthelmy, S., et al. 2005a, GRB Coordinates Network, 3576, 1
- Markwardt, C., Barbier, L., Barthelmy, S., et al. 2005b, GRB Coordinates Network, 3888, 1
- Markwardt, C., Barbier, L., Barthelmy, S., et al. 2006a, GRB Coordinates Network, 4671, 1
- Markwardt, C., Barbier, L., Barthelmy, S., et al. 2006b, GRB Coordinates Network, 5022, 1
- Markwardt, C., Barbier, L., Barthelmy, S. D., et al. 2006c, GRB Coordinates Network, 5882, 1
- Markwardt, C., Barbier, L., Barthelmy, S. D., et al. 2007a, GRB Coordinates Network, 6748, 1
- Markwardt, C., Barthelmy, S. D., Cummings, J., et al. 2007b, GRB Coordinates Network, 7109, 1
- Markwardt, C. M., Barthelmy, S. D., Baumgartner, W. H., et al. 2008, GRB Coordinates Network, 8338, 1
- Markwardt, C. B., Barthelmy, S. D., Baumgartner, W. H., et al. 2009a, GRB Coordinates Network, 9434, 1
- Malesani, D., Fynbo, J. P. U., D'Elia, V., et al. 2009b, GRB Coordinates Network, 9457, 1
- Markwardt, C. B., Barthelmy, S. D., Baumgartner, W. H., et al. 2009c, GRB Coordinates Network, 9724, 1
- Markwardt, C. B., Barthelmy, S. D., Baumgartner, W. H., et al. 2009d, GRB Coordinates Network, Circular Service, No. 1040, #1 (2009), 10040, 1
- Markwardt, C. B., Barthelmy, S. D., Baumgartner, W. H., et al. 2010, GRB Coordinates Network, Circular Service, No. 10685, #1 (2010), 10685, 1
- Markwardt, C. B., Barthelmy, S. D., Baumgartner, W. H., et al. 2012, GRB Coordinates Network, Circular Service, No. 13333, #1 (2012), 13333, 1
- Markwardt, C. B., Barthelmy, S. D., Baumgartner, W. H., et al. 2014, GRB Coordinates Network, Circular Service, No. 16539, #1 (2014a), 16539, 1
- Markwardt, C. B., Barthelmy, S. D., Baumgartner, W. H., et al. 2014, GRB Coordinates Network, Circular Service, No. 16553, #1 (2014b), 16553, 1
- Markwardt, C. B., Barthelmy, S. D., Baumgartner, W. H., et al. 2014, GRB Coordinates Network, Circular Service, No. 16927, #1 (2014c), 16927, 1
- Markwardt, C. B., Barthelmy, S. D., Baumgartner, W. H., et al. 2015, GRB Coordinates Network, Circular Service, No. 17330, #1 (2015a), 17330, 1
- Markwardt, C. B., Amaral-Rogers, A., Barthelmy, S. D., et al. 2015, GRB Coordinates Network, Circular Service, No. 17628, #1 (2015b), 17628, 1
- Markwardt, C. B., Barthelmy, S. D., Cummings, J. R., et al. 2016, GRB Coordinates Network, Circular Service, No. 19240, #1 (2016a), 19240, 1
- Markwardt, C. B., Barthelmy, S. D., Cummings, J. R., et al. 2016, GRB Coordinates Network, Circular Service, No. 19974, #1 (2016b), 19974, 1
- Markwardt, C. B., Barthelmy, S. D., Cummings, J. R., et al. 2017, GRB Coordinates Network, Circular Service, No. 20456, #1 (2017a), 20456, 1
- Markwardt, C. B., Barthelmy, S. D., Cummings, J. R., et al. 2017, GRB Coordinates Network, Circular Service, No. 21331, #1 (2017b), 21331, 1
- McLean, K., Barthelmy, S. D., Cummings, J., et al. 2008, GRB Coordinates Network, 7505, 1
- Melandri, A., Grazian, A., Guidorzi, C., et al. 2006, GRB Coordinates Network, 4539, 1

- Meszaros, P., & Rees, M. J. 1993, ApJ, 405, 278
- Mészáros, P., & Rees, M. J. 1997, ApJ, 476, 232
- Mooley, K. P., Staley, T. D., Fender, R. P., et al. 2016, GRB Coordinates Network, Circular Service, No. 20200, #1 (2016), 20200, 1
- Nasa High Energy Astrophysics Science Archive Research Center (Heasarc) 2014, Astrophysics Source Code Library, ascl:1408.004
- Noosek, J. A., Kouveliotou, C., Grupe, D., et al. 2006, ApJ, 642, 389
- O'Brien, P. T., Willingale, R., Osborne, J., et al. 2006, ApJ, 647, 1213
- Pal'Shin, V. 2006, GRB Coordinates Network, 5984, 1
- Palmer, D., Barthelmy, S., Barbier, L., et al. 2005a, GRB Coordinates Network, 3597, 1
- Palmer, D., Barbier, L., Barthelmy, S., et al. 2005b, GRB Coordinates Network, 3737, 1
- Palmer, D., Ajello, M., Barbier, L., et al. 2006a, GRB Coordinates Network, 4476, 1
- Palmer, D., Barbier, L., Barthelmy, S. D., et al. 2006b, GRB Coordinates Network, 5551, 1
- Palmer, D., Barthelmy, S. D., Baumgartner, W., et al. 2008a, GRB Coordinates Network, 7582, 1
- Palmer, D. M., Barthelmy, S. D., Baumgartner, W. H., et al. 2008b, GRB Coordinates Network, 8759, 1
- Palmer, D. M., Barthelmy, S. D., Baumgartner, W. H., et al. 2009a, GRB Coordinates Network, 9443, 1
- Palmer, D. M., Barthelmy, S. D., Baumgartner, W. H., et al. 2009b, GRB Coordinates Network, 9736, 1
- Palmer, D. M., Barthelmy, S. D., Baumgartner, W. H., et al. 2009c, GRB Coordinates Network, 9888, 1
- Palmer, D. M., Barthelmy, S. D., Baumgartner, W. H., et al. 2012, GRB Coordinates Network, Circular Service, No. 14011, #1 (2012), 14011, 1
- Palmer, D. M., Barthelmy, S. D., Baumgartner, W. H., et al. 2013, GRB Coordinates Network, Circular Service, No. 14163, #1 (2013), 14163, 1
- Palmer, D. M., Barthelmy, S. D., Baumgartner, W. H., et al. 2015a, GRB Coordinates Network, Circular Service, No. 17374, #1 (2015a), 17374, 1
- Palmer, D. M., Amaral-Rogers, A., Barthelmy, S. D., et al. 2015b, GRB Coordinates Network, Circular Service, No. 17637, #1 (2015b), 17637, 1
- Palmer, D. M., Barthelmy, S. D., Baumgartner, W. H., et al. 2015c, GRB Coordinates Network, Circular Service, No. 17907, #1 (2015c), 17907, 1
- Palmer, D. M., Barthelmy, S. D., Cummings, J. R., et al. 2015d, GRB Coordinates Network, Circular Service, No. 18496, #1 (2015d), 18496, 1
- Palmer, D. M., Barthelmy, S. D., Beardmore, A. P., et al. 2016, GRB Coordinates Network, Circular Service, No. 20151, #1 (2016), 20151, 1
- Panaiteescu, A., & Kumar, P. 2001, ApJL, 560, L49
- Panaiteescu, A., & Kumar, P. 2002, ApJ, 571, 779
- Panaiteescu, A., Mészáros, P., Gehrels, N., Burrows, D., & Nosek, J. 2006, MNRAS, 366, 1357
- Parsons, A., Barthelmy, S., Barbier, L., et al. 2005a, GRB Coordinates Network, 3600, 1
- Parsons, A., Barbier, L., Barthelmy, S., et al. 2005b, GRB Coordinates Network, 3757, 1
- Parsons, A., Barthelmy, S., Burrows, D., et al. 2005c, GRB Coordinates Network, 4363, 1
- Parsons, A., Barbier, L., Barthelmy, S., et al. 2006a, GRB Coordinates Network, 5053, 1
- Parsons, A., Barbier, L., Barthelmy, S., et al. 2006b, GRB Coordinates Network, 5214, 1
- Parsons, A., Barbier, L., Barthelmy, S. D., et al. 2006c, GRB Coordinates Network, 5370, 1
- Parsons, A., Barbier, L., Barthelmy, S. D., et al. 2007a, GRB Coordinates Network, 6342, 1
- Parsons, A., Barbier, L., Barthelmy, S. D., et al. 2007b, GRB Coordinates Network, 6468, 1
- Perley, D. A., Bloom, J. S., Modjaz, M., et al. 2008, GRB Coordinates Network, 7889, 1
- Perley, D. A., Cenko, S. B., Bloom, J. S., et al. 2009, AJ, 138, 1690
- Perley, D. A., Levan, A. J., Tanvir, N. R., et al. 2013, ApJ, 778, 128
- Perley, D. A., Ott, C. P., Modjaz, M., & Fierroz, D. 2014, GRB Coordinates Network, Circular Service, No. 17081, #1 (2014), 17081, 1
- Perley, D. A., & Cenko, S. B. 2015a, GRB Coordinates Network, Circular Service, No. 17616, #1 (2015a), 17616, 1
- Perley, D. A., Hillenbrand, L., & Prochaska, J. X. 2015b, GRB Coordinates Network, Circular Service, No. 18487, #1 (2015b), 18487, 1
- Piranomonte, S., D'Elia, V., Fiore, F., et al. 2006, GRB Coordinates Network, 4520, 1
- Rau, A., McBreen, S., & Kruehler, T. 2009, GRB Coordinates Network, 9353, 1
- Rea, N., Gullón, M., Pons, J. A., et al. 2015, ApJ, 813, 92
- Rees, M. J., & Meszaros, P. 1992, MNRAS, 258, 41P
- Rees, M. J., & Meszaros, P. 1994, ApJL, 430, L93
- Rees, M. J., & Mészáros, P. 1998, ApJL, 496, L1
- Retter, A., Racusin, J., Kennea, J., et al. 2005, GRB Coordinates Network, 3525,
- Rowlinson, A., O'Brien, P. T., Tanvir, N. R., et al. 2010, MNRAS, 409, 531

- Rowlinson, A., O'Brien, P. T., Metzger, B. D., Tanvir, N. R., & Levan, A. J. 2013, MNRAS, 430, 1061
- Rowlinson, A., Gompertz, B. P., Dainotti, M., et al. 2014, MNRAS, 443, 1779
- Sakamoto, T., Barthelmy, S., Barbier, L., et al. 2005a, GRB Coordinates Network, 3173, 1
- Sakamoto, T., Barbier, L., Barthelmy, S., et al. 2005b, GRB Coordinates Network, 3273, 1
- Sakamoto, T., Barbier, L., Barthelmy, S., et al. 2006a, GRB Coordinates Network, 4445, 1
- Sakamoto, T., Barbier, L., Barthelmy, S., et al. 2006b, GRB Coordinates Network, 4811, 1
- Sakamoto, T., Barbier, L., Barthelmy, S. D., et al. 2006c, GRB Coordinates Network, 5349, 1
- Sakamoto, T., Barbier, L., Barthelmy, S. D., et al. 2006d, GRB Coordinates Network, 5534, 1
- Sakamoto, T., Barbier, L., Barthelmy, S. D., et al. 2006e, GRB Coordinates Network, 5349, 1
- Sakamoto, T., Barbier, L., Barthelmy, S. D., et al. 2006f, GRB Coordinates Network, 5611, 1
- Sakamoto, T., Barbier, L., Barthelmy, S. D., et al. 2006g, GRB Coordinates Network, 5732, 1
- Sakamoto, T., Barbier, L., Barthelmy, S. D., et al. 2006h, GRB Coordinates Network, 5887, 1
- Sakamoto, T., Barthelmy, S. D., Baumgartner, W., et al. 2008, GRB Coordinates Network, 7938, 1
- Sakamoto, T., Sato, G., Barbier, L., et al. 2009a, ApJ, 693, 922
- Sakamoto, T., Barthelmy, S. D., Baumgartner, W. H., et al. 2009b, GRB Coordinates Network, 8769, 1
- Sakamoto, T., Barthelmy, S. D., Baumgartner, W. H., et al. 2009c, GRB Coordinates Network, 8986, 1
- Sakamoto, T., Barthelmy, S. D., Baumgartner, W. H., et al. 2010a, GRB Coordinates Network, Circular Service, No. 10852, #1 (2010a), 10852, 1
- Sakamoto, T., Barthelmy, S. D., Baumgartner, W. H., et al. 2010b, GRB Coordinates Network, Circular Service, No. 10993, #1 (2010b), 10993, 1
- Sakamoto, T., Barthelmy, S. D., Baumgartner, W. H., et al. 2010c, GRB Coordinates Network, Circular Service, No. 11169, #1 (2010a), 11169, 1
- Sakamoto, T., Barthelmy, S. D., Baumgartner, W. H., et al. 2011a, GRB Coordinates Network, Circular Service, No. 11511, #1 (2011a), 11511, 1
- Sakamoto, T., Barthelmy, S. D., Baumgartner, W. H., et al. 2011b, GRB Coordinates Network, Circular Service, No. 12262, #1 (2011b), 12262, 1
- Sakamoto, T., Barthelmy, S. D., Baumgartner, W. H., et al. 2012, GRB Coordinates Network, Circular Service, No. 13022, #1 (2012), 13022, 1
- Sakamoto, T., Barthelmy, S. D., Baumgartner, W. H., et al. 2014a, GRB Coordinates Network, Circular Service, No. 16029, #1 (2014a), 16029, 1
- Sakamoto, T., Barthelmy, S. D., Baumgartner, W. H., et al. 2014b, GRB Coordinates Network, Circular Service, No. 16258, #1 (2014b), 16258, 1
- Sakamoto, T., Barthelmy, S. D., Baumgartner, W. H., et al. 2015, GRB Coordinates Network, Circular Service, No. 17930, #1 (2015), 17930, 1
- Sakamoto, T., Barthelmy, S. D., Cummings, J. R., et al. 2016a, GRB Coordinates Network, Circular Service, No. 19106, #1 (2016a), 19106, 1
- Sakamoto, T., Barthelmy, S. D., Cummings, J. R., et al. 2016b, GRB Coordinates Network, Circular Service, No. 19861, #1 (2016b), 19861, 1
- Sanchez-Ramirez, R., Gorosabel, J., de Ugarte Postigo, A., & Gonzalez Perez, J. M. 2012, GRB Coordinates Network, Circular Service, No. 13723, #1 (2012), 13723, 1
- Sato, G., Barbier, L., Barthelmy, S., et al. 2006a, GRB Coordinates Network, 5231, 1
- Sato, G., Sakamoto, T., Markwardt, C., et al. 2006b, GRB Coordinates Network, 5538, 1
- Sbarufatti, B., Barthelmy, S. D., Beardmore, A. P., et al. 2007, GRB Coordinates Network, 6560, 1
- Schady, P., & Marshall, F. E. 2008, GRB Coordinates Network, 7953, 1
- Shao, L., & Dai, Z. G. 2007, ApJ, 660, 1319
- Shcherbakov, R. V., Pe'er, A., Reynolds, C. S., et al. 2013, ApJ, 769, 85
- Stamatikos, M., Barbier, L., Barthelmy, S., et al. 2006a, GRB Coordinates Network, 5289, 1
- Stamatikos, M., Barbier, L., Barthelmy, S. D., et al. 2006b, GRB Coordinates Network, 5639, 1
- Stamatikos, M., Barbier, L., Barthelmy, S. D., et al. 2007, GRB Coordinates Network, 6225, 1
- Stamatikos, M., Barthelmy, S. D., Baumgartner, W., et al. 2008a, GRB Coordinates Network, 7656, 1
- Stamatikos, M., Barthelmy, S. D., Baumgartner, W., et al. 2008b, GRB Coordinates Network, 8007, 1
- Stamatikos, M., Barthelmy, S. D., Baumgartner, W. H., et al. 2009, GRB Coordinates Network, 9290, 1
- Stamatikos, M., Barthelmy, S. D., Baumgartner, W. H., et al. 2010a, GRB Coordinates Network, Circular Service, No. 10732, #1 (2010a), 10732, 1
- Stamatikos, M., Barthelmy, S. D., Baumgartner, W. H., et al. 2010b, GRB Coordinates Network, Circular Service, No. 11202, #1 (2010b), 11202, 1

- Stamatikos, M., Barthelmy, S. D., Baumgartner, W. H., et al. 2011, GRB Coordinates Network, Circular Service, No. 11691, #1 (2011), 11691, 1
- Stamatikos, M., Barthelmy, S. D., Baumgartner, W. H., et al. 2012a, GRB Coordinates Network, Circular Service, No. 13414, #1 (2012a), 13414, 1
- Stamatikos, M., Barthelmy, S. D., Baumgartner, W. H., et al. 2012b, GRB Coordinates Network, Circular Service, No. 13720, #1 (2012a), 13720, 1
- Stamatikos, M., Barthelmy, S. D., Baumgartner, W. H., et al. 2014a, GRB Coordinates Network, Circular Service, No. 16063, #1 (2014a), 16063, 1
- Stamatikos, M., Barthelmy, S. D., Baumgartner, W. H., et al. 2014b, GRB Coordinates Network, Circular Service, No. 16827, #1 (2014b), 16827, 1
- Stamatikos, M., Barthelmy, S. D., Baumgartner, W. H., et al. 2015, GRB Coordinates Network, Circular Service, No. 17941, #1 (2015), 17941, 1
- Stamatikos, M., Barthelmy, S. D., Cummings, J. R., et al. 2016, GRB Coordinates Network, Circular Service, No. 18899, #1 (2016), 18899, 1
- Still, A., Kniazev, M., Romero-Colmenero, E., et al. 2006, GRB Coordinates Network, 5226, 1
- Stratta, G., Dainotti, M. G., Dall'Osso, S., et al. 2018, ApJ, 869, 155
- Tagliaferri, G., Goad, M., Chincarini, G., et al. 2005, Nature, 436, 985
- Tanvir, N. R., Wiersema, K., & Levan, A. J. 2010, GRB Coordinates Network, Circular Service, No. 11230, #1 (2010), 11230, 1
- Tanvir, N. R., Wiersema, K., Levan, A. J., et al. 2012a, GRB Coordinates Network, Circular Service, No. 13348, #1 (2012a), 13348, 1
- Tanvir, N. R., Fynbo, J. P. U., Melandri, A., et al. 2012, GRB Coordinates Network, Circular Service, No. 13890, #1 (2012b), 13890, 1
- Tello, J. C., Sanchez-Ramirez, R., Gorosabel, J., et al. 2012, GRB Coordinates Network, Circular Service, No. 13118, #1 (2012), 13118, 1
- Thoene, C. C., Perley, D. A., Cooke, J., et al. 2007, GRB Coordinates Network, 6741, 1
- Thoene, C. C., de Ugarte Postigo, A., Gorosabel, J., et al. 2012, GRB Coordinates Network, Circular Service, No. 13628, #1 (2012), 13628, 1
- Troja, E., Cusumano, G., O'Brien, P. T., et al. 2007, ApJ, 665, 599
- Tueller, J., Barthelmy, S., Barbier, L., et al. 2005a, GRB Coordinates Network, 3615, 1
- Tueller, J., Markwardt, C., Barbier, L., et al. 2005b, GRB Coordinates Network, 3803, 1
- Tueller, J., Barbier, L., Barthelmy, S., et al. 2006a, GRB Coordinates Network, 5242, 1
- Tueller, J., Barbier, L., Barthelmy, S. D., et al. 2006b, GRB Coordinates Network, 5395, 1
- Tueller, J., Barbier, L., Barthelmy, S. D., et al. 2006c, GRB Coordinates Network, 5964, 1
- Tueller, J., Barthelmy, S. D., Baumgartner, W., et al. 2008, GRB Coordinates Network, 8176, 1
- Tueller, J., Barthelmy, S. D., Baumgartner, W. H., et al. 2009a, GRB Coordinates Network, 8808, 1
- Tueller, J., Barthelmy, S. D., Baumgartner, W. H., et al. 2009b, GRB Coordinates Network, 9089, 1
- Ukwatta, T. N., Barthelmy, S. D., Baumgartner, W. H., et al. 2009a, GRB Coordinates Network, 9104, 1
- Ukwatta, T. N., Barthelmy, S. D., Baumgartner, W. H., et al. 2009b, GRB Coordinates Network, 9337, 1
- Ukwatta, T. N., Barthelmy, S. D., Baumgartner, W. H., et al. 2010, GRB Coordinates Network, Circular Service, No. 10615, #1 (2010), 10615, 1
- Ukwatta, T. N., Barthelmy, S. D., Baumgartner, W. H., et al. 2011, GRB Coordinates Network, Circular Service, No. 11533, #1 (2011), 11533, 1
- Ukwatta, T. N., Barthelmy, S. D., Baumgartner, W. H., et al. 2013, GRB Coordinates Network, Circular Service, No. 15354, #1 (2013), 15354, 1
- Ukwatta, T. N., Barthelmy, S. D., Baumgartner, W. H., et al. 2014a, GRB Coordinates Network, Circular Service, No. 16306, #1 (2014a), 16306, 1
- Ukwatta, T. N., Barthelmy, S. D., Baumgartner, W. H., et al. 2014b, GRB Coordinates Network, Circular Service, No. 17010, #1 (2014b), 17010, 1
- Ukwatta, T. N., Barthelmy, S. D., Baumgartner, W. H., et al. 2015, GRB Coordinates Network, Circular Service, No. 17410, #1 (2015), 17410, 1
- Ukwatta, T. N., Barthelmy, S. D., Cummings, J. R., et al. 2016a, GRB Coordinates Network, Circular Service, No. 19301, #1 (2016a), 19301, 1
- Ukwatta, T. N., Barthelmy, S. D., Cummings, J. R., et al. 2016b, GRB Coordinates Network, Circular Service, No. 20032, #1 (2016b), 20032, 1
- Virgili, F. J., Qin, Y., Zhang, B., & Liang, E. 2012, MNRAS, 424, 2821
- von Kienlin, A. 2009, GRB Coordinates Network, 9792, 1
- Vreeswijk, P., Jakobsson, P., Ledoux, C., Thoene, C., & Fynbo, J. 2006, GRB Coordinates Network, 5535, 1
- Vreeswijk, P. M., Thoene, C. C., Malesani, D., et al. 2008a, GRB Coordinates Network, 7601, 1
- Vreeswijk, P. M., Fynbo, J. P. U., Malesani, D., Hjorth, J., & de Ugarte Postigo, A. 2008b, GRB Coordinates Network, 8191, 1

- Wang, X.-G., Zhang, B., Liang, E.-W., et al. 2015, ApJS, 219, 9
- Wang, Y.-Z., Zhao, Y., Shao, L., Liang, E.-W., & Lu, Z.-J. 2016, ApJ, 818, 167
- Waxman, E. 1997, ApJL, 485, L5
- Wiersema, K., Flores, H., D'Elia, V., et al. 2011, GRB Coordinates Network, Circular Service, No. 12431, #1 (2011), 12431, 1
- Willingale, R., O'Brien, P. T., Osborne, J. P., et al. 2007, ApJ, 662, 1093
- Wijers, R. A. M. J., Rees, M. J., & Meszaros, P. 1997, MNRAS, 288, L51
- Wijers, R. A. M. J., & Galama, T. J. 1999, ApJ, 523, 177
- Xu, M., & Huang, Y. F. 2012, A&A, 538, A134
- Xu, D., Fynbo, J. P. U., Malesani, D., et al. 2016a, GRB Coordinates Network, Circular Service, No. 19109, #1 (2016a), 19109, 1
- Xu, D., Heintz, K. E., Malesani, D., Wiersema, K., & Fynbo, J. P. U. 2016b, GRB Coordinates Network, Circular Service, No. 19773, #1 (2016b), 19773, 1
- Xu, D., Heintz, K. E., Malesani, D., & Fynbo, J. P. U. 2017, GRB Coordinates Network, Circular Service, No. 20458, #1 (2017), 20458, 1
- Yost, S. A., Harrison, F. A., Sari, R., & Frail, D. A. 2003, ApJ, 597, 459
- Zhang, B., & Mészáros, P. 2001, ApJL, 552, L35
- Zhang, B., Fan, Y. Z., Dyks, J., et al. 2006, ApJ, 642, 354
- Zhang, B., Liang, E., Page, K. L., et al. 2007a, ApJ, 655, 989
- Zhang, B.-B., Liang, E.-W., & Zhang, B. 2007b, ApJ, 666, 1002
- Zhang, B. 2014a, International Journal of Modern Physics D, 23, 1430002
- Zhang, B.-B., Zhang, B., Murase, K., Connaughton, V., & Briggs, M. S. 2014b, ApJ, 787, 66
- Zhang, B. 2019, The Physics of Gamma-Ray Bursts, Cambridge University Press, DOI: 10.1017/9781139226530.
- Zheng, W., Filippenko, A. V., Yuk, H., Zhu, Y., & Perley, D. A. 2015, GRB Coordinates Network, Circular Service, No. 18273, #1 (2015), 18273, 1